NITRIC OXIDE DEFICIENCY IN CHRONIC KIDNEY DISEASE: LINKS AMONG NEURONAL NITRIC OXIDE SYNTHASE, OXIDATIVE STRESS, AND ASYMMETRIC DIMETHYLARGININE (ADMA)

By

YOU-LIN TAIN

A DISSERTATION PRESENTED TO THE GRADUATE SCHOOL
OF THE UNIVERSITY OF FLORIDA IN PARTIAL FULFILLMENT
OF THE REQUIREMENTS FOR THE DEGREE OF
DOCTOR OF PHILOSOPHY

UNIVERSITY OF FLORIDA

2007

This dissertation is dedication to my family for their constant love

ACKNOWLEDGMENTS

This dissertation would not have been possible without the support of many people. Many thanks go to my adviser: Dr. Chris Baylis gave me the chance to work on many projects and also gave me numerous valuable comments for my manuscripts.

I would like to thank my committee members for their guidance and valuable comments: Dr. Richard Johnson, Dr. Mohan Raizada, and Dr. Mark Segal. I thanks also go to the Chang Gung Memorial Hospital for awarding me a fellowship, providing me with the financial means to complete this dissertation.

I am grateful to many persons who shared their technical assistance and experience, especially Dr. Verlander and Dr. Chang (University of Florida), Dr. Muller and Dr. Szabo (Semmelweis University, Hungary), Dr. Griendling and Dr. Dikalova (Emory University), and Dr. Merchant and Dr. Klein (University of Louisville).

Next, I would like to thank all of the members of Dr. Baylis lab, both past and present, with whom I have been fortunate enough to work: Dr. Aaron Erdely, Gerry Freshour, Kevin Engels, Lennie Samsell, Dr. Sarah Knight, Dr. Cheryl Smith, Dr. Jenny Sasser, Harold Snellen, Bruce Cunningham, Gin-Fu Chen, and Natasha Moningka. I will miss all of them.

Finally, thanks go to my wife, CN, and numerous friends who endured this long process with me, always offering support and love.

TABLE OF CONTENTS

LIST OF TABLES

LIST OF FIGURES

LIST OF ABBREVIATIONS

ADMA	Asymmetric dimethylarginine
A/I	Ablation/infarction
ALLO	Allograft
BP	Blood pressure
CCr	24hr clearance of creatinine
CKD	Chronic kidney disease
CsA	Cyclosporine A
CVD	Cardiovascular disease
DDAH	Dimethylarginine dimethylaminohydrolase
eNOS	Endothelial nitric oxide synthase
5/6 NX	5/6 nephrectomy
ISO	Isograft
nNOS	Neuronal nitric oxide synthase
NO	Nitric oxide
PNOx	Plasma nitrite plus nitrate levels
PRMT	Protein arginine methyltransferase
RAPA	Rapamycin
ROS	Reactive oxygen species
SD	Sprague-Dawley
SDMA	Symmetric dimethylarginine
Tx	Transplant
UNOxV	24hr urinary nitrite plus nitrate levels
UproV	24hr urinary protein excretion
WF	Wistar Furth

Abstract of Dissertation Presented to the Graduate School
of the University of Florida in Partial Fulfillment of the
Requirements for the Degree of Doctor of Philosophy

NITRIC OXIDE DEFICIENCY IN CHRONIC KIDNEY DISEASE: LINKS AMONG NEURONAL NITRIC OXIDE SYNTHASE, OXIDATIVE STRESS, AND ASYMMETRIC DIMETHYLARGININE (ADMA)

By

You-Lin Tain

December 2007

Chair: Chris Baylis
Major: Medical Sciences--Physiology and Pharmacology

Nitric oxide (NO) deficiency is a cause and a consequence of chronic kidney disease (CKD). We focused on three possible causes of NO deficiency in this dissertation: decreased abundance and /or changes in activity of nitric oxide synthase (NOS) enzymes, increased endogenous NOS inhibitors (e.g., asymmetric dimethylarginine (ADMA)), and increased NO inactivation by oxidative stress.

We found reduced renal cortical nNOS abundance as well as NOS activity in various CKD models. Therefore, we evaluated whether oxidative stress and ADMA inhibited nNOS expression in different CKD models. We found that 2 nNOS isoforms expressing in the kidney and that renal cortical nNOSα and nNOSβ isoform expression differentially in various CKD models. In mild CKD, nNOSα abundance can be maintained or compensated by nNOSβ to preserve renal function, while decreased nNOSα abundance results in CKD progression despite increased nNOSβ expression in severe CKD. Both oxidative stress and ADMA may inhibit nNOS expression. The inhibition by oxidative stress can be partially prevented by antioxidant vitamin E; however, vitamin E cannot prevent the elevation of ADMA. In 5/6 nephrectomized rats, we found the increase of ADMA may be due to increased ADMA synthesis by increased

protein arginine methyltransferase (PRMT) expression and decreased ADMA breakdown by decreased dimethylarginine dimethylaminohydrolase (DDAH) activity. In 5/6 ablation/infarction (A/I) model, vulnerable male A/I rats displayed higher oxidative stress but lower nNOSα abundance than resistant female A/I rats, demonstrating decreased nNOSα and increased oxidative stress contribute to CKD progression.

We concluded that decreased cortical nNOSα abundance, increased oxidative stress, and increased ADMA contribute to CKD progression. Targeting on increasing renal nNOS expression, reducing oxidative stress, and lowering ADMA levels to preserve NO bioavailability may be specific therapeutic interventions to prevent CKD progression.

CHAPTER 1
INTRODUCTION

Overview

Chronic Kidney Disease Is a Global Challenge

Increasing numbers of patients with chronic kidney disease (CKD) and consequent end-stage renal disease (ESRD) is becoming a global challenge (34). Cardiovascular disease (CVD) is a major cause of morbidity and mortality in CKD. The therapeutic goal in CKD is not only retarding CKD progression but also preventing adverse cardiovascular complications. Several common pathways of CKD progression have been uncovered, such as activation of renin-angiotensin system, glomerular hypertension, oxidative stress, proteinuria, and inflammation. They are all interrelated and they all interact with the nitric oxide (NO) pathway. Indeed, there is substantial evidence that NO deficiency occurs in CKD in humans and animals and may cause progressive functional deterioration, structural damage and cardiovascular side effects (10, 149). NO is not only a vasodilator but also has anti-inflammatory, anti–proliferative, and anti-oxidant properties (74).

Nitric Oxide Deficiency Is a Common Mechanism of CKD Progression

In clinical studies, patients with CKD develop NO deficiency (120). Animal studies also show that NO deficiency results from CKD and since experimentally induced chronic nitric oxide synthase (NOS) inhibition results in progressive renal injury (164), the development of NO deficiency during CKD is likely to cause progression. In addition, reduced NO bioavailability appears to be a major factor involved in CKD-induced endothelial dysfunction, which is the initial mechanism in atherosclerosis (119).

Nitric oxide deficiency could occur due to reduced substrate (L-arginine) availability, reduced cofactor (e.g., tetrahydrobioterin, BH_4) availability, decreased abundance and /or

changes in activity of NOS enzymes, increased endogenous NOS inhibitors (e.g., asymmetric dimethylarginine (ADMA)), and increased NO inactivation by oxidative stress (10). In clinical studies, both oxidative stress and ADMA have been shown related to the progression of CKD (16) and endothelial dysfunction (161). Thus, both of these causes of NO deficiency affect both renal outcome and CV complications. Oxidative stress can result in both increased ADMA generation and decreased breakdown (128), conversely, ADMA can induce uncoupling NOS causing oxidative stress (23).

Nitric oxide is produced from L-arginine by three nitric oxide synthase (NOS) families: neuronal NOS (nNOS), endothelial NOS (eNOS), and inducible NOS (iNOS). Since there is little iNOS expression in normal kidney (145), we have focused on evaluating eNOS and nNOS in CKD. We have found reduced cortical nNOS abundance as well as in vitro soluble NOS activity (mainly nNOS activity) in various CKD models (10, 36-41, 130, 153). In contrast the eNOS abundance is variable in different CKD models. These findings suggest that nNOS may be involved causally in CKD.

Neuronal Nitric Oxide Synthase

Role of Renal Cortical Neuronal Nitric Oxide Synthase in Chronic Kidney Disease Progression

Nitric oxide derived from nNOS in MD can dilate afferent arterioles, regulate tubuloglomerular feedback, and may also prevent mesangial cell and matrix proliferation (74, 139). Reduction of cortical nNOS may therefore cause renal vasoconstriction, decrease GFR, enhance tubular sodium reabsorption, result in mesangial proliferation and hence hasten progression of CKD. Indeed, cortical nNOS expression was shown to be positively correlated with afferent arteriolar diameter (139) and afferent arteriolar vasoconstriction was considered to participate in the pathogenesis of CKD progression (21, 97). In addition, nNOS in MD has an

essential role for renin production (139) and activation of renin-angiotensin contributes to CKD progression. Although the greatest density of renal cortical nNOS is in the MD, there may also be nNOS in proximal tubular epithelium and in nitrergic nerves that supply tubular and vascular structures in cortex (9, 74).

Neuronal Nitric Oxide Synthase Isoforms in the Kidney

The three NOS isoenzymes share a common structural organization: central calmodulin-binding motif links an oxygenase (N-terminal) and a reductase (C-terminal) domain. The oxygenase domain consists of an arginine, a heme, and a BH_4 binding site. The reductase domain contains binding sites for FAD, FMN, and NADPH (3). Unlike eNOS and iNOS, the 160kDa isoform, nNOSα possesses a unique ~300 aa segment at the N-terminal including a PDZ domain as well as a site for protein binding to allow protein – protein interactions. The protein inhibitor of nNOS (PIN) binds here (63) and was shown to be upregulated in 5/6 nephrectomy (NX) rats (113). At least 11 tissue- or development-specific transcripts of nNOS gene have been reported in rat (102), arising from different promoters or alternative splicing. nNOSα is the most commonly expressed in neural tissues and muscle, and until now, only nNOSα has been reported in rat kidney. As shown in Figure 1-1, the major nNOS isoforms that have been detected in extrarenal tissues, in addition to nNOSα are nNOSβ, nNOSγ, nNOSμ, and nNOS-2. nNOSβ and nNOSγ have part of the N-terminal deleted and consist of aa 236-1433 and 336-1433 of nNOSα, respectively. The nNOSμ (165kDa) is full length and includes an additional 34 aa insert in FMN binding domain, and is mainly located in skeletal muscle. Unlike nNOSα which is exhibited in both soluble and membrane fractions, nNOSβ and nNOS γ are only located in the soluble fraction (no PDZ domain). In nNOS exon 2 knockout mice, nNOSβ and nNOSγ were detected in the brain by Western blot, and nNOSβ has similar functional activity to nNOSα (35). In vitro, NOSβ has ~80% the activity of nNOSα (20), although in vivo the absence of the PDZ and PIN

domains could lead to greater activity (due to resistance to PIN) or decreased activity (due to decreased stability of dimers). In wild type mice, nNOSβ is located in many brain areas and in nNOSα knockout (lacking exon 2), nNOSβ abundance increases (35). In nNOSα knockout mice, nNOSβ was able to maintain normal penile erection, suggesting that there may be an upregulation of nNOSβ when nNOSα-derived NO is deficient (59). Thus, it is likely that nNOSβ may compensate in states of reduced nNOSα to maintain total nNOS activity.

Most of our previous studies used a polyclonal antibody recognizing N-terminal aa 1-231 of nNOS, thus specifically detecting nNOSα in kidney (80). Lately we have also used a C-terminal nNOS antibody (aa #1409-1424, Affinity Bioreagents, Golden, CO, USA), giving bands at both the nNOSα and –β molecular weights. Using a proteomic approach, we have confirmed abundant expression of nNOSβ in rat kidney. In this dissertation I describe studies to characterize the renal nNOSα and -β and determine if they are involved in CKD and their relative expression in different CKD models.

Regulation of Neuronal Nitric Oxide Synthase Expression

Although nNOS is constitutively expressed, its expression is under complex regulation. nNOS mRNA can be upregulated by stress, injury, neurotransmitters, steroid hormones and downregulated by cytokines (17). Most regulatory mechanisms have been studied on extrarenal tissues and relatively little is known about the regulation of the nNOS isoforms in the kidney. In kidney, nNOS in MD can be up- or downregulated by renal perfusion, systemic volume status, distal tubular fluid flow, and NaCl transporter (108). We have evidence that downregulation of nNOSα protein occurs in CKD, which is the subject of this dissertation. In addition to nNOS expression, nNOS activity can be regulated by various mechanisms: dimer stability, post-translational modifications (e.g., phosphorylation), endogenous NOS inhibitors (e.g., ADMA), substrate and cofactor deficiency (L-arginine and BH_4), interacting proteins, and oxidative stress.

Increases in both oxidative stress and ADMA have been implicated in the progression of renal disease in clinical trials (16) and nNOS activity is inhibited by oxidative stress and ADMA in vitro (23), suggesting both factors contribute to CKD progression possibly via modulating nNOS. Therefore we focus on 3 major causes of NO deficiency, decreased nNOS protein abundance and increased oxidative stress and ADMA, to understand whether they regulate nNOS expression/activity in CKD.

Oxidative Stress and Asymmetric Dimethylarginine

Role of Oxidative Stress in Chronic Kidney Disease

Oxidative stress is characterized by the increase of reactive oxygen species (ROS) which cannot be counterbalanced by the antioxidant system (43). In CKD, increased oxidative stress is considered to contribute to the progression as well as CV complications (47, 148). Superoxide ($O2^-$) and NO have counterbalancing actions and reciprocally reduce each other's bioavailability, thus a reduction in NO may shift the kidney toward a state of O_2^- dominance causing renal vasoconstriction, enhanced tubular sodium reabsorption, excessive proliferation and extracellular matrix expansion leading to fibrosis and thus CKD progression (95). In kidney, O_2^- is mainly generated by NADPH oxidase (44) and increased $p22^{phox}$, a major subunit of NADPH oxidase, enhances ROS generation and its expression correlates to NADPH oxidase activity (44). As part of the antioxidant defense, O_2^- can be converted to H_2O_2 by the superoxide dismutases (SOD) which prevents O_2^- from interacting with NO to generate peroxynitrite ($ONOO^-$), an important mediator of lipid peroxidation. Therefore, NOS and NO bioavailability can be inhibited by O_2^- and its metabolites. The activity of nNOS is highly sensitive to changes in oxidative stress (23).

Role of Asymmetric Dimethylarginine in Chronic Kidney Disease

Another important regulator of NOS activity is the endogenous NOS inhibitor, ADMA. Arginine is methylated by protein arginine N-methyltransferase (PRMT) to form

methylarginines: N^W-monomethyl-L-arginine (L-NMMA), asymmetric dimethylarginine (ADMA), and symmetric dimethylarginine (SDMA) (146). L-NMMA and ADMA, but not SDMA are competitive inhibitors of NOS isoenzymes and both are metabolized by dimethylarginine dimethylaminohydrolase (DDAH). Currently, nine PRMT isoenzymes have been identified and are classified as either type I or type II PRMT (12, 105). Both types PRMTs catalyze the formation of L-NMMA as an intermediate, and type I PRMTs lead to the formation of ADMA, whereas type II PRMTs produce SDMA. Since PRMT1 is a predominant type I PRMT and PRMT1 gene expression was increased in 5/6 NX rats (90), it is possible that increased PRMT1 expression may contribute to increased ADMA synthesis in CKD.

Further, DDAH metabolizes ADMA to citrulline and dimethylamine and decreased DDAH activity increased ADMA and diminished L-arginine/ADMA ratio and leading to a decrease of NO production. We have found reduced L-arginine/ADMA ratio in human CKD and ESRD patients and in a rat chronic glomerulonephritis CKD model (153, 159). Elevated ADMA level has also been reported in the presence of various CKD models and is a risk factor for various cardiovascular disorders with endothelial dysfunction (146).

Dimethylarginine dimethylaminohydrolase has been identified in two isoforms, DDAH1 and DDAH2, which have 62% similarity. Rat and human DDAH protein are 95% identical (68). Both DDAHs have distinct tissue distributions but seemingly similar activity. DDAH1 is mainly located in nNOS predominant tissues (neural and epithelial), while DDAH2 is found in tissues with high eNOS expression (84). However, both DDAHs are widely expressed and not confined to NOS-expressing cells. So far, there is little data available on DDAH1/2 expression in kidney because good commercial antibodies have only just become available (138, 140).

Dimethylarginine dimethylaminohydrolase expression and/or activity can be inhibited by tumor necrosis factor α (61), IL-1β (143), homocysteine (126), glycated bovine serum albumin (162), erythropoietin (118), and ox-LDL (135). All of the above pathways provoke oxidative stress and these effects could be prevented by antioxidants (118, 126, 162), suggesting DDAH may be downregulated by oxidative stress (71). On the other hand, DDAH1 and DDAH2 gene expression are induced by farnesoid X receptor agonist (55) and all-trans-Retinoic acid (1), respectively. DDAH activity can also be induced by 17β-estradiol (54). Further, in vitro studies suggest that both DDAH1 and DDAH2 are inhibited by NO via S-nitrosylation on cystiene residues (72, 82). However, little is known about the regulation of DDAH in CKD.

Dimethylarginine dimethylaminohydrolase inhibition decreases NO production in endothelial cells (87). DDAH1 overexpression reduces plasma and tissue ADMA levels and enhances tissue NOS activity both in vitro and in vivo (30, 62) and ADMA levels were attenuated in DDAH2 overexpressing transgenic mice (52). These findings suggest that lowering ADMA levels by increasing DDAH may be a relevant area of intervention. We intended to characterize DDAH1/2 expression in different CKD models by Western blot and determine DDAH activity. This has been determined by measurement of substrate consumption (HPLC measurent of the rate of ADMA consumption or conversion of radiolabeled L -NMMA converted to L –citrulline, however, both methods are time consuming and costly. We have also developed a simple colorimetric method to measure renal DDAH activity that measures rate of citrulline accumulation.

Objective

Nitric oxide deficiency is both a cause and a consequence of CKD. We have found that renal nNOSα expression decreases markedly with injury in the SD rats and is correlated to decreased NOS activity in various rat CKD models. However, WF rats that are protected from

renal injury still show some decrease in nNOSα abundance but maintained NOS activity (39). We intended to test the hypotheses that other nNOS isoforms exist in kidney; that they may compensate for loss of nNOSα in CKD and that this is associated with protection from progression of CKD in different stages of CKD by evaluating different CKD rat models. In this dissertation, four CKD models were studied to elucidate whether nNOS isoform expression differentially in different stages of CKD. There are two transplant (Tx)-indued mild CKD models, ischemia/reperfusion (I/R) isografts (ISO I/R model) and rapamycin-treated allografts (ALLO RAPA model); the other two severe CKD models are 5/6 nephrectomy (NX model) and ablation/infarction models (A/I model). Also, CKD is a state of oxidative stress, known to inhibit NO generation as well as DDAH activity, leading to increased ADMA. We manipulated the level of oxidative stress with antioxidants to investigate the impact on nNOS isoform and DDAH expression/activities. The nNOS activity may be regulated by ADMA and the kidney is a major site of catabolism of ADMA by DDAH. We therefore investigated whether changes in the local ADMA level (due to changes in renal DDAH activity) will also influence renal NOS activity. This dissertation is divided into 5 concurrent studies to determine the impact of nNOS, oxidative stress, and ADMA in CKD (Figure 1-2):

- **Identification of renal nNOS α/β expression in rat kidney:** We compared an N-terminal nNOS antibody to a C-terminal nNOS antibody, to investigate the possibility that different nNOS isoform proteins exist in the rat kidney. nNOS isoforms were identified in rat kidney by a proteomic approach and the presence of the relevant transcripts was also confirmed by RT-PCR.

- **Characterization of renal nNOS α/β expression in transplant-induced CKD models:** We analyzed kidney samples from two renal transplant-induced CKD models; transplanted F344 isografts treated with antioxidants/anti-inflammatory agents and F344 to Lewis allografts treated with rapamycin (RAPA) to elucidate the impact of nNOS expression.

- **Optimization of a colorimetric assay to measure renal DDAH activity:** We established the optimal conditions for use of the Prescott-Jones method (109) of L-citrulline determination to measure kidney tissue DDAH activity. We compared this modified L-citrulline assay to the direct HPLC method measuring rate of ADMA breakdown.

- **Characterization of the renoprotective effects of vitamin E on renal nNOS, oxidative stress, and ADMA in a 5/6 NX CKD model:** We investigated the impact of the 5/6 nephrectomy model on renal nNOS abundance, oxidative stress, and ADMA-related enzymes and also whether the protective effects of vitamin E therapy are associated with preservation of these pathways.

- **Investigation of sex differences on CKD progression in the 5/6 A/I model by regulating renal nNOS, oxidative stress, and ADMA pathways:** We investigated whether L-arginine/ADMA is correlated to renal nNOS abundance, oxidative stress, and renal outcome in A/I rat model and whether there is sex difference in these pathways.

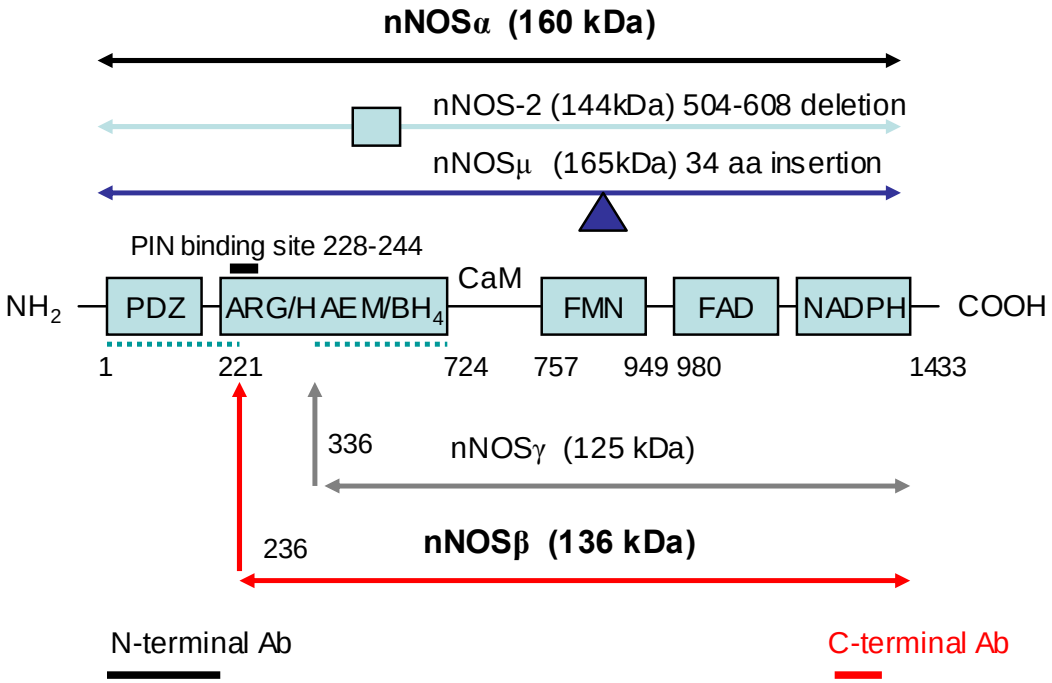

Figure 1-1. Illustration of nNOS isoforms. nNOS isoforms are showed by arrowed lines as follows: black, nNOSα aa #1-1433; red, nNOSβ aa #236-1433; grey, nNOSγ aa #336-1433; blue, nNOSμ aa#1-1433 with a 34 amino acids insertion; and dark blue, nNOS-2 aa 1-1433 with a deletion of aa #504-608. Consensus binding sites for PSD-95 discs large/ZO-1 homology domain (PDZ), protein inhibiter of nNOS (PIN), L-arginine (ARG), heme (HAEM), tetrahydrobiopterin (BH_4), calmodulin (CaM), flavin mononucleotide (FMN), flavin adenine dinucleotide (FAD), and NADPH are indicated. Dimer interfaces are shown by blue dashed line. N-terminal (black) and C-terminal (red) antibodies used in this dissertation recognizing different amino acids sequence are indicated. Based on refs (3, 35, 156).

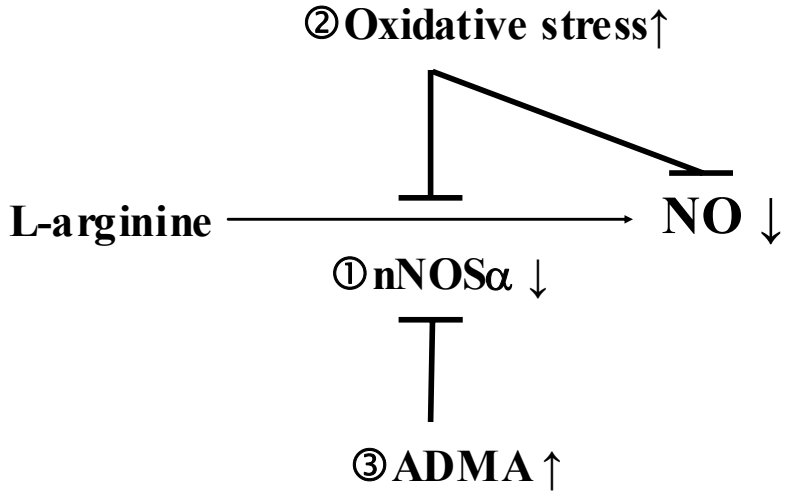

Figure 1-2. Three major mechanisms of NO deficiency in chronic kidney disease studied in this dissertation: (1) Decreased renal cortical neuronal nitric oxide synthase (nNOS) abundance, (2) Increased oxidative stress, and (3) Increased asymmetric dimethylarginine (ADMA).

CHAPTER 2
GENERAL METHODS

Animal Models

Ablation/infarction Model

Ablation/infarction (A/I) model was performed as follows: Renal mass was removed under isoflurane general anesthesia using full sterile technique. By retroperitoneal approach, the right kidney was removed and upper and lower thirds of the left kidney was infarcted by ligation of branches of the renal artery.

5/6 Nephrectomy Model

5/6 nephrectomy (NX) model was perfored as follows: By retroperitoneal approach, 2 poles of the left kidney were removed and then one week later the right kidney was removed.

Renal Transplantation Model

Renal transplantation (Tx) model was performed as follows: Rats were anesthetized by intraperitoneal pentobarbital sodium (32.5 mg/kg; Sigma, St. Louis, MO) and methohexital sodium (25 mg/kg; Brevital sodium, Eli Lilly and Co, Indianapolis, IN). After median laparatomy the left kidney was removed. In the donor the abdominal aorta and vena cava were clamped, a cannula placed into the left renal artery and the kidney flushed with cold (4ºC) solution, removed with the artery, vein and ureter and placed into cold solution for 10 min. Donor and recipient renal artery and vein were then anastomized with 10-0 prolene sutures and after a warm ischemia time of 35 min (total ischemia time 45 min), vascular clamps were removed and the ureter was anastomized end to end near to the hilus. To avoid infections, rats received 10 mg/kg/day rocephin (Ceftriaxone sodium, Roche, Nutley, NJ) for 10 days then rats were again anesthetized and the right native kidney removed.

Tissue Harvest

Tissue harvest was performed as follows: Tissue harvesting was done in isoflurane anesthetized rats. Initially a 20G butterfly was inserted into the abdominal aorta at the bifurcation and clamped in place. BP was measured then a blood sample withdrawn, then the vasculature was perfused with 60ml ice-cold PBS at 25ml/min and the vena cava vented. For frozen tissue harvesting for WB etc, tissues were harvested on to dry ice and snap frozen in liquid nitrogen and then stored in -80ºC freezer until analysis. For immunohistochemistry and histology the perfusate was switched to 2% paraformaldehyde-lysine-periodate (PLP) and perfused for 5 minutes, then removed, sliced longitudinally, then stored in the same fixative overnight at 4ºC. At the end of experiments, rats were euthanized with isoflurane overdose.

Metabolic cage studies/general chemical analyses: Rats were placed in metabolic cages for collection of 24 h urines. In all studies where NO_X (NO_2^- + NO_3^-) output was measured, rats were maintained on a low NO_X diet (ICN, AIN 76, MP Biomedicals, Solon, OH, USA) for 24h before and during the measurements. Measurements were made of total urinary protein by the Bradford assay; plasma and urine creatinine by a HPLC method previously described by us (130).

Biochemical Analysis

Nitric Oxide Assay

Urine and plasma NOx (NO_2^- + NO_3^-) assay was perfored as follows: The NOx levels were measured with Griess reaction according to Stuehr et al. (125) using the nitrate reductase enzyme which reduced NO_3^- to NO_2^-. Briefly, 125µl of samples plus 100µl of HEPES/ammonium formate (1:1) were mixed with 25µl of nitrate reductase, incubated for 60 minutes at 37ºC. After the incubation, samples were centrifuged (2000rpm for 15min) and 100µl of supernatant was transferred into a 96-well plate. Griess reagent was made by 1:1 (V/V) mixed

1% sulfanilamide with 0.1% naphthylethylene diamine. 150µl of Griess reagent was added into each well. Samples were incubated for 15 minutes at room temperature. Absorbance was determined at a wavelength of 543 nm spectrophotometrically. All chemicals for NOx assay were from Sigma (St Louis, MO, USA). A standard curve was constructed ranged from 0-400µM. Details of this method have been published by us previously (130).

Nitric Oxide Synthase Activity

In vitro NOS activity was determined as the following procedures: NOS activity was measured from the conversion of L-[^{3}H]-arginine to L-[^{3}H]-citrulline in the kidney cortex as described by us previously (39). Briefly, tissues were homogenized in iced homogenization buffer, ultracentrifuged, and both supernatant (soluble) and membrane fractions assayed; the soluble fraction contains predominantly nNOS (and iNOS when stimulated), whereas the membrane fraction contains mostly eNOS. Endogenous arginine was removed from the supernatant using Dowex while the pellet was reconstituted in homogenization buffer, then ultracentrifuged and resuspended. Samples were run at baseline and in the presence of nonselective NOS inhibitor cocktails: 2mM trifluoperazine, 5 mM NG-methyl-L-arginine (L-NMA), and 10 mM Nw-nitro-L-arginine methyl ester (L-NAME, Sigma-Aldrich, St. Louis, MO, USA). Data were expressed as pmol citrulline/min/mg protein minus any activity not inhibited by the NOS inhibitor cocktail and adjusted for background.

Pathology

Pathology was determined as follows: Pathology was performed on 5 micron sections of formalin-fixed kidney, blocked in paraffin wax, stained with PAS (Periodic acid-schiff staining system, Sigma-Aldrich, St. Louis, MO, USA). The level of renal injury was assessed on a blinded basis by determining the sclerotic damage to glomeruli using the 0 to 4+ scale, where 1+ injury involved less that 25% damage to the glomerulus, 2+ = 25 - 50% injury, 3+ = 51-75%

damage and 4+ = 76 – 100% damage. Data were represented as % of damaged glomeruli (N=100) showing any level of injury (scale 1+ to 4+). The total numbers of damaged glomeruli including all levels of injury were also measured and represented as total % of damaged glomeruli (N=100).

Western Blot

Western blot was performed as follows: Samples were loaded to 7.5-12% polyacrylamide gels, in aliquots of 50–300μg total protein with concentration adjusted to give fixed volume = 50μl. MW markers were run in one lane and positive control was also run. The proteins were separated by electrophoresis (200 V, 1h5min-2.5hr), transferred onto nitrocellulose membranes (1hr 45 min, 0.18Amps). We stained each membrane with Ponceau red to correct variations during protein loading and transfer. Then the membranes were incubated in 5% non-fat milk with TBS-T blocking solution for 60 min and washed in TBS-T (0.05%-0.5%) then incubated in the appropriate dilution of the primary then secondary antibody. The nNOSα was detected with 2 N-terminal antibodies: a rabbit polyclonal antibody (76) (1:10,000 dilution, 1 hr incubation) followed by a secondary goat anti-rabbit IgG-HRP antibody (Bio-Rad; 1:3,000 dilution, 1 hr incubation), or a mouse monoclonal antibody (Santa Cruz, 1:200 dilution, overnight incubation) followed by a goat anti-mouse IgG-HRP secondary antibody (Bio-Rad, 1:2000 dilution, 1-hour incubation). For nNOSβ detection we used a C-terminal rabbit polyclonal antibody (Affinity BioReagents, 1:250 dilution, overnight incubation), followed by a goat anti-rabbit IgG-HRP secondary antibody. Membranes were stripped and reprobed for eNOS using a mouse monoclonal antibody (Transduction Laboratories 1:250 dilution, 1-hour incubation), followed by a goat anti-mouse IgG-HRP secondary antibody. For PRMT1 we used a rabbit anti-PRMT1 antibody (Upstate, 1:2000 dilution, overnight incubation) and a goat anti-rabbit antibody. For DDAH we used a goat anti-rat DDAH1 antibody (Santa Cruz, 1:500 dilution, overnight

incubation) or a goat anti-rat DDAH2 antibody (Santa Cruz, 1:100 dilution, overnight incubation), followed by a secondary donkey anti-goat antibody (Santa Cruz, 1:2000 dilution, 1h incubation). For p22phox we used a goat anti-rat antibody (Santa Cruz, 1:200 dilution, overnight incubation), followed by a secondary donkey anti-goat antibody. Bands of interest were visualized using SuperSignal West Pico reagent (Pierce, Rockford, IL) and quantified by densitometry, as integrated optical density (IOD) after subtraction of background. The IOD was factored for Ponceau red staining to correct for any variations in total protein loading and for an internal standard (rat cerebellum for nNOS, endothelial cell lysate for eNOS, rat kidney cortex for PRMT1 & DDAH1/2, rat heart for p22phox). The protein abundance was represented as IOD/Ponceau Red/Std. We used Ponceau red method for standardization because in some situations β-actin may change.

Electronic Spin Resonance

NADPH oxidase-dependent superoxide was detected by electronic spin resonance (ESR) as follows: For this we collaborated with Dr. Griendling, Emory University to measure superoxide production by ESR with spin trapping. Membrane samples from kidneys were prepared as described previously (33, 51). 10μg of protein was added to 1 mM CPH, 200 μM NADPH, and 0.1 mM diethylenetriaminepentaacetic acid in a total volume of 100 μl of Chelex-treated PBS. In duplicate samples, NADPH was omitted. Samples were placed in 50 μl glass capillaries (Corning, New York, NY, USA). The ESR spectra were recorded using an EMX ESR spectrometer (Bruker) and a super-high-Q microwave cavity. Superoxide formation was assayed as NADPH-dependent, SOD-inhibitable formation of 3-carboxyproxyl.

Reverse Transcription Polymerase Chain Reaction

Reverse transcription polymerase chain reaction (RT-PCR) was performed as follows: End-point RT-PCR was used for semi-quantitative analysis of mRNA. RNA was isolated from

tissue using TRI Reagent (Sigma, St.Louis, MO, USA) and treated with DNase I (Ambion, Austin TX, USA). RNA (1 µg) was reversed transcribed (RT; SuperScriptTM II RNase H-Reverse Transcriptase, Invitrogen, Bethesda, MD, USA) with random primers (Invitrogen, Bethesda, MD, USA) in a total volume of 20 µl. Primers were designed using GeneTool Software (Biotools Incorporated, Edmonton, Alberta, Canada) with annealing temperatures at 58-61°C. Ribosomal 18S (r18S; Ambion, Austin, TX, USA) was used as an internal reference since r18S expression remained constant throughout. For nNOSα and nNOSβ, a forward primer targeting Exon 1a, a 5' untranslated region (5'UTR), was made according to Lee et al. and reverse primers targeting exon 2 (R2:5' tccgcagcacctcctcgaatc 3') and exon 6 (R6: 5' gcgccatagatgagctcggtg 3') were designed from rat-specific sequences (NM_052799). For each primer set, the cDNA from all samples was amplified simultaneously using aliquots from the same PCR mixture. PCR was carried out using 1-0.5 µg of cDNA, 50ng of each primer, 250 µM deoxyribonucleotide triphosphates, 1 x PCR Buffer, and 2 units Taq DNA Polymerase (Sigma, St. Louis, MO, USA) in a 50 µl final volume. Following amplification, 20 µl of each reaction was electrophoresed on 1.7% agarose gels. Gels were stained with ethidium bromide, images were captured and the signals were quantified in arbitrary units (AU) as optical density x band area using a VersaDoc Image Analysis System and Quantity One, v.4.6 software (Bio-rad, Hercules, CA, USA). PCR signals were normalized to the r18S signal of the corresponding RT product to provide a semi-quantitative estimate of gene expression.

CHAPTER 3
IDENTIFICATION OF NEURONAL NITRIC OXIDE SYNTHASE ISOFORMS IN THE KIDNEY

Introduction

The vulnerable Sprague-Dawley (SD) rats develop decreased nNOSα abundance as well as NOS activity and structural damage; however, the protected Wistar-Furth (WF) rats showed some decrease in nNOSα abundance but maintained NOS activity (39). These findings suggest the possibility that other nNOS isoforms, lacking the unique N-terminal of the nNOSα, might exist in the kidney and be influenced by injury which prompted our current investigation on identification of nNOS isoforms in the SD kidney.

In this study we compared an N-terminal antibody (that recognizes the unique PDZ-PIN region of the full length nNOSα), to a C-terminal antibody (that theoretically recognizes all nNOS variants), to investigate the possibility that structurally and functionally different nNOS proteins exist in the rat kidney. A targeted proteomics approach was used to determine if different nNOS proteins were present in the rat kidney and the presence of the relevant transcripts was also investigated using RT-PCR.

Materials and Methods

Tissue was harvested under isofluorane anesthesia from male (n=4) and female (n=3) Sprague Dawley (Harlan, Indianapolis, IN) rats (200-250g). The aorta was perfused with ice-cold PBS, the kidneys removed, separated into cortex and medulla, flash frozen in liquid nitrogen and stored at –80°C for analysis. Other tissues were collected similarly (skeletal muscle, heart, lung, liver, aorta, small intestine, testis, and cerebellum). Supplies were from Sigma, St Louis MO, unless otherwise specified. For Western blot, analysis was performed as described in chapter 2.

Peptide competition was performed by Western blot on two identical membranes, run as described above, on which were loaded 200 µg of kidney cortex, 100 µg of kidney medulla, and 5 µg of cerebellum. For peptide competition 150 µg of neutralizing peptide (ABR PEP-190) was incubated with 3.75 µg of the C-terminal nNOS antibody (ABR PA1-033) overnight at 4 °C, centrifuged and supernatant diluted in blocking solution (1:4000) and used for nNOS detection. The control membrane was probed with the ABR PA1-033 alone. Both membranes were then probed with a secondary goat anti-rabbit IgG-HRP antibody (BioRad, Hercules, CA; 1:60,000 dilution, 1 hr incubation).

Immunoprecipitation was carried out on kidney cortex (KC), kidney medulla (KM), and cerebellum (Cer) and tissues were homogenized with lysis buffer (20 mM Tris-HCl, 150 mM NaCl, 1% Triton X-100, 0.5% Nonidet P-40, 1 mM EDTA, 1 mM EGTA, 20 mM sodium orthovanadate, 20 mM NaF, 5 mM phenylmethylsulfonyl fluoride, 21 µg/ml aprotinin, and 5 µg/ml leupeptin) and after centrifugation the supernatant (KC = 1.5 ml, 26 µg protein /µl; KM = 1 ml, 25 µg /µl; Cer = 1 ml, 11.5 µg /µl) was incubated with 20-80µl of C-terminal nNOS antibody (ABR PA1-033) overnight at 4°C with continuous rotation. Protein A-Sepharose beads (30-50 µl, Amersham Biosciences, Piscataway, NJ) were added, continuously rotated for 2 h at 4 °C, washed, resuspended in 50 µl of 2× Laemmli buffer, boiled for 3 min and loaded onto 7.5% SDS polyacrylamide gels. Proteins were separated by SDS-PAGE (200 V, 2.5 hr), gels were stained overnight with Coomassie blue (Sigma, St. Louis, MO) and the bands of interest excised from the gel under fully sterile conditions and analyzed by proteomics.

For proteomic analysis we collaborated with Dr. Klein, University of Louisville. Protein digestion, peptide mass fingerprinting and sequence tagging was conducted on individual bands excised as 1-3 mm^3 plugs from the 1D-SDS PAGE gels, conditioned and de-stained with 20 µL

0.1 M NH_4HCO_3 for 15 minutes followed with 30 µL 99.9% acetonitrile. The gel pieces were dried, re-hydrated with 20 µL of 0.02 M dithiothreitol in 0.1 M NH_4HCO_3 and heated at 56ºC for 45 minutes for reduction of disulphide bonds. The solution was replaced with 0.055 M iodoacetamide in 0.1 M NH_4HCO_3 for alkylation of reduced thiols (30 minutes in the dark). The alkylation solution was removed, the gel plug conditioned for 15 minutes with 200 µL 0.05 M NH_4HCO_3, then gel plugs were dehydrated with 200 µL 99.9% acetonitrile. After 15 minutes the solution was removed, gel plugs were dried by vacuum centrifuge and re-hydrated with 3 µL of 20 ng/µL modified trypsin (Promega, Madison, WIA) in 0.05 M NH_4HCO_3. Re-hydrated gel pieces were covered with 5-6 µL 0.05 M NH_4HCO_3 and incubated overnight at 37ºC. The samples were cooled and the trypsinization reaction was stopped by the addition of 1 µL 0.1% trifluoroacetic acid (TFA).

MALDI matrix used throughout the analysis was α-cyano-4-hydroxycinnamic acid (α-CN) containing 10 mM $NH_4H_2PO_4$. Samples were a) spotted as 1:1 (v/v) samples of protein digest: α-CN (or b) desalted sample aliquots (0.7 µL - 1.0 µL, 4 mg/mL α-CN, 50% acetonitrile, 0.1% TFA) spotted directly onto MALDI sample targets using C18 Zip Tips® (Millipore, Salem, MA). Samples were air-dried in the dark and cleared of particulate matter with compressed gas prior to sample plate loading into the mass spectrometer.

Positive ion MALDI -TOF mass spectra were acquired using an Applied Biosystems (Foster City, CA) AB4700 protein analyzer operating in reflectron mode and with ion source pressure ~0.5 µTorr. After a 400 ns time-delayed ion extraction period, the ions were accelerated to 20 kV for TOF mass spectrometric analysis. A total of 600 to 1000 laser shots (355 nm Nd:YAG solid state laser operating at 200 Hz) were acquired and signal averaged. Individual sample plates were calibrated and plate modeling performed using a six peptide calibration

standard with - 1) des-Arg1-Bradykinin, 2) angiotensin I, 3) Glu1-Fibrinopeptide B, 4) ACTH (1-17), 5) ACTH (18-39), and 6) ACTH (7-38). Data was analyzed using Mascot (version 1.9) against the 20051115 or 20061212 Swiss Protein database (all taxonomy) assuming: a.) monoisotopic peptide masses, b.) cysteine carbamidomethylation, c.) variable oxidation of methionine, d.) no missed trypsin cleavage sites, e.) a MS mass accuracy of greater than 50 ppm and f.) a MSMS mass accuracy of greater than 0.3 Da. Limitation of the original protein mass was not employed within the Mascot search. A Mascot score of ≥ 65 was considered to be statistically significant ($p<0.05$).

Major ion peaks and suspect modified peptides were subjected to MALDI TOF-TOF analysis by collision induced fragmentation (CID) using 1 KeV collision energy and atmospheric gases (medium pressure). Mascot search of the MALDI TOF-TOF data proceeded with search parameters listed above with the inclusion of a mass accuracy of 0.3 Da for peptide fragment masses. MALDI TOF-TOF spectra were used for combined analysis using Applied Biosystems Global Protein Server software and Mascot.

End-point RT-PCR was used for qualitative analysis to differentially detect nNOS mRNA. RNA as described in chapter 2.

Results

Homogenates of male and female kidney cortex and medulla were immunoblotted using both N-terminal and C-terminal polyclonal nNOS antibodies. Figure 3-1A shows a representative western blot using the antibody targeting the N-terminal of rat nNOS (AA#1-231) (80). This antibody detects a single band at ~160 kDa in the kidney cortex, kidney medulla and cerebellum which corresponds to the nNOSα isoform. Figure 3-1B shows the same samples probed with the ABR nNOS antibody, which detects a conserved region within the C-terminal of nNOS (AA#1409-1424) and should detect all the potential nNOS isoforms within the kidney. Multiple

bands are shown including those marked by arrows at ~160 kDa (putative nNOSα), ~140 kDa (putative nNOSβ), and ~125 kDa (putative nNOSγ).

Homogenates of female kidney cortex, medulla and cerebellum were immunoblotted onto 2 identical membranes which were probed with the C-terminal ABR antibody in the absence and presence of neutralizing peptide (x40). As shown in Figure 3-2, the bands at ~160 kDa (putative nNOSα), ~140 kDa (putative nNOSβ), and ~125 kDa (putative nNOSγ) were faded or abolished when incubated with the neutralizing peptide.

Next, homogenates from male kidney cortex, kidney medulla and cerebellum were immunoprecipitated with the C-terminal ABR nNOS antibody and electrophoresed by 1D-SDS PAGE. MALDI-TOF MS and MS/MS data were acquired. Mascot analysis used a combination of peptide mass fingerprinting (PMF) and tandem MS fragmentation data. We identified nNOS in both the ~170 kDa and ~160 kDa band of cerebellar lysate control (C3, C4, Table 3-1). The observed peptide coverage for cerebellar nNOS (C4) spans the nNOS protein sequence from amino acid residue 36 to 1407, consistent with nNOSα. Although nNOS was also detected in the ~170 kDa band (C3, Table 3-1), we were unable to determine if this slightly larger isoform was nNOS-μ since the tryptic peptide mass/fragments associated with the 34 AA insert (starting at AA# 839, K -> KYPEPLRFFPRKGPSLSHVDSEAHSLVAARDSQHR) were not observed.

In kidney medulla nNOS was identified in both the ~160 kDa and ~140 kDa bands (KM 4 and 5). Band KM4 contained peptide ions mapping to the rat nNOSα sequence from amino acids 36 – 1400. Multiple analyses of the nNOS in KM band 5 identified only peptides spanning amino acids 360 through 1400, consistent with the identification of the KM5 as nNOS-β (Table 3-1).

Due to relatively low abundance we were unable to detect any nNOS protein in the kidney cortex by MS analysis (Table 3-1) instead observing myosin-6, spectrin-α-chain, clathrin heavy chain and α-S1-casein in the putative bands of interest (KC3-5). The clathrin heavy chain and myosin-6 were also seen in the same fractions in which the ABR antibody was omitted. To further evaluate the presence of nNOS variants in the kidney medulla, RT-PCR was performed on the same tissue sample used for proteomic analysis using various untranslated regions of exon 1.4 Two bands were detected with Exon 1a-Exon 5 primer pairing indicating the presence of nNOSα (~1365bp) and nNOSβ (~310bp) mRNA expression. To test for the presence of the nNOSγ transcript, Exon 1a-Exon 6 primer pairing was performed. Following PCR, only two bands were detected indicating the presence of nNOSα (~1603bp) and nNOSβ (~548bp), but no nNOSγ mRNA expression.

As shown in Figure 3-3 nNOSα and/or nNOSβ mRNA was present in various rat tissues including kidney cortex, medulla, skeletal muscle, liver, small intestine, lung, testis, and cerebellum.

Discussion

The novel finding in this study is that both the nNOSα and nNOSβ proteins are present in the normal SD rat kidney. In addition, we have confirmed the presence of two nNOS mRNA transcripts (nNOSα, nNOSβ) arising from the same 5' untranslated region (UTR).

It was the presence of residual NOS activity in the brain of the nNOSα knockout mouse (generated by an exon 2 deletion), that led to the identification of the nNOSβ isoform (57). Since then, a number of nNOS isoforms have been identified that arise from the alternative splicing of nNOS pre-mRNAs. The greatest diversity of nNOS transcripts occur in the 5' UTR (Exon 1). In human tissues nine different first exons have been identified (117, 160) whereas in rat four first exons are known (58, 81, 102). Lee et al. identified three nNOS mRNA each with distinct 5'

untranslated first exons which all splice to Exon 2 while Oberbaumer et al. identified different nNOS mRNA splice variants in rat (81, 102). In rat kidney, a novel first exon was identified with five nNOS mRNA variants, four of which encoded for nNOSα (Exon 2) and one which encoded for nNOSβ (Exon 3) (102).

Most renal researchers use commercially available C-terminal antibodies to detect renal nNOS but we have used an N-terminal antibody synthesized by Lau et al. (80) that is highly selective for nNOSα. We selected the ABR C-terminal nNOS antibody (#PA1033; polyclonal rabbit anti rat) since the neutralizing peptide was also available for competition assays. Using this C-terminal antibody in Western blots we observed bands in normal kidney cortex and medulla at the molecular weights of nNOS-α (~160 kDa), nNOS-β (~140 kDa) and nNOS-γ (~125 kDa). These were all competed when incubated with the neutralizing peptide, suggesting that they were either nNOS isoforms or other proteins with structural homogeneity in the AA #1409-1424 region of the C-terminal.

We then immunoprecipitated these proteins with the ABR nNOS C-terminal antibody, separated the proteins by 1D-PAGE and performed proteomic analysis on the bands of interest (4). Repeated MALDI-TOF MS analysis demonstrated that the cerebellum and kidney medulla contained peptide ions mapping to the rodent nNOS sequence (NCBI Accession #P29476) from amino acids 36 – 1400 thereby identifying the ~160 kDa protein band as nNOSα. In the ~140 kDa protein band, peptide ions mapping to the rodent nNOS sequence from amino acids 359 – 1400 were observed. Of note, we did not identify the R.VSKPPVIISDLIR.G, the R. GIASETHVVLILR.G or the R.GPEGFTTHLETTFTGDGTPK.T tryptic peptides, predicted to be present within amino acids 1 through 358 of the nNOSα, consistent with the identification of the ~140 kDa band as nNOSβ. To verify the existence of transcripts coding for nNOSα and

nNOSβ in rat kidney we used RT-PCR using three forward primers for Exon 1 as previously published by Lee et al. (81) and two reverse primers designed to target Exon 5 (aa. #318-326) and Exon 6 (aa. #398-405). Two bands were detected with Exon 1a-Exon 5 (1365bp, 310bp) and Exon 1a-Exon 6 (1603bp, 548bp) primer pairing indicating the presence of both nNOSα and nNOSβ transcripts in both renal cortex and medulla.

Although an immunoreactive protein band at ~125 kDa (nNOSγ) was detected with the ABR nNOS C-terminal antibody by Western blot analysis, we were unable to confirm the presence of nNOSγ by proteomic analysis. While this absence could simply be due to low protein abundance, the fact that we could not detect any nNOSγ mRNA suggests that nNOSγ is not present in normal rat kidney. We speculate that this ~125 kDa band (which was competed by neutralizing peptide), may contain a novel nNOS variant.

Despite detecting both nNOSα and nNOSβ transcripts in the rat kidney cortex, we could not confirm the presence of any nNOS protein in the kidney cortex by proteomic analysis. This presumably resulted from a relatively low abundance of nNOS in the kidney cortex. Given the large body of literature demonstrating that nNOS is present in very high concentrations in the macula densa, we hypothesize that the abundance of nNOS in the macula densa relative to total cortex is beneath the level that can be detected by the MS methods we have used (3). In the kidney cortex five proteins were identified by MS in the MW bands that should contain nNOS: clathrin heavy chain (CLH), spectrin-α chain brain (SPTA2), myosin-6 (MYO6) and aminopeptidase N (AMPN). There is no homology between CLH, SPTA2, MYO6 and AMPN and the immunogen of the COOH-terminal ABR antibody or the nNOS. In addition, CLH, SPTA2, and MYO6 were identified in the absence of ABR antibody control suggesting protein-protein interactions and/or non-specific binding to Protein A. AMPN was identified by MALDI-

TOF MS/MS-MS in only one immunoprecipitation and not in repeated studies, suggesting contamination rather than a lack of ABR nNOS antibody specificity (85).

Based on the present findings we suggest that nNOSβ is present in the normal rat kidney. Unlike full-length nNOSα, nNOSβ lacks amino acids 1-236, which contains the PDZ- and PIN-domains. The PDZ-domain is important in targeting nNOSα to the membrane, thus nNOSβ would only occur in the cytosol as shown by Huber et al. (58) in the rat intestine. The PIN-domain contains a binding site for protein-inhibitor of NOS which may inhibit the dimerization and activity of nNOSα (63). Since nNOSβ does not contain a PIN-domain, nNOSβ can not be inhibited by PIN or influenced by any protein-protein interaction. Heterologous transfection assays have shown the nNOSβ to be catalytically active (~80% of the activity of nNOSα) (35), thus the renal nNOSβ is likely to be a functional enzyme.

In wild type mice, nNOSβ is located in many brain areas and with nNOSα knockout, nNOSβ abundance increases (35). In nNOSα knockout mice, nNOSβ was able to maintain normal penile erection (59), suggesting that there may be an upregulation of nNOSβ when nNOSα-derived NO is deficient.

Table 3-1. Proteins identified by MALDI-TOF MS/MS-MS

Band	Protein ID	Protein Accession Number	MASCOT Score	Sequence Coverage (%)	Number of matching Non-redundant peptides	Estimated MW (kDa)	Calculated MW (kDa)
C3	nNOS	P29476	169	15	20	190	161.8
C3	Clathrin heavy chain	P11442	141	13	19	190	193.2
C4	nNOS	P29476	600	33	37	160	161.8
C4	α-S1-Casein	BAA00313	115*	20	3	160	24.6
KM3	Clathrin heavy chain	P11442	251	23	28	190	193.2
KM4	nNOS	P29476	138	18	19	160	161.8
KM5	nNOS	P29476	187	17	21	150	161.8
KC3	Clathrin heavy chain	P11442	458	32	42	190	193.2
KC4	Spectrin-α-chain brain	P16546	136	15	18	160	168
KC4	Myosin-6	Q9UM54	78	11	14	160	150
KC5	Aminopeptidase N	P15684	76	12	9	150	109.6

Peptide masses were searched against the Swiss Protein data (20051115) and all taxa (197228 sequences and 71581181 residues) assuming complete alkylation of Cys with iodoacetamide, partial oxidation of Met, no missed cleavages by trypsin, and a MS mass tolerance of 50ppm & MSMS mass tolerance of 0.3Da. The Mascot Score is the absolute probability that the observed match is a random event. The Mascot Score is reported as -10 x Log10 (P), where P is the absolute probability; therefore the lower the probability that an observed match is a random event the higher the score. In this study, a score of ≥65 was considered significant. The sequence coverage is the number of amino acids (AA) identified by peptide sequence tagging compared to the parent protein (AA identified/total AA in parent protein). *Protein identification significance achieved by peptide sequence tagging of one peptide. C, cerebellum; KM, kidney medulla; KC, kidney cortex.

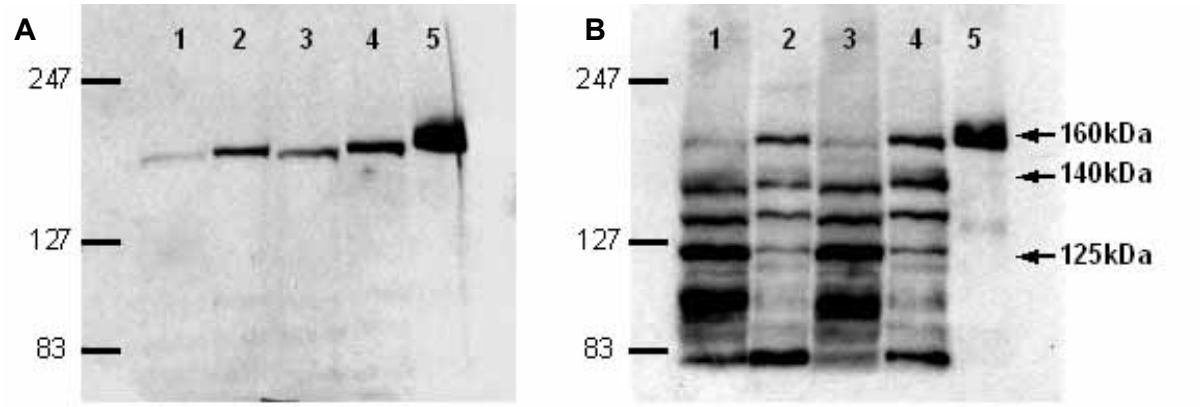

Figure 3-1. Immunoblots of male and female kidney cortex (KC), kidney medulla (KM), and control cerebellar lysate (Cer). A) with N-terminal nNOS antibody. B) with ABR C-terminal nNOS antibody. Lanes: 1 = male KC, 2 = male KM, 3 = female KC, 4 = female KM, 5 = Cer.

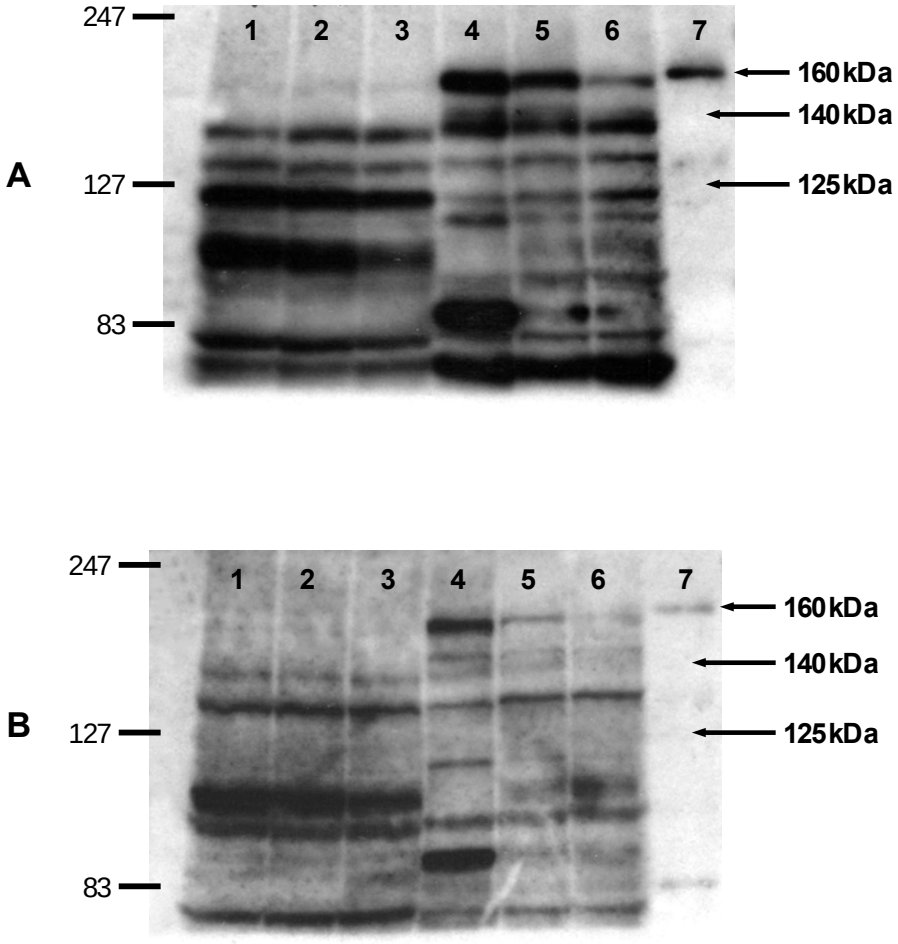

Figure 3-2. Immunoblots of female kidney cortex (KC), kidney medulla (KC), and control cerebellar lysate (Cer) with ABR C-terminal nNOS antibody. A) In the absence of neutralizing peptide. B) In the presence of neutralizing peptide. KC (lanes 1-3) and KM (lanes 4-6) samples were from three separate females. Lanes: 1-3 = KC, 4-6 = KM, 7 = Cer.

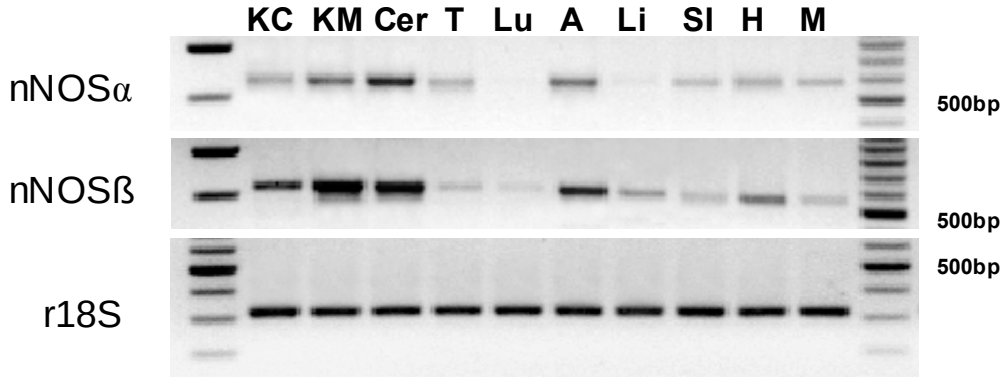

Figure 3-3. End-point RT-PCR of nNOS transcripts in various male tissues: kidney cortex (KC), kidney medulla (KM), cerebellum (Cer), testis (T), lung (Lu), aorta (A), liver (Li), small intestine (SI), heart (H), and skeletal muscle (M). nNOSα transcript was detected using a forward primer targeting exon 1a and a reverse primer targeting exon 2. nNOSβ transcript was detected using a forward primer targeting exon 1a and a reverse primer targeting exon 6. Ribosomal 18S was used as an internal control. The KC and KM samples used for end-point RT-PCR were the same tissue samples used in generating the KC and KM proteomic data. DNA ladders are shown on the left and right.

CHAPTER 4
RENAL CORTEX NEURONAL NITRIC OXIDE SYNTHASE IN KIDNEY TRANSPLANTS

Introduction

Nitric oxide (NO) derived from iNOS has been implicated as damaging in kidney transplants while NO derived from constitutive NOS might protect the allograft (152). We previously reported that decreased renal nNOS abundance was associated with renal injury in a wide variety of CKD models (10), including the 5/6 ablation/infarction (A/I) (130), chronic glomerulonephritis (153), puromycin aminonucleoside-induced CKD (PAN) model (38), normal aging (40), chronic NOS inhibition model (36), Zucker obese rat which develops type 2 diabetes (37), and DOCA/NaCl-induced CKD model (39). Renal transplantation-induced injury could be due to high iNOS-derived NO which could compromise constitutive NOS availability via substrate limitation (65, 152). It is also possible that decreased renal nNOS abundance might occur in the transplanted kidney and contribute to injury. We intended to elucidate the nNOS expression in two kidney transplant (Tx) models: a rapamycin-treated allograft model (RAPA) and an I/R injury model using renal isografts (ISO).

Although calcineurin inhibitors (CNIs) have improved 1-year survival rates for kidney grafts, long-term graft failure still occurs (92), perhaps reflecting ischemia/reperfusion (I/R) injury and CNI-related nephropathy. In the first series we investigated the long-term (22w) outcome (structural/functional) of renal Tx and renal nNOS expression using 2 different short-term (10d) immunosuppressive regimens (Cyclosporine vs. rapamycin) to prevent acute rejection. Rapamycin (RAPA), a mammalian target of rapamycin (mTOR) inhibitor, is used as a substitute for, or given in combination with CNIs to prevent rejection and reduce nephrotoxicity. In male rats, a wide therapeutic dosage of RAPA between 0.3-6 mg/kg/day was effective for prolongation of allograft survival (32) although RAPA at 6.5mg/kg/day resulted in acute

nephrotoxicity in a male rat isograft model with I/R (101). In this study, the dose sufficient to suppress the initial acute rejection of rapamycin (1.6mg/kg/day) and Cyclosporine (3mg/kg/day) were used.

In the second series, we investigated whether perioperative (10 day) anti-inflammatory/ antioxidant treatment designed to give endothelial protection (EP) and preserve NO would prevent long-term graft injury using a Tx-induced (isograft) I/R injury model. Although many antioxidants and anti-inflammatory agents have been tested to prevent I/R injury and ameliorate short-term graft dysfunction, it is unclear whether these acute effects may affect the long-term graft function (29, 107). Tempol (4-hydroxy-tempo), a membrane permeable, superoxide dismutase (SOD) mimetic that removes superoxide (O_2^-) and facilitates hydrogen peroxide (H_2O_2) dismutation, was reported to prevent renal I/R injury at the dose of 30mg/kg/hr for 6hr (25). Deferoxamine (DFO), an iron chelator, has been included in preservation solutions (for 18hr) and reduces renal I/R injury at 9 days after Tx (56). L-arginine is a substrate for nitric oxide synthase (NOS) and reduces renal I/R injury when administered once before I/R (24). Glucocorticoids are anti-inflammatory agents and also prevent the induction of the damaging iNOS. The individual strategies above were combined in this study to prevent I/R injury in the 10 day period immediately before and after Tx.

Materials and Methods

Orthotopic renal Tx was performed as described in chapter 2. Male Fisher 344 (F344, RT1v1, from Harlan Indianapolis, USA) served as donors. Lewis (LEW, RT1, from Harlan, Indianapolis, USA) male rats were used as recipients in the ALLO groups (n=14), while F344 male rats were used in the ISO groups (n=12). In addition to ALLO and ISO rats, 2-kidney age-matched male rats (n=7) of both Lewis and F344 stains were used as age control. All rats were aged 9-14 weeks and maintained with free access to standard rat chow and water ad libitum.

In the RAPA series Tx recipients were treated for the first 10 days after surgery with rapamycin derivative sirolimus (n=7) (1.6 mg/kg/day; Rapamune, Wyeth Laboratories, Philadelphia, PA) by gavage or with 3 mg/kg/day cyclosporin s.c. (n=7) (CsA, Sandimmune, Novartis, Basle, Switzerland). Rats also received the antibiotic ceftriaxone sodium, 10 mg/kg/day (Rocephin, Roche, Nutley, NJ) i.m. for 10 days.

In the I/R series, ISO rats were separated into 2 groups: untreated group, ISO-UN (n=6) in which lactated Ringers was used to flush the donor kidney at the time of Tx. A second group (n=6) were given treatments to provide endothelial protection, ISO-EP. The donors received 10 mg/kg dexamethasone, iv (APP, Los Angeles, CA, USA) 30 minutes before kidney removal. The donor kidney was flushed with 2 ml/g kidney weight cold lactated Ringers solution containing 1 mM deferoxamine mesylate (Sigma-Aldrich, St. Louis, MO, USA) and 3 mM 4-hydroxy-tempo (Sigma-Aldrich, St. Louis, MO, USA) removed and placed in the same cooled solution for 10 minutes. Recipients were treated with 1% L-arginine (Fresenius Kabi Clayton, Clayton, NC, USA) and 1 mM 4-hydroxy-tempo in the drinking water one day before Tx and for 10 days thereafter to provide overall EP.

We used additional tissue solely as positive control for the NADPH oxidase-dependent superoxide production assay. Female Lewis recipients received renal grafts from female Fisher donors (30 min ischemia time) and were treated with cyclosporine (Novartis, Basel, Switzerland) at 1.5 mg/kg/day for 10 days. The contralateral donor Fisher kidney was harvested at Tx and the allograft was harvested at week 7 because of severe rejection; these provided normal control and severely inflamed samples, respectively.

Urine samples were collected in metabolic cages at 22 wks after Tx for determination of urinary NOx and total protein excretion. Just prior to sacrifice, blood pressure (BP) was

measured, under general anesthesia and a blood sample taken for analysis of plasma creatinine. Kidneys were then perfused until blood-free, decapsulated, removed and weighed. A thin section of kidney including cortex and medulla was fixed for histology and the remaining cortex and medulla was separated, flash frozen in liquid nitrogen and stored at –80°C for later analysis. Kidney sections were fixed in 10% buffered formalin, blocked in paraffin and 5 μm sections were stained with PAS. Glomerular sclerosis, interstitial, tubular, and vascular lesions were graded according the Banff classification. Renal nNOS and eNOS abundance were determined by Western blot. In addition, cerebellum (5 μg) and skeletal muscle (150 μg) were also used for detection of nNOSα in this study. End-point RT-PCR was used for semi-quantitative analysis of mRNA. In I/R series, NADPH-dependent superoxide production in kidney cortex was measured by Electron Spin Resonance (ESR) spectroscopy with hydroxylamine spin probe 1-hydroxy-3-carboxypyrrolidine (CPH). All analyses were performed as described in chapter 2.

Results are presented as mean±SEM. Parametric data was analysed by t-test and ANOVA. Nonparametric data was analysed by the Mann-Whitney test. $P<0.05$ was considered significant.

Results

All ALLO rats survived to 22 weeks post Tx. As shown in Table 4-1 both CsA and RAPA groups had higher urine NOx excretion than control. Both CsA and RAPA groups developed renal failure represented as increased plasma Cr, BUN, and decreased clearance of Cr. BP was lower in both ALLO vs. control possibly reflecting a lower BP in the Lewis ALLO recipients. Both ALLO groups had greater kidney weight vs. control presumably due to compensatory hypertrophy.

We found RAPA group exhibited significantly more sclerotic glomeruli than CsA group and their respective control (Figure 4-1). Banff score summarizing glomerular, tubular, interstitial and vascular changes demonstrated more severe injury in RAPA group compared to

CsA group. CsA group displayed lower urine protein excretion than control, while there was no dofference between RAPA group and control. Using the N-terminal antibody, cortical nNOSα protein was nearly undetectable in RAPA group (Figure 4-2). In contrast, there was no difference in nNOSα abundance in skeletal muscle (0.0076 ± 0.0005 vs. 0.0084 ± 0.0005 IOD/Int Std/Ponc) and cerebellum (0.0064 ± 0.0024 vs. 0.0088 ± 0.0006 IOD/Int Std/Ponc) between CsA and RAPA groups. As shown in Fig 4-3, nNOSα mRNA significantly increased in CsA group compared to controls (Fig 4-3A), whereas nNOSβ mRNA significantly increased in RAPA group (Fig 4-3B). Using the C-terminal nNOS antibody, nNOSβ protein (~140kDa) was significantly higher in the cortex of RAPA group compared to CsA and normal 2 kidney controls (Fig 4-4).

In I/R series, ISO-UN and ISO-EP groups had similar body weights (BW), kidney weights and the ratio of KW/BW, which was higher than in controls due to compensatory hypertrophy (Table 4-2). Ccr, plasma Cr and BUN were similar in both groups of ISO and lower vs. normal controls (Table 4-2).

Mild proteinuria developed in the ISO-UN rats (Table 4-2) while the ISO-EP group showed no change from baseline or from controls at week 22. By histology, the ISO-EP and ISO-UN rats, developed moderate and similar glomerulosclerosis and tubulointerstitial injury vs. controls (Figure 4-5). Despite the lack of proteinuria the EP group was not protected from structural damage compared to the UN rats.

The EP protocol should provide protection against inflammation and oxidative stress pre- and for the 10 days post Tx; the period where I/R injury would likely be developing. However, as shown in Figure 4-6, by 22 weeks post Tx there was no difference in renal NADPH-dependent O_2^- production in ISO-EP and ISO-UN kidney cortex. This assay is able to detect oxidative stress

since we observed increased renal NADPH-dependent O_2^- production in female Lewis allograft recipients undergoing severe graft rejection compared to normal kidney (Fig 4-6).

By Western blot, ISO-EP rats showed lower nNOS and eNOS protein abundance in renal cortex vs. ISO-UN (Figure 4-7A) but the in vitro NOS activity in both soluble (main location of the nNOS) and membrane (main location of the eNOS) fractions were similar between the 2 groups (Figure 4-7B).

Discussion

The novel finding of this study is that short-term RAPA treatment (10d) had a long-term (22w) effect to reduce the renal cortical nNOSα protein abundance, but with increases in the nNOSβ abundance. This may explain why the almost total loss of nNOSα seen in RAPA group was associated with same degree of renal dysfunction as that in CsA group.

In the renal mass reduction model there is a linear inverse relationship between increasing glomerular injury and decreasing renal cortical nNOSα abundance, once glomerular injury exceeds ~20 % (130). Consistent with this finding, CsA-treated allografts developed ~20% of glomerulosclerosis and their nNOSα abundance was maintained. However, the RAPA treated allograft showed marked reduction (near zero) in nNOSα in renal cortex. Based on our 5/6 A/I studies in the SD rat (130) we would expect this to result in massive renal damage and yet the F344 to Lewis RAPA treated allograft showed only ~30% of glomerular injury, suggestive of compensatory changes, perhaps by another nNOS isoform.

Of note, there was no difference in abundance of nNOSα in either skeletal muscle or cerebellum in RAPA compared to CsA treated ALLO rats. Why RAPA specifically inhibits nNOSα protein expression only in renal cortex but not other nNOS abundant tissues is unclear. One possibility is that tubular reabsorption and concentration of RAPA leads to elevated tissue concentrations compared to e.g., skeletal muscle (99) and that the nNOSα isoform may be

particularly sensitive to RAPA. There is no data available on the impact of RAPA on nNOS expression although RAPA induced increases in aortic eNOS protein expression have been reported in Apo E knock out mice (98).

We have identified mRNA and protein of nNOSα and –β in rat kidney as described in chapter 3. Here we demonstrated that ALLO male rats given RAPA showed increases in both nNOSβ mRNA and protein abundance vs. CsA treated male rats. Since NOSβ has ~80% the activity of nNOSα in vitro (20), this suggests that the increased nNOSβ may compensate for the decreased nNOSα activity in response to RAPA. With regard to renal Tx, experimental NOS inhibition worsens injury, while L-arginine supplementation decreases renal damage suggesting that NO plays a protective role (2, 124). Although the RAPA group displayed a moderately higher degree of glomerulosclerosis than CsA group, both groups had similar reduction of renal function. It suggests that the increased nNOSβ compensates for the decreased nNOSα activity to maintain similar renal function in RAPA group vs. CsA group.

In the 2nd series we found that short-term (10 day) intensive endothelial protection (EP) with combined antioxidant and anti-inflammatory treatment at the time of Tx (ISO) has no long-term benefit in terms of structure or function. While much of the chronic renal Tx damage is antigen-dependent, non-immunological mechanisms also contribute (92). Because uninephrectomized Fisher kidneys are functionally, morphologically and immunologically identical to two-kidney controls (6), the injury must come from Tx-induced I/R injury. Not all strains show susceptibility to I/R-injury since ISO kidneys in Brown Norway rats showed normal function and structure at 1 year after Tx (76).

We also found that there was no structure/function protection with EP therapy nor was the long-term increase in renal NADPH-dependent O_2^- production prevented. This contrasts to

studies in ALLO (Fisher to Lewis) where function/structure is improved by short term immunosuppressive/anti-inflammatory treatment to the donor (112). Short term L-Arginine has functional benefit to human ALLO recipients (121). Although the individual agents that we used in this study have been shown to provide short-term renoprotection (1 hr to 9 days) against I/R injury, their long-term effects are unclear. Thus, our findings suggest that the "optimal" donor kidney, in the absence of alloreactivity, does not benefit from EP therapy. There is likely to be benefit from treatment of ALLO in man, particularly where "expanded donor criteria" are used.

Despite similar structural damage there was a lower renal cortex nNOS and eNOS protein abundance in the treated ISO-EP vs. ISO-UN kidneys. Of note, however, the in vitro NOS activity of both soluble and membrane fractions of renal cortex were similar in ISO-EP and ISO-UN. This highlights the complexity of the regulation of NOS enzyme activity which is influenced by many posttranslational modifications as well as by protein abundance. Although the oxidative state is a major regulator of nNOS protein abundance and activity, there was no difference in the amount of O_2^- generated by NADPH oxidase between untreated and treated groups. These findings suggest that EP therapy partially restores NO synthesis and endothelial function so that lower abundance of nNOS and eNOS are required in ISO-EP rat. However, the net renal NOS activity is not improved.

In summary, nNOSα abundance can be maintained in mild Tx-induced CKD in the CsA ALLO and although the RAPA ALLO rats showed almost no nNOSα, increased nNOSβ compensated to limit injury and preserve renal function. In the ISO studies, short term combined antioxidant therapy did not prevent the chronic Tx-induced I/R injury in donor kidneys that were optimally harvested from living donors.

Table 4-1. Functional parameters in Tx and control groups 22 weeks after transplantation

	BW (g)	UprotV (mg/day)	UNOxV (μM/day/100g BW)	PCr (mg/dl)	BUN (mg/dl)	CCr (ml/min/ Kg BW)	BP (mmHg)	TX weight (g)
CsA	451±12	16±2*	1.29±0.10*	0.45±0.04*	30±1*#	5.4±0.3*	63±3*#	2.18±0.10*
RAPA	436±9	37±17	1.45±0.17*	0.49±0.03*	26±1*	5.0±0.3*	79±5*	2.21±0.12*
Control	456±8	36±4	0.81±0.03	0.30±0.02	18±2	7.3±0.5	113±3	1.84±0.14

Values are represented as mean ± SEM. UproV, 24hr urine protein; CCr, 24hr clearance of creatinine; TX, transplanted kidney. *$p<0.05$ vs control, #$p<0.05$ vs. RAPA.

Table 4-2. Weight and renal function measures at 22 wk after kidney transplantation or similar time in control

	ISO-UN	ISO-EP	CON
Body weight (g)	408±15*	396±13*	456±8
Kidney weight (g)	2.20±0.14	2.36±0.16	1.84±0.14
Kidney weight/body weight x1,000	5.36±0.02*	5.96±0.36*	4.07±0.35
Blood urea nitrogen (mg/dl)	23±1*	21±1	18±1
Plasma creatinine (mg/dl)	0.50±0.02*	0.44±0.02*	0.30±0.02
CCr/BW (ml/min/kg BW)	4.3±0.4*	4.6±0.1*	7.3±0.5
UprotV (mg/24hr)	51±9	31±4$^{\#}$	36±4

Values are represented as mean ± SE; abbreviations are: ISO-UN, isograft without therapy; ISO-EP isograft with endothelial protection; CON, time control; CCr, 24hr clearance of creatinine; UproV, 24hr urine protein; *$p<0.05$ vs. CON; $^{\#}p < 0.05$ vs. ISO-UN. Reprinted with permission from S. Karger AG, Basel (134).

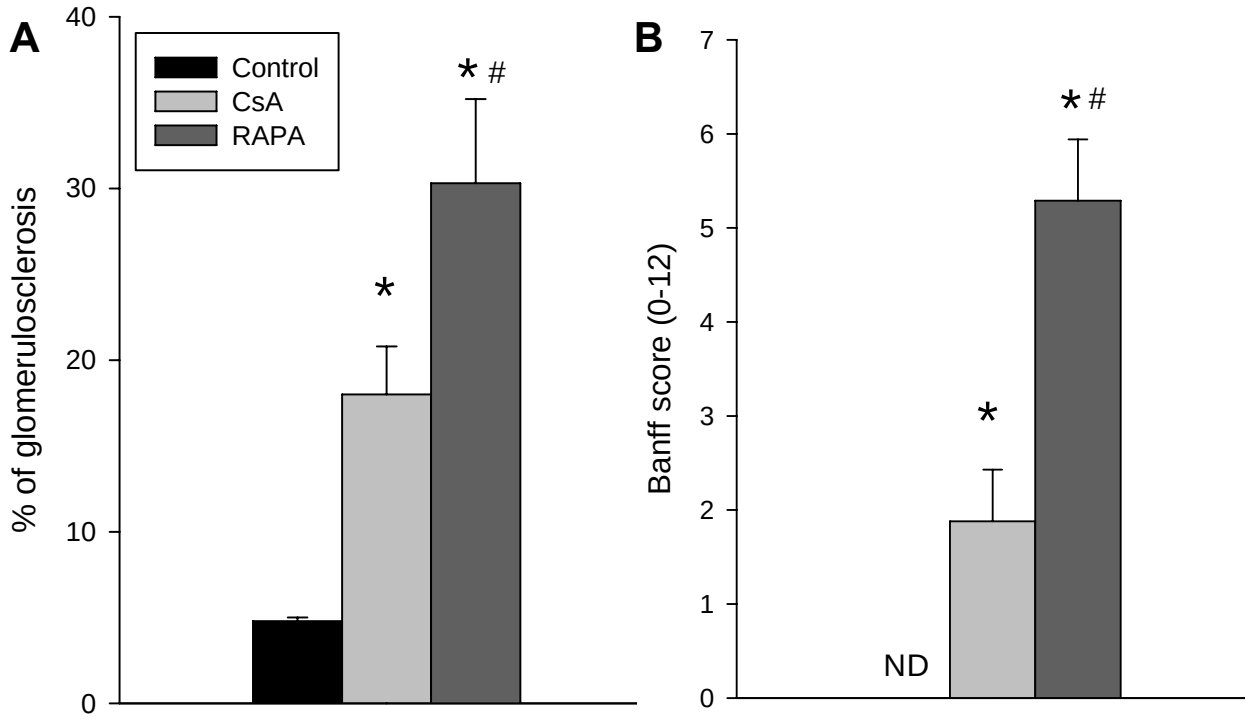

Figure 4-1. Renal outcome in ALLO grafts at 22 weeks after Tx. A) % of Glomerulosclerois. B) Banff score. *p<0.05 vs. control, #p<0.05 vs. CsA.

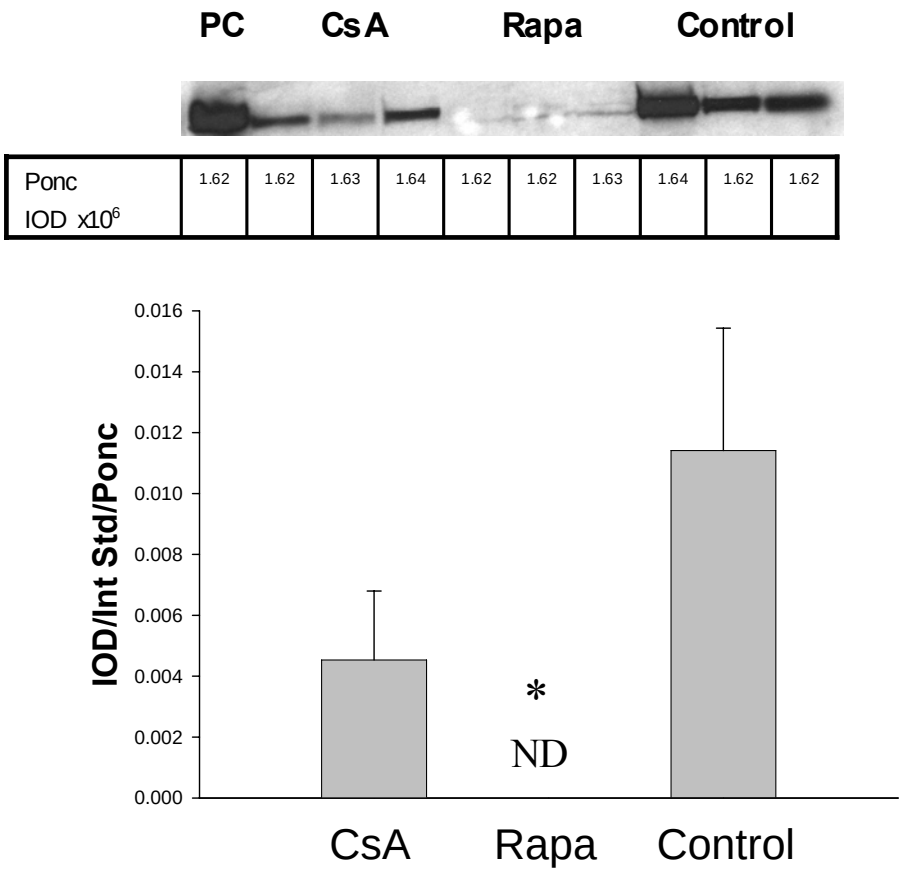

Figure 4-2. Renal cortical nNOSα protein abundance in CsA and RAPA ALLO rats. The molecular weight marker is in the first line. PC represents positive control. The bands were analyzed and represented as integrated optical density (IOD). The Ponc IOD represents total protein loading detected by Ponceau red staining, which shows equal loading in all lanes. The nNOSα protein abundance was factored for Ponc to correct for any variations in total protein loading and for an internal standard (Int Std). ND represents not detectable. *$p<0.05$ CsA vs. RAPA.

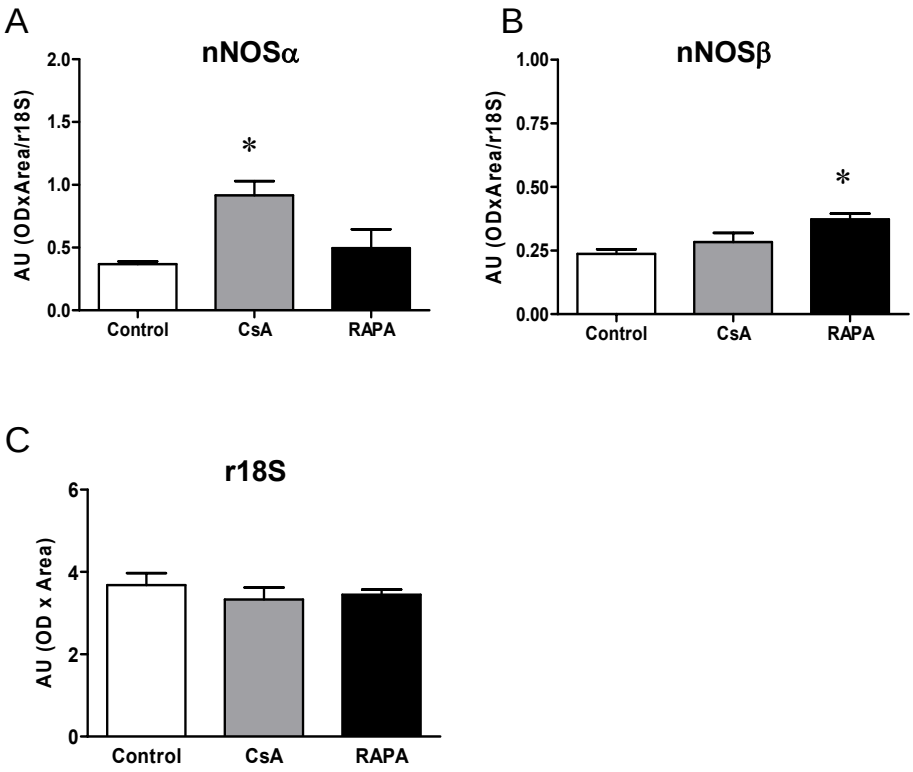

Figure 4-3. Renal cortical nNOSα and nNOSβ mRNA abundance in CsA and RAPA treated ALLO male rats and controls (n=5 in each group). A) nNOSα. B) nNOSβ. C) The r18S was used as an internal standard. *$p<0.05$ vs. control.

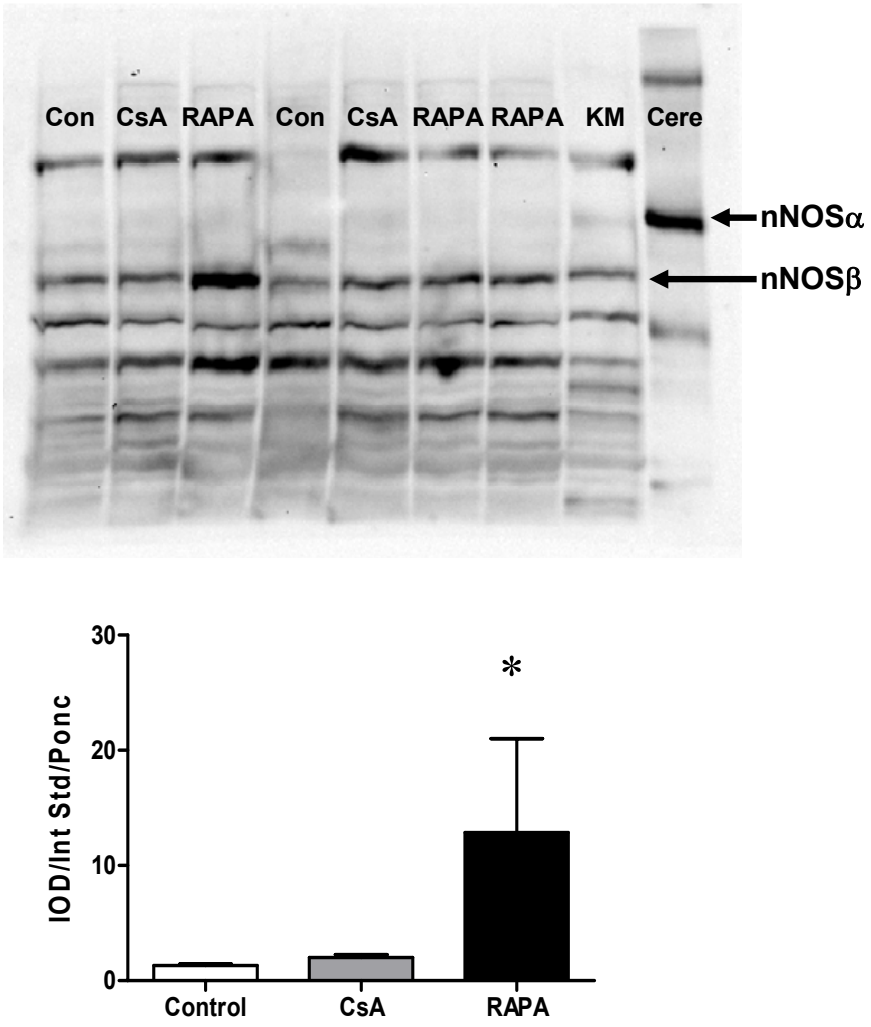

Figure 4-4. Renal cortical nNOSβ protein abundance in CsA and RAPA treated male rats and controls. A) Representative western blot whole membranes show nNOSα band (~160 kDa) and nNOSβ band (~140 kDa). Cere represents cerebellum used as positive control for nNOSα. KM represents kidney medulla used as positive control for nNOSβ. B) Densitometry (n=5 in each group). *$p<0.05$ vs. control.

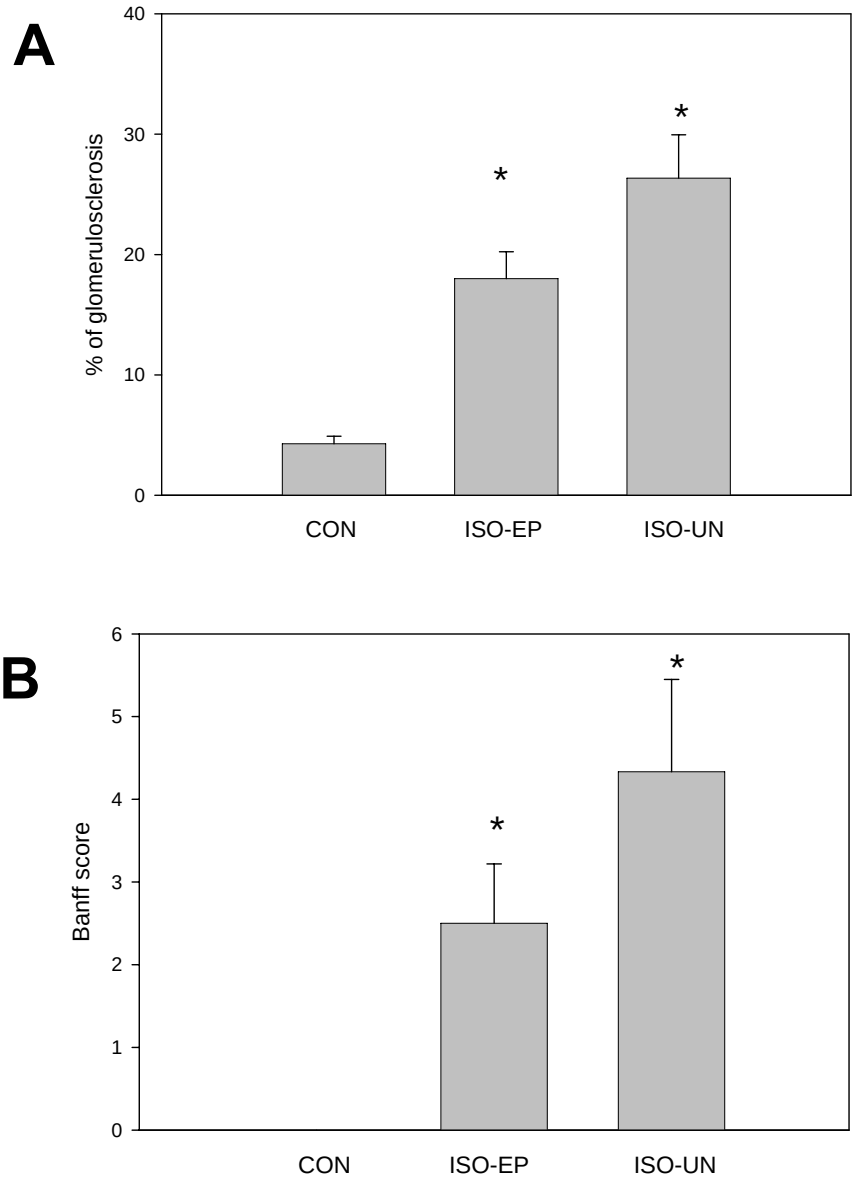

Figure 4-5. Renal pathology at 22 wk after kidney transplantation. A) % of glomerulosclerosis. B) Banff score (0-12). *$p < 0.05$ vs. CON. Reprinted with permission from S. Karger AG, Basel (134).

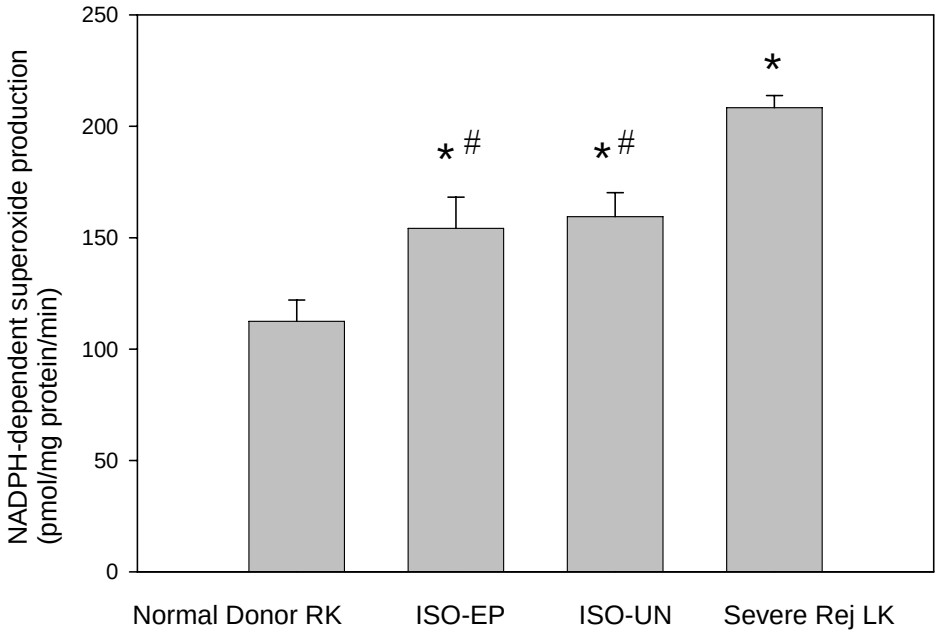

Figure 4-6. NADPH-dependent superoxide production of ISO-UN, ISO-EP, and acutely rejecting allografts and the control kidneys. *$P < 0.05$ vs. normal donor RK; $^{\#}P < 0.05$ vs. severe rejection LK. Reprinted with permission from S. Karger AG, Basel (134).

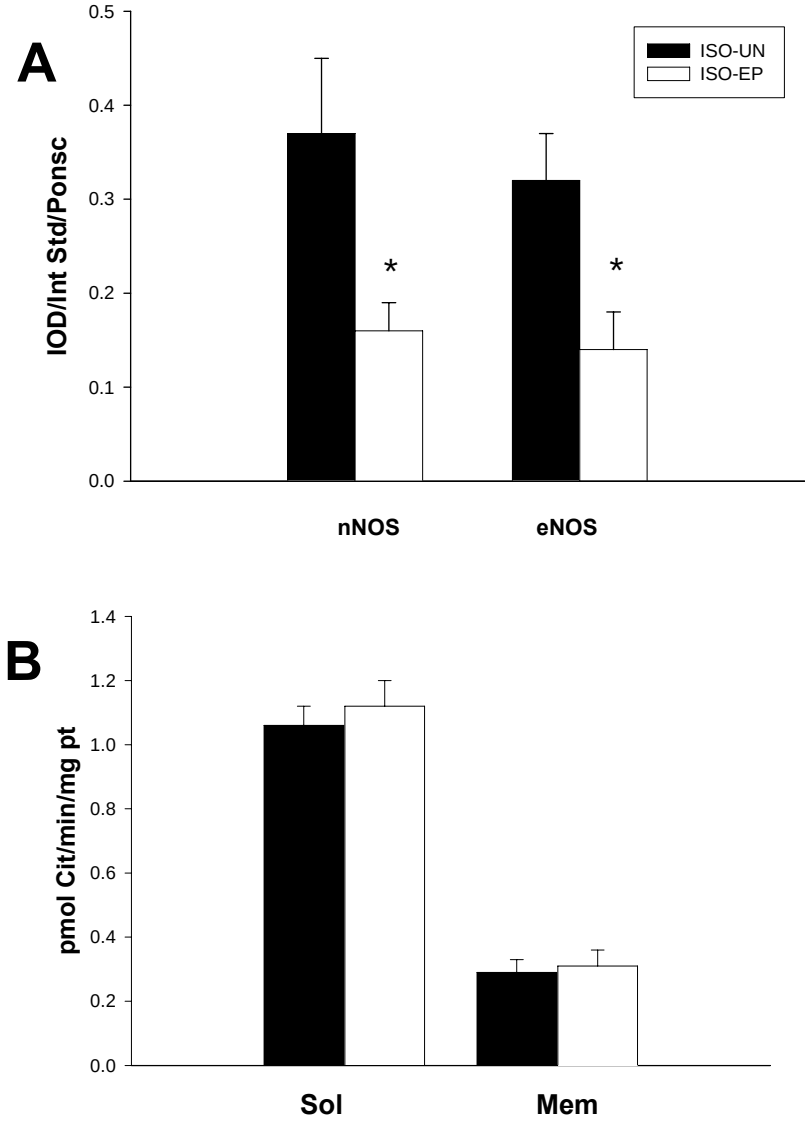

Figure 4-7. NOS protein abundance and activity in ISO-UN and ISO-EP rats. A) Relative abundance of renal cortex neuronal (nNOS) and endothelial nitric oxide synthase (eNOS). B) *In vitro* NOS activity in the soluble (Sol) and membrane fraction (Mem) of cortical homogenates. *$P < 0.05$ vs. ISO-UN. Reprinted with permission from S. Karger AG, Basel (134).

CHAPTER 5
DETERMINATION OF DIMETHYLARGININE DIMETHYLAMINOHYDROLASE ACTIVITY IN THE KIDNEY

Introduction

Dimethylarginine dimethylaminohydrolase (DDAH) metabolizes the methylarginines asymmetric dimethylarginine (ADMA) and N^W-monomethyl-L-arginine (L-NMMA), to generate L–citrulline, and is highly expressed in the kidney (84). ADMA is elevated in many systemic diseases, including renal failure, possibly due to impaired renal DDAH activity.

Dimethylarginine dimethylaminohydrolase activity can be measured by rate of substrate (e.g., ADMA) consumption but these assays are time consuming and costly (61, 87). A colorimetric method that detects L-citrulline production can also be used providing that 1). Other pathways that generate or remove L-citrulline are inactivated and 2). Interfering compounds have been removed.

Here, we have optimized the Prescott-Jones method (109) using diacetyl monoxime (DAMO) derivatization of the ureido group in L-citrulline to form color that has been adapted to a 96-well format (73). Particular attention was paid to nonspecific color generation by urea (46). Furthermore, we compared this modified L-citrulline assay to the direct HPLC method measuring rate of ADMA consumption.

Materials and Methods

Male Sprague Dawley rats from Harlan (Indianapolis, IN, USA) were used. Tissues were collected after perfusion with cold PBS and stored at –80°C. Protein concentration was determined by Bradford assay. Tissue homogenate was adjusted to the concentration of 20mg/ml. Several pilot studies were conducted to optimize the assay including evaluation of homogenization buffer, deproteinization reagents and other pathways if citrulline metabolism.

Optimization of Homogenization Buffers

We tested 4 different homogenization buffers: HB1, pH=6.8 which contained 20 mM Tris, 1% Triton X-100, 5 mM EDTA, 10 mM EGTA, 2mM DTT, 1 mM sodium orthovanadate, 0.1 mg/ml phenylmethylsulfonyl fluoride, and 10 μg/ml leupeptin and aprotinin; HB2 contained 0.1M sodium phosphate, pH=6.5 containing 2mM 2-mercaptoethanl; HB3 contained 0.1M sodium phosphate, pH=6.5; and HB4 was RIPA buffer (Santa Cruz Biotechnology, Santa Cruz, CA, USA), which contained 20 mM Tris, pH=7.6, 137mM sodium chloride, 0.2% Nonidet P-40, 0.1% sodium deoxycholate, 0.02% SDS, 0.0008% sodium azide, and protease inhibitor cocktail.

L-citrulline, sulfosalicylic acid, trichloroacetic acid, sulfuric acid, antipyrine, sodium nitrite and urease were purchased from Sigma. ADMA and diethylamine NONOate (DEA NONOate) were purchased from Cayman, 2,3-Dimethoxy-1,4-naphthoquinone (DMNQ) was from AG Scientific Inc., N^{W}-Hydroxy-nor-L-arginine (nor-NOHA) was from Calbiochem. Diacetyl monoxime was from Fisher. The 96-well polystyrene plate and thermo resistant sealing tape were from Costar Corning Inc.

In pilot studies, in the presence of 25μM L-citrulline, we tested the effect on background color of 4 different homogenization buffers (HB1-4) and the following common additives: 0.1M sodium phosphate buffer (pH=6.5), 1% Triton X-100, 1M HEPES, 0.3M sucrose, 100nM urea, 0.9% NaCl, 0.1M DTT, 1% 2-mercaptoethanol, 0.5% Tween, 1% SDS, 0.5M EDTA, and 0.2M EGTA. 0.1M sodium phosphate buffer, pH=6.5 containing protease inhibitors (0.1 mg/ml phenylmethylsulfonyl fluoride, and 10 μg/ml leupeptin and aprotinin) was examined for the effect of protease inhibitors on color formation. We also determined whether protease inhibitors were required for stability of DDAH in this assay. We found that protease inhibitors were not required and that the simple HB3 gave optimal color. Other reagents, 1mM ADMA and 4% sulfosalicylic acid, used in this assay were also examined for their impact on color formation.

The effect of protein content was tested by using BSA and kidney homogenate at the concentrations of 1 and 2 mg/ml. Serial diluted L-citrulline standards (0-100 μM) were prepared in distilled water. All samples were analyzed in triplicate. The contribution of buffer/additive to color formation was represented as percent of mean absorbance of each sample compared to 25μM L-citrulline (=100%). The findings from these pilot studies were used to optimize the assay for kidney tissue.

Optimization of Deproteinization

One mM ADMA in sodium phosphate buffer 0.1M, pH=6.5 were prepared for use as substrate. 4-20% sulfosalicylic acid, 4% sulfuric acid, and 1N hydrochloric acid were prepared as deproteinization solutions. As shown in Table 5-1, in the absence of deproteinization the absorbance was very high (due to detection of protein-bound L-citrulline and increased turbidity) and the optimum deproteinization solution (giving the minimal absorbance was 4% sulfosalicylic acid). L-citrulline standard solution was made by adding 17.5mg of L-citrulline to 1000ml sodium phosphate buffer to make 100μM standard, used as stock solution. Oxime reagent (0.8%) was made by adding 0.8g of diacetyl monoxime in 100ml of 5% (v/v) acetic acid. This solution was stored in the dark at 4°C. Antipyrine/H_2SO_4 reagent (0.5%) was made by adding 0.5g antipyrine in 100ml of 50% (v/v) sulfuric acid. 1mM and 0.1mM DMNQ was prepared as superoxide donor; 1mM and 0.1mM sodium nitrite and DEA NONOate were used as NO donors; 0.01mM, 0.1mM, and 0.5mM nor-NOHA was prepared for inhibition of arginase.

Tests for Other Pathways That Could Alter Citrulline Concentration

It is theoretically possible that citrulline could be simultaneously consumed by the ASS/ASL enzymes that are abundant in kidney. We incubated kidney homogenate with excess citrulline (200μM) in the absence of ADMA (n=4). At incubation time was 0 and 90min, 0.5ml

of 4% sulfosalicylic acid was added for deproteinization and assayed. We found citrulline formation at t=0 and 90 min were similar, suggesting no citrulline consumption.

The activity of the NOS enzymes (which can also generate citrulline) was automatically inhibited by the presence of a high concentration of ADMA, as well as the lack of essential cofactors (NADPH, FMN, FAD, BH_4 etc). When the assay had been optimized for kidney we also investigated the impact of NO and superoxide (using DEA NONOate, nitrate, and DMNQ) on DDAH activity. Kidney homogenate was pre-incubated with urease at 37ºC for 15min, then 400ul of mixture of ADMA and drugs were added to the homogenate and incubated at 37ºC for 45min.

To determine the inter- and intra-assay variability we ran supernatant of kidney cortex (which after deproteinization could be stored at -80ºC and remained stable after 1 freeze/thaw cycle) in 12 different assays and 9 times in one assay.

Recommended assay procedures are summarized in Table 5-2. A time course study was conducted with pre-incubation of urease with homogenates of rat kidney cortex, liver, cerebellum, and aorta, then incubation with 1mM ADMA from 0 to 120min. We also investigated the impact of NO and superoxide (diethylamine NONOate, sodium nitrate, and 2,3-Dimethoxy-1,4-naphthoquinone, DMNQ) on DDAH activity.

Comparison of Citrulline Assay and Asymmetric Dimethylarginine Degradation by High Performance Liquid Chromatography

We compared the rate of L-citrulline production by DDAH with the rate of ADMA degradation at t=0, 30, 45, 90 and 120min. In this study 400 µl of 1mM ADMA was mixed with the 100µl of kidney homogenate (20mg/ml) and 100µl of the mixture was collected for HPLC analysis of ADMA at the various times, given above. ADMA (and L-arginine) levels were

measured in tissue homogenate using reverse-phase HPLC with the Waters AccQ-Fluor fluorescent reagent kit as described in chapter 2.

Statistical Analysis

Data are presented as mean ± SEM. The effects of arginase inhibitor, NO and superoxide were compared by unpaired t test. The correlation between L-citrulline formation and ADMA consumption was analyzed by Pearson correlation coefficient.

Results

Optimization of Citrulline Assay

The enzyme is saturated at between 100 μM and 1 mM substrate (ADMA) and we therefore use 1mM ADMA in all studies. We compared 4 different homogenization buffers and found sodium phosphate buffer, pH=6.5, was without effect on color formation (Table 5-3). Without deproteinization both BSA and the kidney homogenate caused turbidity. 4% sulfosalicylic acid gave the lowest blank absorbance and was used for deproteinization (Table 5-1). With deproteinization, there was no background color with BSA although the kidney homogenate still had high color, suggesting the presence of interfering factors.

Effect of Urea on Citrulline Assay

As shown in Figure 5-1, the high background color seen in the deproteinized kidney homogenate was reduced by >95% at t=15min after incubation with urease. Added urea: 1, 5, 10, 50, and 100 mM gave color equivalent to ~21, 49, 106, 195, and 221 μM L-citrulline, respectively but gave no background color at t=0 when pre-incubated with urease for 15 min.

After pre-incubation with urease, citrulline production in kidney and other tissue homogenates incubated with 1mM ADMA was linear from 0 to 120 min (Figure 5-2). Without urease treatment, the high background color due to urea obscures DDAH-dependent L -citrulline formation until ~ t=45min (Figure 5-3). We used a 45min incubation in subsequent studies.

Comparison of Dimethylarginine Dimethylaminohydrolase Activity Measured by Citrulline Accumulation with Asymmetric Dimethylarginine Consumption

In kidney cortex the rate of production of L-citrulline = 0.3976μM / g protein/min and the corresponding rate of consumption of ADMA =0.4378μM /g protein/min are similar (Figure 5-4), suggesting that this assay gives a faithful measurement of DDAH activity.

Tests for Other Pathways That Could Alter Citrulline Concentration

Further, when we measured the rate of ADMA degradation under the same assay conditions, we found that at t=0, 30, 45, 90 and 120min the L-arginine concentration was stable (89, 85, 87, 85, and 91 μM respectively), suggesting no net synthesis of arginine. This constancy of L-arginine also suggested that arginase activity was not active under the conditions of this assay, a finding confirmed by the lack of effect of the arginase inhibitor (nor-NOHA; 0.01 – 0.5mM) when incubated with urease treated kidney homogenate for 45min (Figure 5-5). The renal cortex and medulla DDAH activity was 0.39±0.01 (n=15) and 0.30±0.01 (n=3) μM/g protein/min, respectively. Inter- and intra-assay coefficient of variation are 5.61±0.28 % (n=12) and 4.82±0.19 (n=9). The NO donors and superoxide donor inhibited DDAH activity (Figure 5-6).

Discussion

We have used the Prescott-Jones method to measure kidney DDAH activity from rate of L–citrulline production and found: Urea markedly raises background and must be removed; deproteinization is essential and the choice of deproteinization method influences background color; the modified method correlates well with rate of ADMA consumption, and both superoxide and NO, known to inhibit DDAH activity, produce declines in rate of L–citrulline formation in kidney homogenates.

Knipp and Vasak (73) adapted the Prescott-Jones assay to a 96-well plate method for measurement of activity of the purified DDAH enzyme. However, in complex tissues there may be agents that reduce or increase color development and alter L–citrulline metabolism. Of particular note, the development of color is not specific for L-citrulline but also occurs with urea (46) and there is a urea concentration gradient in kidney (~4mM in cortex and ~20mM in inner medulla) (114). Even in renal cortex, urea accounts for more than 90% of baseline absorbance, and therefore obscures DDAH-induced changes in color due to citrulline formation. In the presence of urease, the effect of urea (up to 100mM) can be completely removed from kidney cortex and medulla. Kulhanek et al. (78) reported that urease treatment was not required for citrulline assay in liver and brain. Our results, however, demonstrate that where urea concentration is measurable, urease should be used. Although the urea effect can be prevented by initial ion-exchange chromatography (103), this is more costly and time consuming compared to urease.

Another difficulty is that the DAMO reagent can detect protein-bound L-citrulline as well as free L-citrulline. Although no separate protein-removing step was required in the purified enzyme system (73), in tissues, protein precipitation is mandatory. We found that 4% sulfosalicylic acid gave lowest background.

Buffer/additives also influence color development, for example 2-mercaptoethanol (in HB2) reduces color formation which might explain our observation of a higher renal DDAH activity than a previous study using HB2 (68). Without urease treatment, the high background color due to urea obscures DDAH-dependent L -citrulline formation until ~ t=45min, which might also explain the longer incubation time used previously (26, 126, 162).

In addition to DDAH, ornithine carbamoyltransferase (OCT) and NOS generate L-citrulline. In this assay, activity of both enzymes can be ignored since OCT is not detectable in kidney and 1mM ADMA used as substrate is a potent NOS inhibitor. On the other hand, L-citrulline can be converted to L-arginine by argininosuccinate synthase (ASS) and lyase (ASL). However, in tissue homogenate citrulline consumption by ASS & ASL requires added aspartate (110) and ATP and we found no citrulline consumption under the conditions of our assay. Furthermore, arginases, which might indirectly increase L-citrulline consumption by increasing rate of L–arginine utilization (28), are not active since arginase inhibition did not affect L-citrulline formation and there was no L-arginine consumption.

Both oxidative and nitrosative stress have been reported to inhibit DDAH activity (71, 82) and in this study we show that both superoxide and NO donors have an acute inhibitory action on renal cortex DDAH activity, measured from L–citrulline production.

In conclusion, this colorimetric assay of L-citrulline accumulation is a simple and inexpensive method optimized for detection of renal tissue DDAH activity in vitro, which agrees well with the more costly and time consuming method of measuring ADMA consumption. This can also be adapted for other tissues, even with low activity such as cerebellum, but should be optimized prior to use.

Table 5-1. Effect of deproteinization reagents on absorbance of blank

	Absorbance
2mg/ml kidney homogenate without deproteinization	1.114±0.275
Sulfosalicylic acid	
4%	0.227±0.006
10%	0.254±0.023
Trichloroacetic acid	
10%	0.790±0.016[a]
20%	1.332±0.085[a]
Sulfuric acid 4%	0.355±0.022
Hydrochloric acid 1N	0.357±0.011

All measurements were analyzed in triplicate.

[a] The supernatant was opalescent.

Reprinted with permission from Nature Publishing Group (132).

Table 5-2. Effect of buffers and additives on the L-citrulline assay in the presence of 25μM L-citrulline

	L-citrulline μM	Color as % of control
Homogenization buffer[a]		
HB1	17.0±0.8	68
HB2	<Minimal	<1
HB3	24.9±0.6	100
HB4	>100[c]	464
Buffer base		
1% Triton	13.0±0.9	52
1M HEPES	27.5±0.4	110
0.3M sucrose	>100	500
0.9% normal saline	24.6±0.6	98
0.1M sodium phosphate	24.9±0.6	100
100mM urea	>100	1419
Additives		
0.1M DTT	>100	384
1% 2-mercaptoethanol	<Minimal	<1
0.5% Tween	22.2±1.0	89
1% SDS	22.3±3.7	89
0.5M EDTA	25.6±3.0	102
0.2M EGTA	33.6±0.6	134
1mM ADMA	22.2±0.8	89
Protease inhibitors[b]	23.2±0.3	95
4% sulfosalicylic acid	28.2±1.0	113
Protein		
1 mg/ml BSA	33.6±2.8[c]	134
2 mg/ml BSA	43.3±7.8[c]	173
1 mg/ml kideny homogenate	76.3±12.1[c]	305
2 mg/ml kidney homogenate	>100[c]	415
Protein with deproteinization		
1 mg/ml BSA	26.1±0.8	107
2 mg/ml BSA	25.7±0.8	103
1 mg/ml kidney homogenate	63.4±1.1	253
2 mg/ml kidney homogenate	82.6±1.2	330

The values reflect effect of an additive on the color generated by a 25μM L-citrulline standard (taken as 100%).

[a] HB1, pH=6.8 contained 20 mM Tris, 1% Triton X-100, 5 mM EDTA, 10 mM EGTA, 2mM DTT, 1 mM sodium orthovanadate, 0.1 mg/ml phenylmethylsulfonyl fluoride, 10 μg/ml leupeptin and aprotinin; HB2 contained 0.1M sodium phosphate, pH=6.5 containing 2mM 2-mercaptoethanl (66); HB3 contained 0.1M sodium phosphate, pH=6.5; and HB4 was RIPA buffer (Santa Cruz), containing 20 mM Tris, pH=7.6, 137mM sodium chloride, 0.2% Nonidet P-40, 0.1% sodium deoxycholate, 0.02% SDS, 0.0008% sodium azide, and protease inhibitors.

[b] Protease inhibitors: 0.1 mg/ml phenylmethylsulfonyl fluoride, 10 μg/ml leupeptin and aprotinin. [c] The supernatant was opalescent.

Table 5-3. Recommend assay procedures/conditions for the measurement of renal cortical DDAH activity

1. Homogenize tissue with 5X sodium phosphate buffer, pH=6.5
2. Adjust protein concentration to 20mg/ml
3. Pre-incubate urease (100U/ml homogenate) with tissue homogenate in 37°C water bath for 15min
4. Add 100µl sample to 400µl 1mM ADMA in sodium phosphate buffer
   * respective blank is sample omitting ADMA
5. Incubate mixture in 37°C water bath for 45min
6. Stop reaction by addition of 0.5 ml of 4% sulfosalicylic acid
7. Vortex and centrifuge at 3,000g for 10min
8. Add 100µl supernatant into a 96-well plate in triplicate
9. Serially dilute 100µM L-citrulline standard to 0, 3.125, 6.25, 12.5, 25, 50, and 100µM
10. Add 100µl of standard into the 96-well plate in triplicate
11. Mix one part of oxime reagent with 2 parts of antipyrine/ H_2SO_4 reagent to make the "color mixture"
12. Add 100µl of color mixture into the wells
13. Cover the plate with a sealing tape
14. Shake on a plate shaker for 1min
15. Incubate the plate in 60°C water bath for 110 min in the dark
16. Cool the plate in an ice bath for 10min

Reprinted with permission from Nature Publishing Group (132).

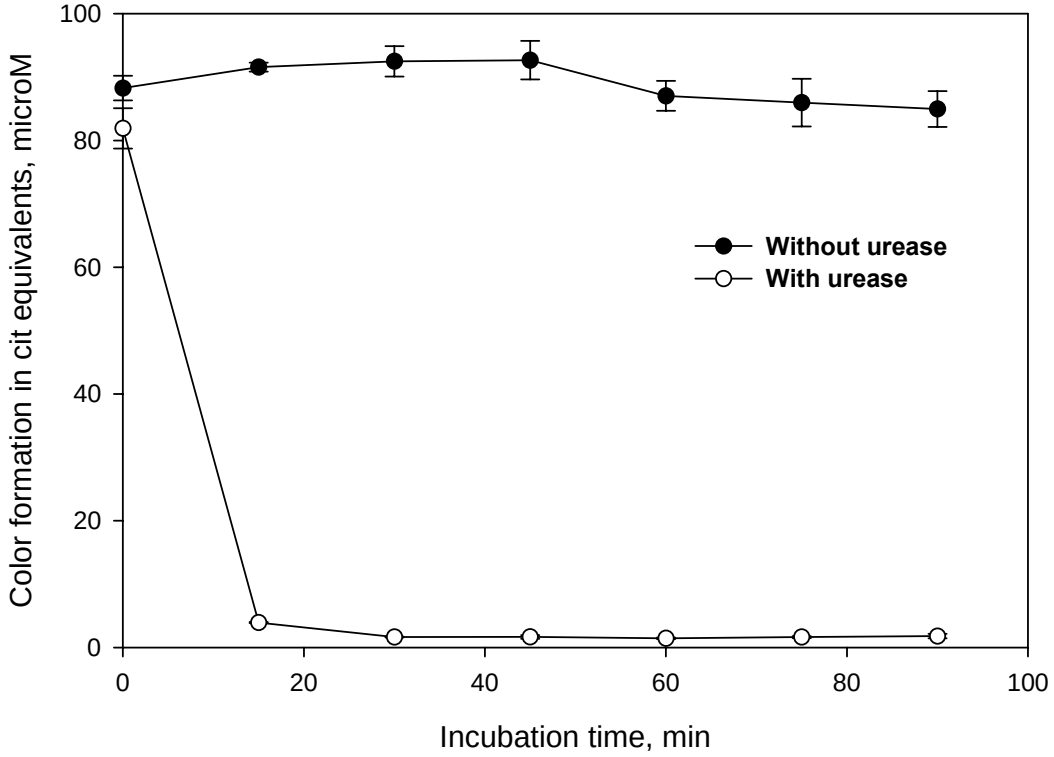

Figure 5-1. Time course of the urea effect on color formation without substrate (ADMA) in the absence (solid circle) and presence of urease (open circle). Each time point determined in triplicate. Reprinted with permission from Nature Publishing Group (132).

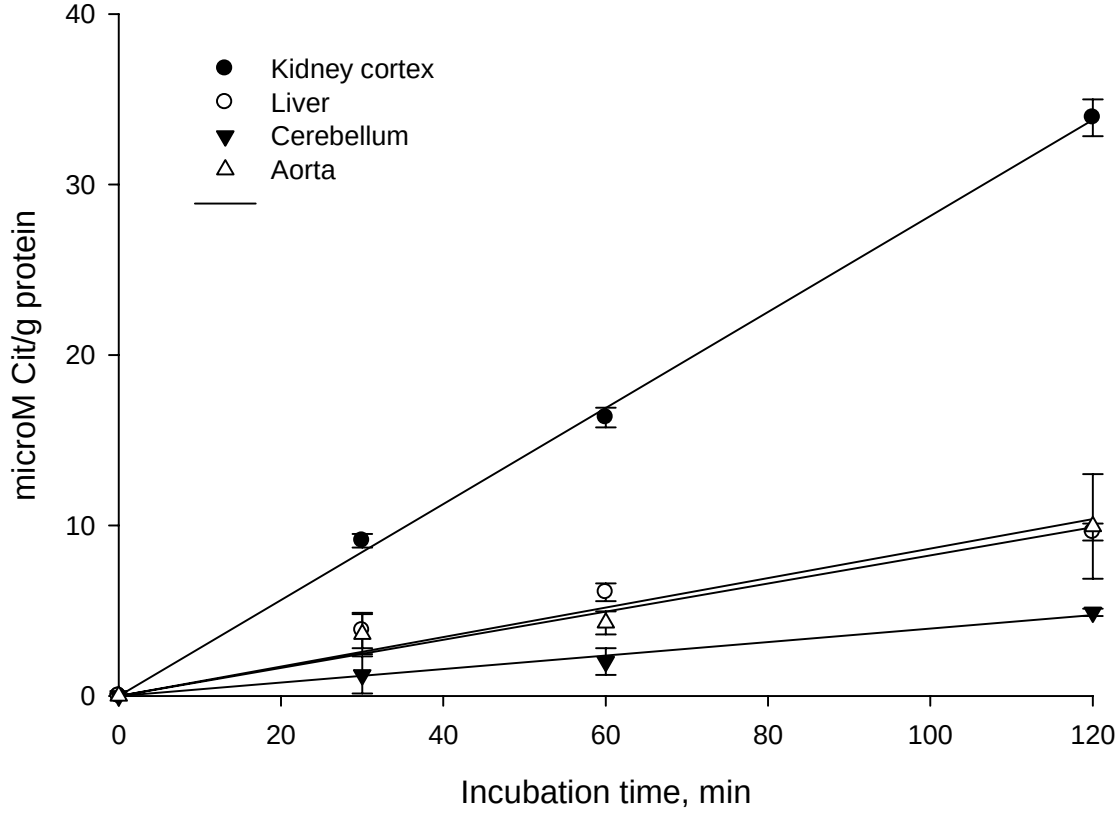

Figure 5-2. Time course of DDAH activity in different rat tissues: kidney cortex (solid circle), liver (open circle), cerebellum (inverted solid triangle), and aorta (open triangle). Each time point determined in triplicate. Reprinted with permission from Nature Publishing Group (132).

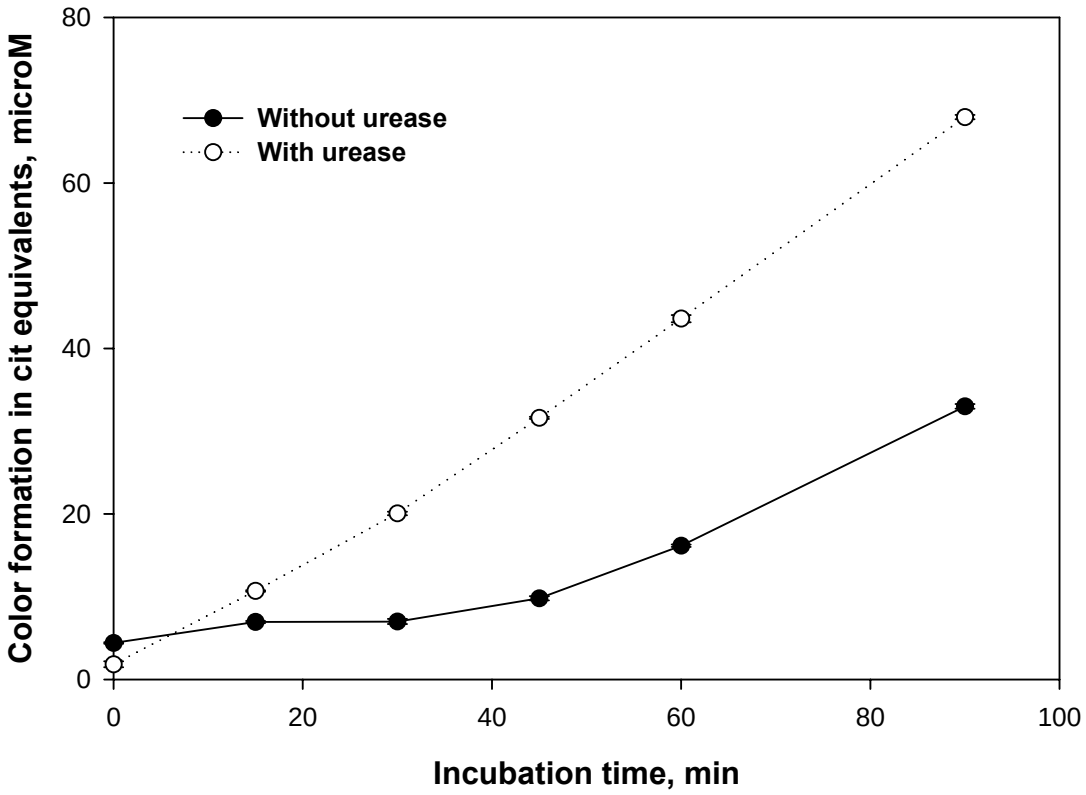

Figure 5-3. Time course of color formation in citrulline equivalents in the presence of the DDAH substrate (ADMA) in the absence (solid circle) and presence of urease (open circle). Each time point was determined in triplicate. Reprinted with permission from Nature Publishing Group (132).

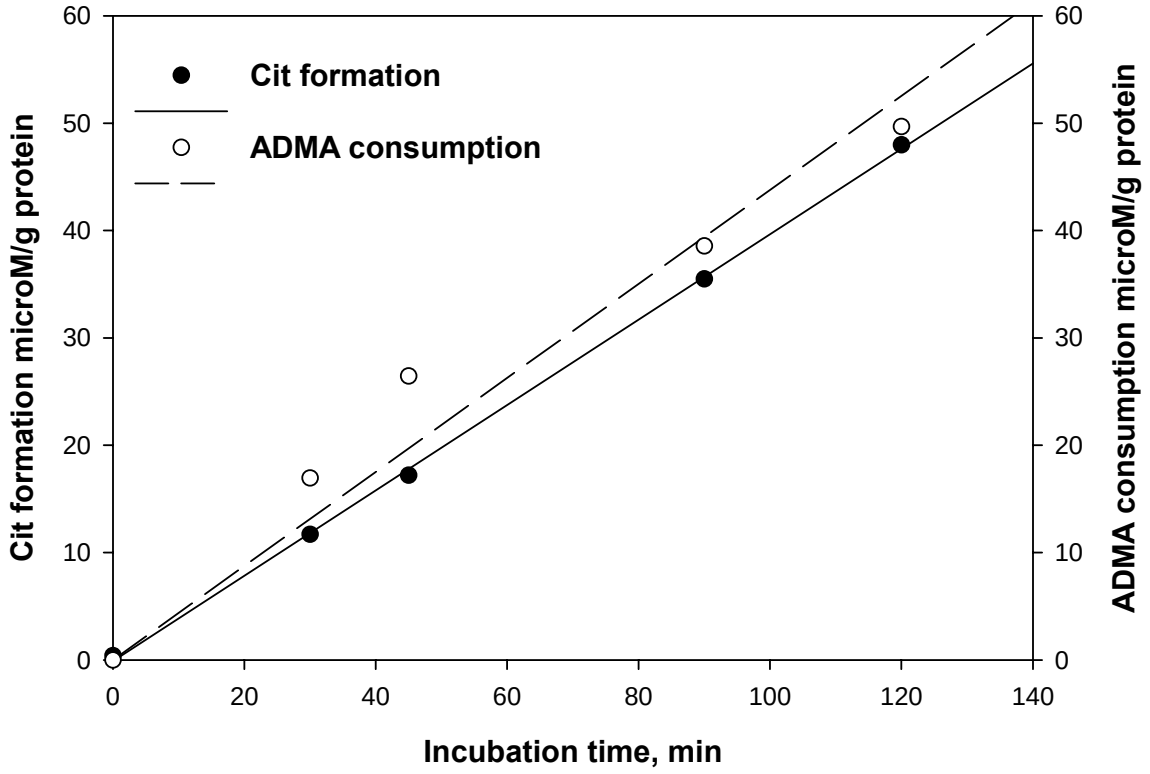

Figure 5-4. Correlation of L-citrulline formation as a measure of DDAH activity (solid circle, solid line) with the rate of ADMA consumption (open circle, dashed line). Reprinted with permission from Nature Publishing Group (132).

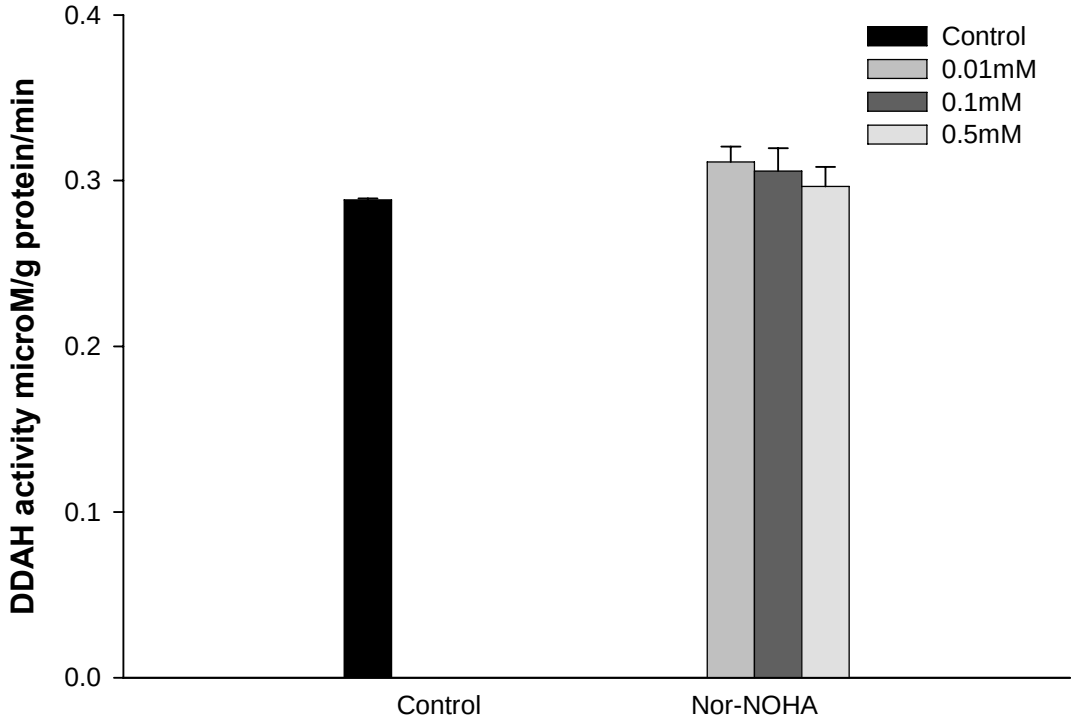

Figure 5-5. The effect of arginase on the L -citrulline assay to detect renal DDAH activity. Nor-NOHA was used as arginase inhibitor. All measurements were analyzed in triplicate. Reprinted with permission from Nature Publishing Group (132).

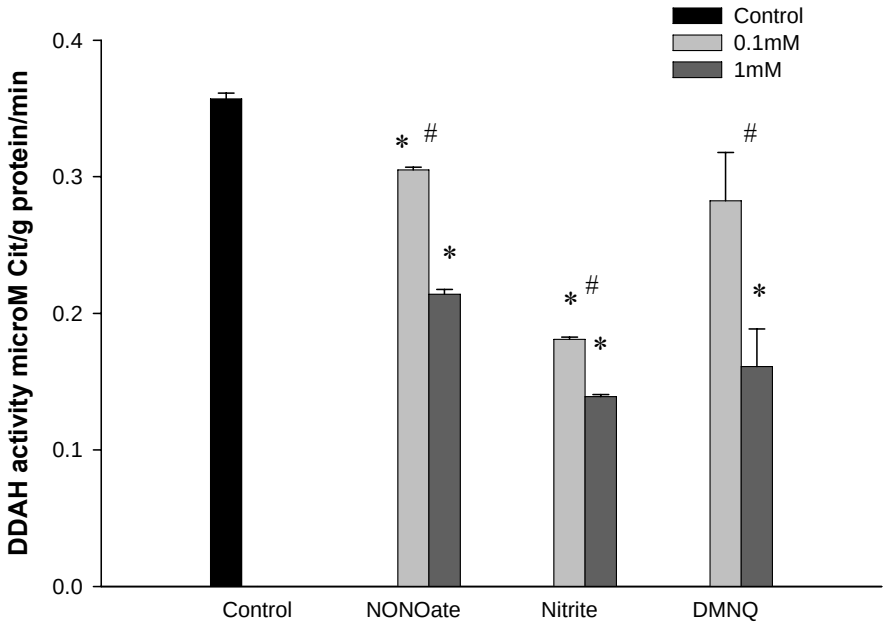

Figure 5-6. The effect of NO and superoxide on the L-citrulline assay to detect renal DDAH activity. DEA NONOate and nitrite were used as NO donors; and DMNQ was used as superoxide donor. All measurements were in triplicate. *$p<0.05$ vs. control; #$p<0.05$ 0.1mM vs. 1mM. Reprinted with permission from Nature Publishing Group (132).

CHAPTER 6
VITAMIN E REDUCES GLOMERULOCLEROSIS, RESTORES RENAL NEURONAL NITRIC OXIDE SYNTHASE, AND SUPPRESSES OXIDATIVE STRESS IN THE 5/6 NEPHRECTOMIZED RAT

Introduction

Chronic kidney disease (CKD) is accompanied by oxidative stress and nitric oxide (NO) deficiency (10, 95). In CKD, oxidative stress results from increased production of reactive oxygen species (ROS) as well as decreased antioxidant enzyme capacity. The major ROS is superoxide and in kidney this is said to be mainly generated by NADPH oxidase (44). NO deficiency in CKD has many causes including inactivation of NO by oxidative stress; inhibition of NOS enzyme activity by increased levels of endogenous inhibitors and in kidney there is reduced neuronal nitric oxide synthase-α (nNOSα) enzyme abundance/activity (10, 95, 150). Because superoxide (O_2^-) and NO have counterbalancing actions and reciprocally reduce each other's bioavailability, an imbalance of NO and superoxide may shift the kidney toward a state of O_2^- dominance causing renal vasoconstriction, enhanced tubular sodium reabsorption, increased cell and extracellular matrix proliferation and CKD progression (95). Therefore, antioxidants have been considered for prevention of CKD progression by reducing oxidative stress and/or preserving NO bioavailability.

Vitamin E is a potent, naturally occurring lipid-soluble antioxidant that scavenges ROS and lipid peroxyl radicals. The most active and predominant form of vitamin E is α-tocopherol and this has been used therapeutically in many conditions although the impact of vitamin E on CKD progression is controversial (5, 19, 22, 45, 50, 69, 111, 147). In this study we investigate the impact of the 5/6 renal ablation model on renal nNOS isoform abundance and also whether the protective effects of vitamin E therapy are associated with preservation of renal nNOSα abundance and reduction in NADPH-dependent superoxide generation. The endogenous NOS

inhibitor asymmetric dimethylarginine (ADMA), generated by type I protein arginine methyltransferase (PRMT) and metabolized by dimethylarginine dimethylaminohydrolase (DDAH), is increased in CKD (10). In this study we also determined the impact of vitamin E treatment on the circulating level of ADMA and on PRMT1 abundance as well as abundance and activity of DDAH.

Materials and Methods

Studies were conducted on 17 male Sprague Dawley rats (12 week-old) purchased from Harlan (Indianapolis, IN, USA). Rats were kept under standard conditions and fed rat chow and water ad libitum. All rats had baseline metabolic cage measurements and were subjected to either sham surgery or 5/6 NX. 5/6 NX was performed under isoflurane general anesthesia using full sterile technique. By retroperitoneal approach, 2 poles of the left kidney were removed and then one week later the right kidney was removed. All rats were assigned to the following groups at the time of the first surgery: Group 1 (sham, n=6), sham-operated rats kept on regular rat chow (powdered) and tap water; Group 2 (5/6 NX, n=6), 5/6 NX rats maintained on regular rat chow and tap water; and Group 3 (5/6NX + VitE, n=5), 5/6 NX rats treated with vitamin E supplementation (Sigma Diagnostics, St. Louis, MO, USA) of regular rat chow containing α-tocopherol 5000 IU/kg of chow, begun at the polectomy surgery.

In all rats, 24h urine was collected in metabolic cage for measurement of protein by Bradford method and total NO production (from NOx $=NO_3^- + NO_2^-$) by Greiss reaction every other week after surgery. Rats were followed for 15 weeks after surgery and then sacrificed. At sacrifice, blood pressure was measured via abdominal aorta then an aortic blood sample was collected for measurement of plasma creatinine, ADMA, and NOx levels. The left kidney remnant was perfused blood free with cold PBS, removed and a section placed in 10% buffered formalin for pathology and the remainder separated into cortex and medulla, flash frozen in

liquid nitrogen and stored at –80°C for analysis of NOS protein and superoxide. Plasma and urine creatinine levels were measured by HPLC as described in chapter 2.

eNOS, nNOSα, nNOSβ, PRMT1, DDAH1, and DDAH2 protein abundances were detected by Western blot. ADMA levels were measured in plasma using reverse-phase HPLC with the Waters AccQ-Fluor fluorescent reagent kit as described in chapter 2. Renal DDAH activity was measured by a colorimetric assay measuring the rate of citrulline production, as optimized by us in chapter 5 (132). NADPH-dependent O_2^- production was measured by Electron Spin Resonance (ESR) spectroscopy with hydroxylamine spin probe 1-hydroxy-3-carboxypyrrolidine (CPH) as described in chapter 2. Pathology was performed on 5 micron sections of formalin-fixed kidney, blocked in paraffin wax, stained with PAS.

Statistical analysis: Results are presented as mean ± SEM. Parametric data was analyzed by unpaired t test and 1-way ANOVA. Histologic (non-parametric) data were analyzed by Mann-Whitney U test. $P<0.05$ was considered statistically significant.

Results

As shown in Table 6-1, 5/6 NX + Vit E group had higher body weight (similar to shams) vs. 5/6 NX group at 15th weeks after renal mass reduction, whereas the BWs were similar between all 3 groups prior to surgery (Sham: 429±13g; 5/6 NX: 435±10g; 5/6 NX + Vit E: 449±5g). Left kidney weights and the ratio of KW/BW were higher in 5/6 NX rats than in shams due to compensatory hypertrophy, while values were intermediate in 5/6 NX + Vit E group and were not different from sham. Rats with 5/6 NX remained normotensive and blood pressure was similar in all groups. Plasma creatinine and urine protein excretion were increased similarly, and CCr was similarly reduced, in both 5/6 NX groups compared to sham (Table 6-1). As shown in Figure 6-1, however, the appearance of the proteinuria was delayed by ~2 weeks in the 5/6 NX +Vit E group (week 6) compared to the 5/6 NX rats (week 4). The total number of damaged

glomeruli (all levels of injury) was 10±2 % in shams, which is normal for this strain and age (38, 130), and greater in both 5/6 NX groups (5/6 NX: 40±3 %, $p<0.01$; 5/6 Nx + VitE: 24±2 %, $p<0.01$). The total injury was also greater in the untreated 5/6 NX group vs the 5/6 NX + vit E ($p=0.01$). As shown in Figure 6-2, there were more damaged glomeruli at 1+, 2+, and 4+ levels of severity in the 5/6 NX group vs. sham, while only the 2+ injury severity was greater in 5/6 NX + VitE group vs. sham. In general the severity of injury was intermediate in the 5/6 NX + VitE between shams and 5/6 NX but was significantly less ($p<0.05$) compared to 5/6NX at the 4+ level. The 5/6 NX group also showed increased renal cortex NADPH-dependent O_2^- production vs. sham (Figure 6-3) which was completely prevented by vitamin E therapy.

As shown in Figure 6-4, the 24h UNOxV fell in all groups with time and at 14 weeks after surgery there was a greater reduction in both 5/6 NX groups vs. shams, suggesting that CKD contributed to the reduced total NO independent of the age effect. This was supported by the lower plasma NOx in both NX groups (expressed as a ratio factored for creatinine to eliminate an effect of reduced renal clearance) of 0.12±0.02, 5/6 NX & 0.11±0.01, 5/6 NX + Vit E vs. 0.31±0.06 for shams (both $p=0.01$ vs sham).

By Western blot we found no difference in eNOS abundance in renal cortex and medulla among 3 groups (Figure 6-5A). Further, there was no difference in nNOSα abundance in renal medulla, however, renal cortex nNOSα abundance was lower in the 5/6 NX group than sham, and this reduction was prevented by vitamin E therapy (Figure 6-5B). Using the C-terminal antibody we found that nNOSα is decreased while there is an increased nNOSβ abundance following injury (Figure 6-6)

Both 5/6 NX groups showed similar increases in plasma ADMA concentration (5/6 NX: 0.35±0.06 and 5/6 NX +Vit E: 0.28±0.05 μM, respectively) vs. sham (0.17±0.02 μM, both

$p<0.05$). Renal cortex PRMT1 abundance was higher in both 5/6 NX group vs. sham (Figure 6-7A). We found no difference in DDAH1 and DDAH2 abundance in renal cortex among 3 groups (Figure 6-7B &C), but in contrast, renal cortex DDAH activity was lower in both 5/6 NX groups than sham (both $p<0.05$) and was not influenced by vitamin E treatment (sham: 0.41±0.01; 5/6 NX: 0.34±0.02; and 5/6 NX +Vit E: 0.36±0.02 μM citrulline formation/g protein/min). For the DDAH2 Western blot many non-specific bands were detected. In the presence of neutralizing peptide, however, only the DDAH2 band (~30 kDa) was competed (Figure 6-8).

Discussion

The novel finding in this study is that long-term vitamin E administration prevents the increased NADPH-dependent superoxide generation and reduction in renal cortical nNOS abundance, in the 5/6 NX model of CKD. Since both reduced renal nNOS and increased renal superoxide are viewed as pathogenic in progression of CKD, this likely accounts for the protection against structural damage seen with vitamin E supplementation.

This is the first time we have used the 5/6 NX model of CKD. In this model the right kidney is removed and the 2 poles of the left kidney are cut off leaving a true 1/6 remnant. With 5/6 NX the rat remains relatively normotensive, whereas in the 5/6 A/I model (which involves infarction of 2/3rds of the left kidney, leaving large amounts of scar tissue) BP increases rapidly and exacerbates the CKD due, at least in part, to greater activity of the renin, angiotensin, aldosterone system (60). In the present study we found no difference in BP between shams or 5/6 NX groups although we only obtained a terminal BP, under anesthesia which may not reflect the awake values. However, Griffin et al. (48) used telemetry for conscious BP measurement and also reported that rats with 5/6 NX remained normotensive over 15 wk (48). Another factor that could contribute to the lack of hypertension in the 5/6 NX model, vs. the 5/6 A/I is that

medullary nNOS is unchanged with NX, but fell with A/I (130). There is considerable evidence to suggest that loss of medullary NO can lead to salt sensitive hypertension (131).

The abundance of eNOS in renal cortex was unchanged by 5/6 NX vs. control. In other CKD models renal eNOS abundance is increased, reduced and unchanged depending on the primary insult which suggests that the eNOS varies secondary to the injury (10). In contrast, we observe that the renal cortex nNOS abundance decreased in 5/6 NX – induced CKD as we previously reported in 5/6 A/I (130), accelerated 5/6th A/I (high sodium and protein intake), chronic glomerulonephritis (153), chronic puromycin aminonucleoside- induced nephrosis (PAN) (38), diabetic nephropathy (37), and aging (40). This reinforces our hypothesis that renal cortex nNOS abundance is a primary marker of renal injury (130).

The treatment arm of this study involved antioxidant therapy with Vitamin E (α-tocopherol) given in the diet (5000 IU/kg chow). In previous studies this dose has been shown to significantly increase plasma α-tocopherol levels in 5/6 NX rats at 6 weeks and in the aging rat after 9 months of treatment (111, 151). We observed that the treatment with vitamin E significantly reduced the degree of kidney structural damage in the 5/6 NX rats. This is in agreement with earlier studies that showed a reduction in glomerulosclerosis with vitamin E therapy in 5/6 NX rats (50, 151). However, there was no improvement in renal function, as assessed by 24h CCr and this also agrees with other observations where vitamin E did not improve renal function in the renal mass reduction models after 2-3 weeks (22, 48). Although slightly delayed in appearance, the proteinuria was not reduced by vitamin E despite the concurrent reduction in severity and extent of glomeruluosclerosis. This perhaps reflects the relatively mild protective effect of vitamin E at this time point. Nevertheless, prevention of structural damage is of benefit and long term (9 months) high dose vitamin E supplements were

able to improve structure, decrease proteinuria, and improve function (111). Importantly, this was achieved without increased mortality. It should be noted, however, that a meta-analysis of 136,000 subjects in 19 clinical trials suggested that high-dosage (> 400 IU/d) vitamin E supplements increased all-cause mortality in man (94); limiting the utility of this therapy in man.

Our rationale for use of vitamin E therapy was based on its known antioxidant properties and the protective effects on CKD progression are presumably by decreasing oxidative stress. Vitamin E acts as a scavenger of ROS/RNS and lipid peroxyl radicals and most studies on CKD have measured lipid peroxidation products or antioxidant enzymes (48, 111, 147). Lipid peroxidation is certainly a marker of redox imbalance due to excess superoxide but could be associated with either decreased or increased NO bioavailability. Measurement of antioxidant enzyme activity/abundance can be misleading since both decreased (presumably primary) and elevated (presumably secondary, compensatory) changes have been correlated to oxidative stress in CKD (106). Because NADPH oxidase is the major source of ROS in kidney (44), we used NADPH-dependent superoxide production as a marker of oxidative stress. A previous study reported that renal NADPH oxidase expression increased in 5/6 NX rats (151) and our data confirm this. The novel finding in the present study is that vitamin E treatment completely prevents this increased kidney cortex NADPH oxidase-dependent superoxide production in 5/6 NX rats. While conventional wisdom holds that vitamin E exerts its antioxidant effects by scavenging harmful radicals, it also inhibits protein kinase C dependent events, which include NADPH oxidase assembly (7, 22). As pointed out by Vaziri (150) the best strategy for prevention of oxidative stress is to identify and inhibit the source of the ROS. Thus, in situations where increased NADPH oxidase is the source of damaging ROS, vitamin E is likely to be

highly effective. It is also worth pointing out that the deleterious effects of high dose vitamin E in clinical studies probably relate to its non radical scavenging actions (150).

In addition to reducing NADPH oxidase dependent superoxide production, vitamin E also reverses the decline in renal nNOS abundance. We have repeatedly found that development of renal structural injury in diverse models of CKD is associated with decreases in the renal cortex nNOS abundance (10). Here we again see an association between injury and renal cortex nNOS abundance, in yet another model of CKD, reinforcing our earlier suggestion that cortex nNOS abundance is a marker of renal injury (130) and that decreased nNOS abundance is also a potential mediator of injury. Since in this study vitamin E not only reduces renal cortex superoxide production but also preserves nNOS abundance (and presumably activity), vitamin E helps to restore the local balance between NO and superoxide in kidney. We cannot tell whether vitamin E has a direct action on the nNOS or whether this is a consequence of the injury-prevention.

We used plasma and urine NOx levels as indices of total NO production, and vitamin E did not reverse the reduction in total NO production due to 5/6 NX. In contrast to vitamin E, tempol increased total NO production in this model (151) which may be due to tempol- induced inactivation of superoxide which cannot be directly achieved by vitamin E. Despite the lack of vitamin E effect on total NO production, renal cortical nNOS was restored. It is important to note, however, that renal NO production represents just a small fraction of total NO and we have several times observed dissociation between total and renal NO production in different forms of CKD (37, 38, 41). In fact it is likely that a persistent decline in overall NO generation will occur despite vitamin E therapy since the elevation in plasma ADMA concentration seen in 5/6 NX rats was not prevented by vitamin E.

The lack of reduction of plasma ADMA by vitamin E was unexpected since decreasing ROS should boost DDAH activity and thus lower ADMA (10, 61). Vitamin E was reported to lower ADMA levels in CKD patients (115). However, the renal DDAH enzymes play an important role in ADMA degradation and in this 5/6 NX model it is possible that such severe reduction in renal mass irreversibly impaired ADMA breakdown. Indeed, our data suggest increased ADMA production (secondary to increased PRMT1 abundance) and decreased ADMA degradation (secondary to decreased DDAH activity), which was not prevented by vitamin E therapy. Matsuguma and colleagues have recently reported increased renal PRMT1 gene expression at 12 weeks after 5/6 NX although they also reported decreased DDAH1 and 2 protein expression (90). In contrast to our finding that DDAH1 and 2 protein abundance was unaltered in 5/6 NX rats; however, we do observe decreased renal DDAH activity.

In conclusion, long-term vitamin E therapy reduces structural damage in rats subjected to 5/6 NX and protection is associated with a direct action to inhibit NADPH oxidase-dependant superoxide production. As with other models renal cortex nNOSα abundance was reduced with injury in 5/6 NX rats, and was preserved by vitamin E therapy. However, increased nNOSβ abundance in 5/6 NX rats suggests the upregulation of nNOSβ in response to renal injury. The renoprotective effect of vitamin E is likely via both reducing superoxide production and preserving renal NO generation. However, vitamin E had no effect on plasma ADMA levels and renal ADMA related enzymes.

Table 6-1. Measurements at 15 wk after surgery

	Sham	5/6NX	5/6NX + Vit E
Body weight (g)	533±12	492±15	535±8[#]
Kidney weight (g)	1.50±0.07	2.40±0.14*	2.12±0.43
Kidney weight/body weight (%)	2.82±0.18	4.94±0.40*	3.99±0.86
Blood pressure (mmHg)	91±3	82±8	81±5
Plasma creatinine (mg/dl)	0.38±0.02	2.10±0.62*	1.80±0.41*
CCr/BW (ml/min/kg BW)	6.5±0.4	1.5±0.3*	1.5±0.2*
Proteinuria (mg/24hr)	38±7	72±15*	100±19*

Values are means ± SE; CCr, 24hr clearance of creatinine;
*, $p<0.05$ vs. Sham; [#], $p<0.05$ vs. 5/6NX.
Reprinted with permission from the American Physiological Society (133).

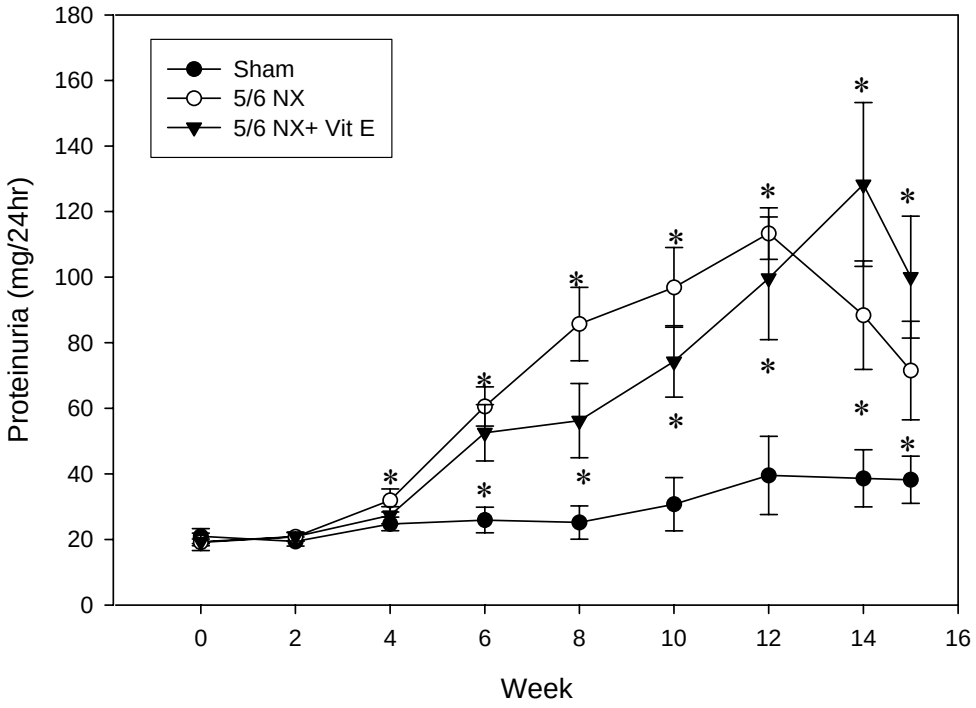

Figure 6-1. Urinary protein excretion at baseline (week 0) and during the 15 wk period after surgery in shams (solid circles), 5/6 NX (open circles) and 5/6 NX + Vit E (closed inverted triangles). *p<0.05 vs. Sham. Reprinted with permission from the American Physiological Society (133).

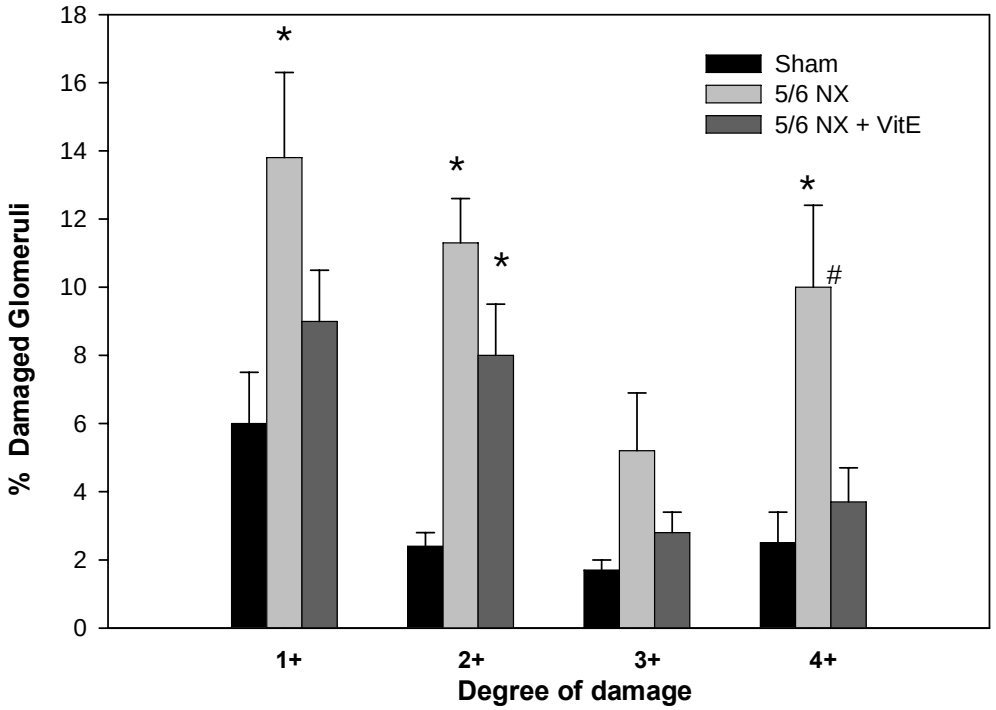

Figure 6-2. Summary of the % and severity of glomerulosclerosis on the 1+-4+ scale 15 weeks after surgery in shams (black column), 5/6 NX (gray column) and 5/6 NX + Vit E (dark gray column). *p<0.05 vs. Sham; # p<0.05 5/6 NX vs. 5/6 NX + Vit E. Reprinted with permission from the American Physiological Society (133).

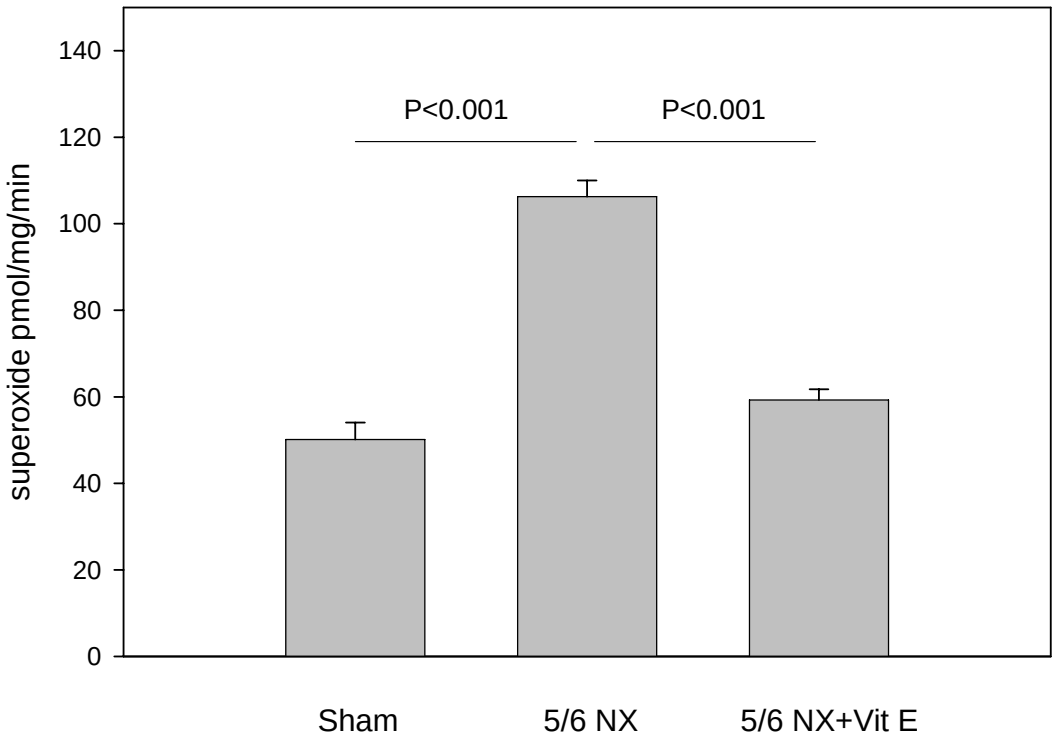

Figure 6-3. Renal cortex NADPH-dependent superoxide production at 15 wk after surgery. Reprinted with permission from the American Physiological Society (133).

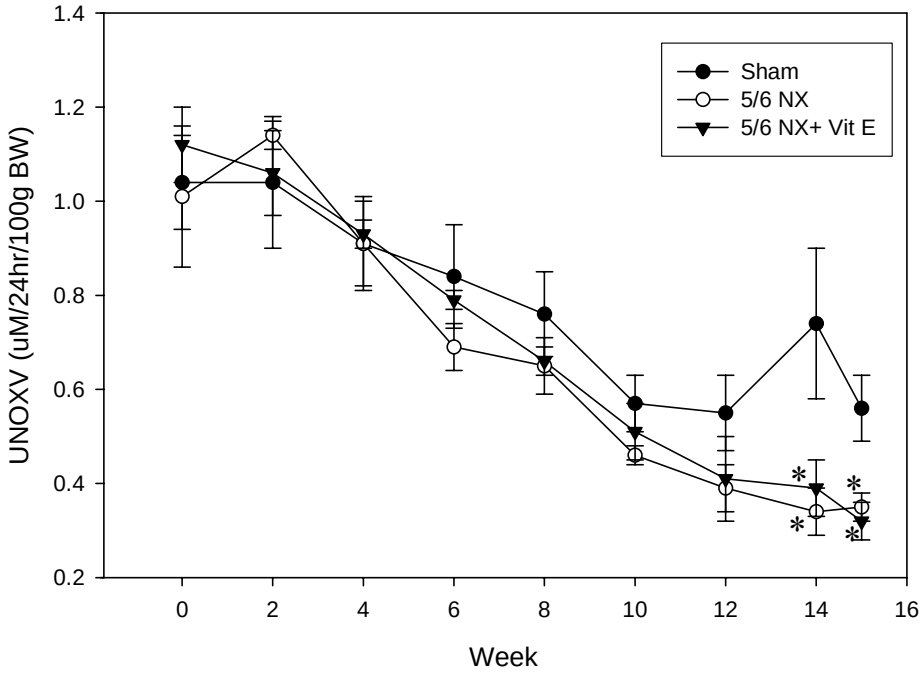

Figure 6-4. Total urinary NOx (NO_3^- +NO_2^-) excretion at baseline (week 0) and during the 15 wk period after surgery in shams (solid circles), 5/6 NX (open circles) and 5/6 NX + Vit E (closed inverted triangles). *$p<0.05$ vs. Sham. Reprinted with permission from the American Physiological Society (133).

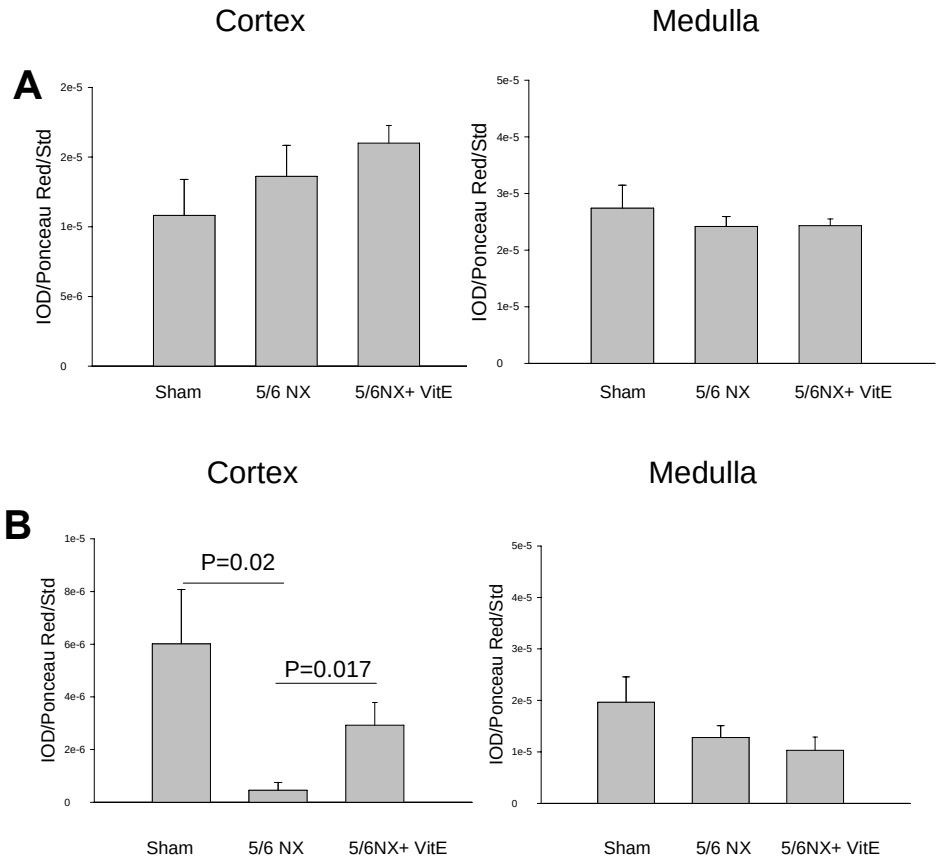

Figure 6-5. NOS protein expression in sham and 5/6 NX rats at 15 wk after surgery. A) Relative abundance of renal cortex and medulla endothelial nitric oxide synthase (eNOS). B) Relative abundance of renal cortex and medulla neuronal nitric oxide synthase (nNOS). Reprinted with permission from the American Physiological Society (133).

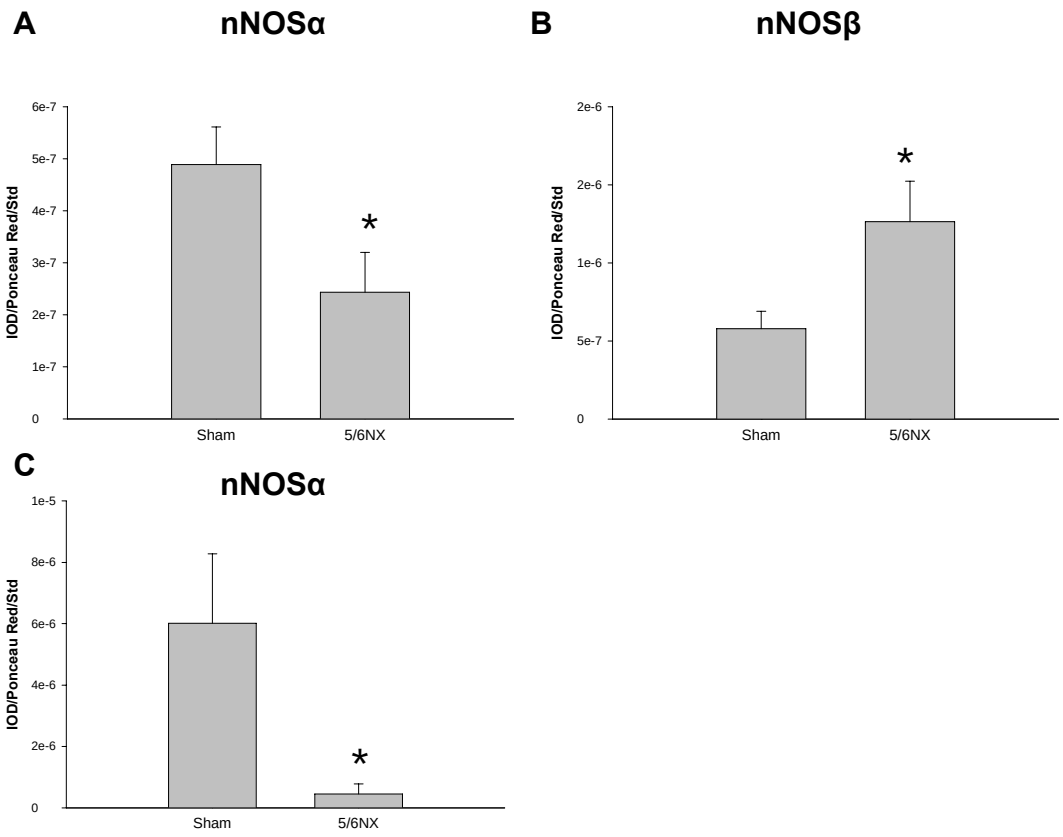

Figure 6-6. Densitometry showing abundance of nNOSα and nNOSβ in renal cortex of sham and 5/6 NX rats studied 15 wks after surgery. A) nNOSα using the C-terminal nNOS antibody. B) nNOSβ using the C-terminal nNOS antibody. C) nNOSα using the N-terminal antibody. *$p<0.05$ vs. sham.

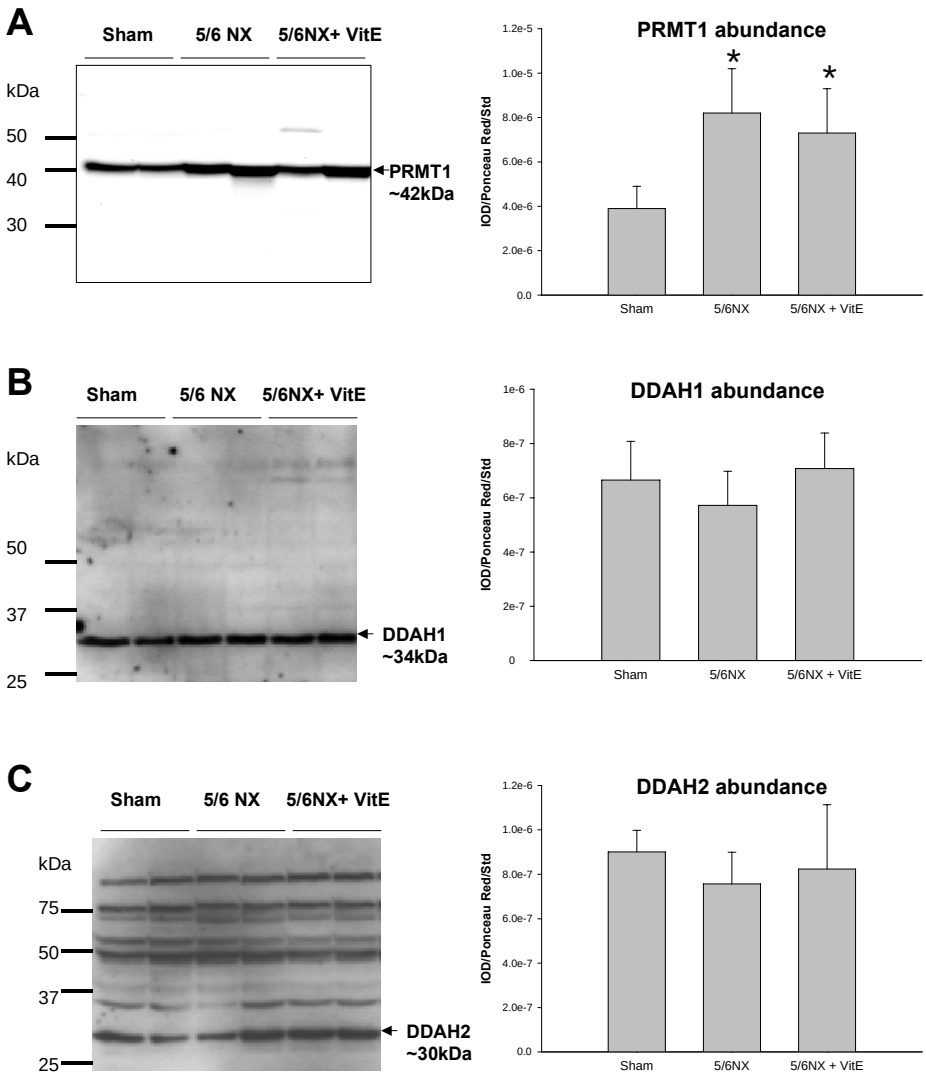

Figure 6-7. ADMA-related enzyme expression in renal cortex at 15 wk after surgery. A) PRMT1. B) DDAH1. C) DDAH2. Representative western blots of whole membranes show PRMT1 (~42kDa), DDAH1 (~34 kDa), and DDAH2 bands (~30 kDa). *$p<0.05$ vs. sham. Reprinted with permission from the American Physiological Society (133).

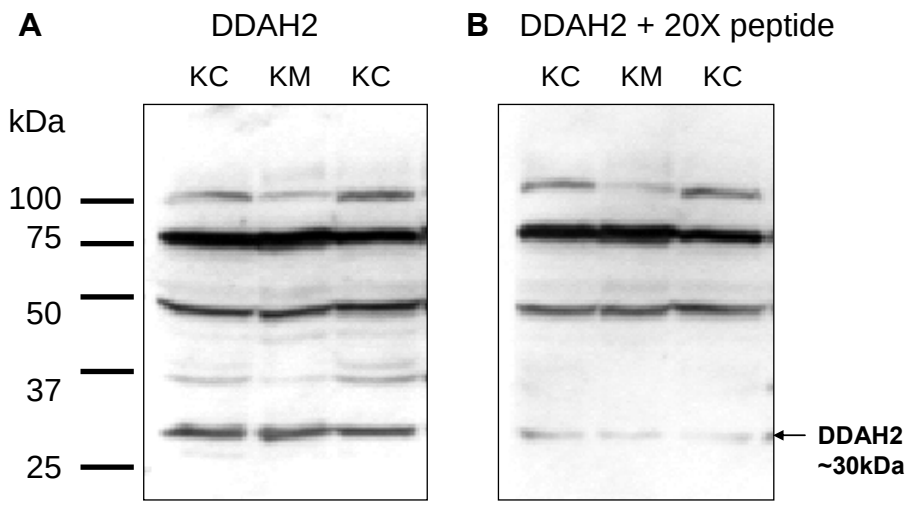

Figure 6-8. Immunoblots of rat kidney cortex (KC) and kidney medulla (KM) with DDAH2 antibody. A) In the absence of neutralizing peptide. B) In the presence of neutralizing peptide. Reprinted with permission from the American Physiological Society (133).

CHAPTER 7
SEX DIFFERENCES IN NITRIC OXIDE, OXIDATIVE STRESS, AND ASYMMETRIC DIMETHYLARGININE IN 5/6 ABLATION/INFARCTION RATS

Introduction

As discussed in previous chapters, nitric oxide (NO) deficiency occurs in humans and animals with chronic kidney disease (CKD) and may contribute to the progression (10). A higher constitutive nitric oxide synthase (NOS) expression was noted in young female rat kidney than that in male and a decrease in NO production in aging male rat but not in aging female (11, 100). This suggests that the ability to preserve renal NO might contribute to the relative protection of females against progression of renal damage.

Possible mechanisms of NO deficiency in CKD include decline in NOS expression, inactivation of NO and NOS by oxidative stress, and inhibition by endogenous NOS inhibitors, such as asymmetric dimethylarginine (ADMA). We found that renal cortical neuronal nitric oxide synthase-α (nNOSα) expression decreased markedly with injury and correlated to decreased NOS activity in various rat CKD models (10), such as the renal mass reduction model, 5/6 ablation infarction (A/I) (130). We have also found that another nNOS isoform, nNOSβ, increases in response to loss of nNOSα in the transplanted kidney and that this may be associated with protection from progression of CKD (chapter 4). In this study we investigated the renal nNOS isoforms, nNOSα and -β in the 5/6 A/I model to determine whether sex-dependent differences in isoform abundance might correlate with the severity of renal injury.

Oxidative stress, another mechanism causing NO deficiency, is associated with the progression of CKD (148). We have shown that vitamin E prevents the increased NADPH oxidase-dependent superoxide (O_2^-) production and reduction of renal nNOS abundance in a 5/6 nephrectomy (NX) model in Chapter 6 (133). Because $p22^{phox}$ is a major regulatory subunit of NADPH oxidase and its expression is correlated to NADPH activity (44), because O_2^- is

converted to hydrogen peroxide by superoxide dismutase (SOD), and because increased ROS causes lipid peroxidation and tissue injury, we have evaluated renal $p22^{phox}$, plasma malondialdehyde (MDA), and urine hydrogen peroxide levels to elucidate the impact of sex on the regulation of reactive oxygen species (ROS) metabolism and NO.

In addition to oxidative stress renal NOS activity can be inhibited by ADMA. Both ADMA and symmetric dimethylarginine (SDMA) are dimethylarginines generated by protein arginine methyltransferases (PRMTs) and PRMT1 is specific for ADMA production. Only ADMA (not SDMA) is metabolized by dimethylarginine dimethylamino-hydrolase (DDAH) in the kidney, liver etc (27). We have previously shown that increased PRMT1 expression and decreased renal DDAH activity were associated with the accumulation of ADMA in 5/6 NX rats (133). Here we investigated the impact of sex on dimethylarginine metabolism in this A/I model.

Materials and Methods

Studies were conducted on 16 male and 15 female Sprague-Dawley (SD) rats from Harlan (Indianapolis, IN, USA) at age 10 to 12 weeks. Rats were allowed ad libitum access to tap water and standard rat chow. A/I surgery was performed by removal of the right kidney and infarction of 2/3 of the left kidney by ligation of branches of the left renal artery. Rats were assigned to the following groups: male sham (N = 6); male A/I (N=10); female sham (N=5), and female A/I (N=10). Rats were sacrificed 7 weeks after surgery. All surgical procedure was done using full sterile technique. Twenty-four–hour urine was collected in metabolic cages for measurement of protein by Bradford method before surgery and every other week after surgery. Total NO production (from 24h urine NOx $=NO_3^- + NO_2^-$) was measured by Greiss reaction before and 7 weeks after surgery. When rats were sacrificed, blood pressure was measured via abdominal aorta and a blood sample was taken for plasma creatinine, L-arginine and dimethylarginines, and NOx levels. A thin section of cortex was fixed in 10% formalin for pathology and the reminder

separated into cortex and medulla and stored at -80°C for later analysis. Plasma and urine creatinine levels were measured by HPLC. Plasma MDA levels were determined by a modified fluorometric method for measuring thiobarbituric acid-reactive substances (TBARS) (157). Urine hydrogen peroxide levels were measured by Amplex Red Hydrogen Peroxide/Peroxidase Assay Kit (Molecular Probes, Eugene, OR). Plasma L-Arginine and dimethylarginine levels were measured using reverse-phase HPLC with the Waters AccQ-Fluor fluorescent reagent kit. More detailed descriptions of these analyses were described in chapter 2.

Western blot was used to analyze nNOSα, nNOSβ, eNOS, PRMT1, DDAH1, DDAH2, and p22phox abundance in kidney and/or other tissues. DDAH activity was measured by a colorimetric assay measuring the rate of citrulline production, as described in chapter 5 (132). Whole blood was centrifuged at 2,000 rpm for 8min and after removal of plasma and buffy coat, RBC was washed by 2ml of normal saline, then lyzed by sonication (Fisher, dismembrator model 100, setting=8) for 3 cycles (10 second sonication and 10 second rest). RBC lysate was centrifuged at 15,000 rpm for 10min at 4ºC, the RBC supernatant was collected and stored in -80ºC freezer until analysis. Tissue was homogenized in sodium phosphate buffer, pre-incubated with urease for 15 min, then 100µl (2mg for kidney cortex and liver; 6mg for RBC) of homogenate was incubated with 1mM ADMA for 45 min (kidney cortex) or 60min (for RBC and liver) at 37ºC. After deproteinization, supernatant was incubated with color mixture at 60ºC for 110 min. The absorbance was measured by spectrophotometry at 466 nm. The DDAH activity was represented as µM citrulline formation/g protein/min at 37ºC. Histology was performed on kidneys and stained with periodic acid-Schiff kit (PAS, Sigma, St. Louis, MO) and examined for level of renal injury.

Statistics: Results were presented as mean±SEM. Data were analyzed by general linear univariate model using gender (Male vs. female) and injury (Sham vs. A/I) as fixed factors, followed by LSD post-hoc test for multiple comparisons. The Kruskal-Wallis and Pearson tests were for correlation, followed by the regression analysis. Gender effect on the reduction of CCr and plasma NOx levels were analyzed by nested ANOVA. $p< 0.05$ was considered statistically significant.

Results

Data of Renal Outcome and Clinical Parameters

As shown in Table 7-1, 7 weeks after A/I males had lower body weight (BW) vs. sham, whereas the BWs were similar in female sham and A/I rats and always lower that the males. Left kidney weight increased in the A/I groups and the left kidney weight to BW ratios were higher in both male and female A/I rats than shams, reflecting compensatory renal hypertrophy. In male A/I rats terminal BP was similar to shams whereas BP was low in sham females and increased in females with A/I. The 24-hour urine protein excretion was not different at baseline (before surgery) between sham and A/I groups within each sex, although males had a greater baseline urine protein excretion than females (male vs. female: 25±2 vs. 3±1 mg/day, $p<0.05$). Urine protein excretion increased in male A/I vs sham as early as the 2^{nd} wk (41±9 vs. 16±2 mg/day, $p<0.05$) and female A/I rats also developed proteinuria which became statistically significant at 6^{th} wk (Table 7-1). The 24h urinary NOx excretion (factored for BW) was lower in females than males in both sham and A/I groups and did not fall significantly with A/I in either group. Plasma NOx (factored for creatinine to correct for differences in renal function) levels were lower in sham females vs males, decreased in both sexes with A/I with a greater reduction in males (63±4 % vs. 54±6 % reduction. $p<0.001$). Plasma creatinine levels increased in both A/I groups, but

less in females. The clearance of Cr (CCr) was lower in sham females than males, was reduced by A/I in both sexes with a greater % fall in males (90±2 % vs. 71±6 %, $p<0.001$) (Table 7-1). The % of damaged glomeruli was significantly increased in both A/I groups, to a lesser extent in female.

Renal Neuronal Nitric Oxide Synthase Isoform Expression

As shown in Figure 7-1A, the nNOSα abundance in cortex was higher in sham females than males and fell significantly in male A/I rats, whereas female A/I rats maintained their nNOSα abundance. To confirm this finding we ran 2 identical membranes probed with two different N-terminal anti-nNOS antibodies (Fig 7-1A, upper panel, Ab from Dr. Kim Lau (76) vs. lower panel, Santa Cruz Ab) and the results were comparable. In contrast, nNOSβ abundance in cortex was very variable in male A/I, tending to increase but only rose significantly in females (Fig 7-1B). The cortical eNOS protein abundance was not different between 4 groups (Figure 7-1C).

Since the rate of progression in the A/I model is quite variable (depending on exact amount of infarct), we looked at the regression relationship between renal nNOS isoform abundance and glomerular damage. As shown in Figure 7-2, the more severe the glomerular sclerosis, the greater the decline in cortical nNOSα abundance ($r = -0.554$, $p=0.001$), but the greater the increase in nNOSβ abundance ($r = 0.408$, $p<0.05$). We found the same general trends when comparing plasma creatinine and nNOS isoforms but the relationships were not so robust (data not shown).

Reactive Oxygen Species Metabolism

As shown in Fig 7-3A, there was no sex difference in renal cortical $p22^{phox}$ in shams and the abundance increased with A/I only in males. Both plasma MDA levels (a marker of lipid

peroxidation) and urine hydrogen peroxide levels were similar in shams of both sexes and increased significantly in male A/I rats but not in females (Fig 7-3B &C).

L-Arginine and Dimethylarginines

As shown in Table 7-2, plasma L-arginine levels were similar in shams and fell significantly in female A/I rats but not in males. There were no sex differences in baseline (sham) values of plasma ADMA and SDMA and the only response to A/I was an increase of SDMA in males. However, the L-arginine to ADMA ratio, a determinant of systemic NO metabolism (13, 15), was significantly decreased in both sexes with A/I and the L-arginine to ADMA ratio correlated directly with plasma NOx levels (Fig 7-4). In kidney cortex, L-arginine and SDMA levels were similar in shams but females had higher baseline ADMA levels vs. males. In response to A/I the L-arginine and ADMA levels in kidney cortex rose significantly in female A/I rats but did not change in males. There was no effect of A/I on renal cortical SDMA levels in either sex. The L-arginine to ADMA ratio in kidney cortex was lower than that in the plasma in all groups. As shown in Table 7-2, the ratio significantly decreased in both sexes in response to A/I injury with a greater reduction in male A/I rats.

Asymmetric Dimethylarginine Related Enzymes

Renal cortex PRMT1 abundance was similar in shams and increased similarly with A/I in both sexes (Figure 7-5A). We also measured PRMT1 expression in the liver and found that female shams had higher abundance than males, and that liver PRMT1 increased in males but not females in response to renal injury (Figure 7-5B). There was no difference in DDAH1 abundance in renal cortex among 4 groups (Fig 7-5C), whereas DDAH2 expression was similar in both sham groups and fell similarly with A/I in both sexes (Figure 7-5D). Despite the similar falls in renal DDAH2 abundance, renal cortex DDAH activity was decreased only in male A/I rats however, absolute renal cortex DDAH activity was similar between the sexes after A/I (Fig 7-

6A). DDAH activity in RBC and liver was lower in female sham than male sham (Fig 7-6B &C), however, female A/I rats maintained DDAH activity, which was significantly decreased in male A/I groups. The RBC DDAH activity was correlated to renal DDAH activity ($r = 0.557$, $p < 0.05$) (Figure 7-7).

Discussion

The novel finding in this study is that decreased nNOSα and increased oxidative stress are associated with the worse renal outcome in male vs. female A/I rats. These sex differences possibly contribute to greater renoprotection of female rats against A/I injury due to preserved renal NO bioavailability.

Sex differences in NOS have previously been observed in rats. Normal male rats displayed lower renal nNOS expression than females (18, 155). In the present study we specifically address the possible sexual dimorphism of the different nNOS isoforms in renal disease. Under baseline (sham) conditions we find that the male rat has lower renal nNOSα abundance than females. This observation is similar to our previous finding in aged female SDs at 20 months of age who show little renal structural damage and preserved nNOSα abundance whereas male SDs have severe injury and marked falls in renal nNOSα (40). In addition, male Wistar Furth (WF) rats are resistant to renal injury induced by A/I and PAN (38, 41), relative to male SD rats and show elevated baseline and only small falls in renal nNOSα abundance in both models of CKD. Also, despite moderate falls in nNOSα abundance, the WF actually also showed maintained or increased NOS activity in the soluble fraction of kidney cortex (38, 39, 41), suggesting that other nNOS isoforms may exist and be recruited in the kidney. At the time these studies were conducted we had not characterized the presence of nNOSα and nNOSβ proteins in the rat kidney and do not have data in the WF on the presence of nNOSβ. However, we have now shown that these 2 isoforms exist in the normal SD kidney cortex (chapter 3) and also in the

transplanted F344 kidney, where we found upregulation of renal cortical nNOSβ with CKD-induced reduction in nNOSα which seemed to be protective (chapter 4). In the transplant study, we demonstrated that nNOSβ is positively correlated with renal injury in contrast to nNOSα. In the present study a strong negative correlation between nNOSα and nNOSβ suggests that an upregulation of renal cortical nNOSβ occurs with A/I-induced reduction in nNOSα.

We also examined several markers of oxidative stress and found that there were no differences between male and female shams although the male A/I rats did exhibit enhanced oxidative stress in response to A/I injury, detected by several measures (renal cortical $p22^{phox}$ abundance, plasma MDA levels, and urine hydrogen peroxide levels) while female A/I rats were resistant to ROS. Several studies have reported that the male SHR produces more systemic ROS compared to the female, that this is testosterone –dependent and contributes to the higher BP in males (42, 127). Whether other strains/species also exhibit a sexual dimorphism in oxidative stress is not certain, although both pro-oxidant actions of testosterone and antioxidant actions of estrogen have been implicated in the cardiovascular protection seen in pre-menopausal women (93, 116). Our study also suggests that there is a sex difference in renal oxidative stress, females protected since p22phox abundance is less in female rat kidney cortex after A/I. A similar finding has been reported in the renal wrap model where there is estrogen-dependent protection of kidney damage associated with decreased NAPDH oxidase activity and decreased renal p22phox (64). Males kidneys are also at increased risk of injury due to oxidative stress in ischemia/reperfusion injury (67), polycystic kidney disease (89) and toxicity due to potassium bromate exposure (144). Our data suggest that increased oxidative stress seen in the males with A/I is associated with decreased nNOSα and that may predict the poor renal outcome in males. This is consistent with our previous study in the male showing increased NADPH oxidase-

dependent O_2^- production and reduction of renal nNOSα abundance in a 5/6 NX model, reversible with antioxidant therapy (133).

Protein turnover results in the release of free ADMA from protein-incoporated ADMA, and two counterbalancing pathways, type I PRMT and DDAH, control free plasma and tissue ADMA levels (146). Regarding ADMA and sex differences, clinical data suggests that in young adult males and females plasma ADMA concentration is similar and that levels increase with age in both sexes but are delayed in the female (122). Otherwise, little is known about sex differences in abundance of ADMA and its' regulating enzymes. In the present study we found no sex difference in sham plasma ADMA levels in young adults although the in vitro red blood cell and liver DDAH activity was lower in females than males. Female shams also had higher PRMT1 expression in liver which would tend to promote increased ADMA formation. Thus, there was no obvious correlation between organ PRMT level/ DDAH levels/activity and plasma ADMA. Similarly, although sham females had higher renal cortical ADMA levels than males, renal PRMT1 and DDAH1 and 2 protein abundance, as well as DDAH activity were similar in sham males and females. Thus, neither renal PRMT nor DDAH expression/activity can predict plasma or kidney ADMA levels.

There is a report that plasma ADMA may be controlled by DDAH activity of the whole blood (13) and DDAH1 expression has been detected in human RBCs (66). We were able to detect DDAH activity in rat RBC and found that it correlates with renal DDAH activity. This may provide a useful tool as a surrogate measure of renal DDAH activity in patients with CKD.

After A/I there was no increase in plasma ADMA level in either sex, which was unexpected given the findings of increased plasma ADMA in end stage renal failure in man, although plasma ADMA is very variable in CKD (10). There was no change in renal ADMA

levels in males with A/I but an increase was seen in females. As in the sham rats, there was no obvious correlation with the abundance of the ADMA regulatory enzymes since renal PRMT1 increased similarly, renal DDAH1 was unchanged and DDAH2 fell similarly in both sexes with A/I and liver PRMT1 increased only in males. It was unexpected that the tissue ADMA level was higher in the "protected" female kidney vs. the male and that the renal and plasma L-arginine/ADMA ratios were similar after A/I in both sexes. Of note, the changes in the L-arginine: ADMA ratio in plasma and kidney in both sexes post A/I reflected both changes in L-arginine as well as ADMA levels.

There is no sex difference in baseline plasma and renal SDMA levels although male A/I rats displayed higher plasma SDMA levels, which were correlated to greater loss of renal function. Our finding is supported by previous studies showing that SDMA is a marker of renal function, which is predictable given that SDMA is excreted unmetabolised in the urine (14). Although SDMA is not a NOS inhibitor, it may compete with L-arginine to enter the cells and cause a decreased NO production (14).

In conclusion, male A/I rats displayed a more rapid CKD progression associated with reduced renal nNOSα abundance and increased oxidative stress. The decreased nNOSα abundance was correlated to increased oxidative stress markers suggesting that oxidative stress may inhibit nNOSα expression in the kidney. Sex differences exist in nNOS expression, oxidative stress, and ADMA metabolism, reinforcing the notion that sex specific treatment may be needed in CKD.

Table 7-1. Renal outcome and clinical parameters

	Male sham N=6	Male A/I N=10	Female sham N=5	Female A/I N=10	p-value
Body weight (g)	431±12	388±7*	250±5$^{\#}$	241±6$^{\#}$	<0.001
Left kidney weight (g)/100g BW	0.43±0.03	0.58±0.03*	0.49±0.05	0.61±0.03*	0.002
Mean arterial pressure (mmHg)	123±10	108±4	88±4$^{\#}$	111±6*	0.01
UprotV (mg/day)	54±25	80±29	4±4	69±16	0.166
UNOxV (μM/24h/100g BW)	0.66±0.10	0.47±0.08	0.24±0.08$^{\#}$	0.07±0.05$^{\#}$	<0.001
PNOx/Cr	0.91±0.05	0.34±0.04*	0.74±0.08$^{\#}$	0.34±0.04*	<0.001
Plasma creatinine (mg/dl)	0.34±0.01	1.18±0.14*	0.30±0.03	0.87±0.08*,$^{\#}$	<0.001
CCr/BW (ml/min/100g BW)	1.25±0.25	0.13±0.03*	0.68±0.19$^{\#}$	0.20±0.04*	<0.001
GS %	6.83±1.34	38.82±3.24*	4.00±1.83	31.18±3.79*,$^{\#}$	<0.001

Values are means ± SEM; UprotV, total urine protein excretion; PNOx, plasma nitrite plus nitrate levels; PCr, plasma creatinine level; CCr, 24hr clearance of creatinine; GS%, total % of damaged glomeruli. *$p<0.05$ vs. sham, $^{\#}p<0.05$ vs. respective male.

Table 7-2. L-arginine and dimethylarginine levels in plasma and kidney cortex

Plasma	N	L-Arginine (μM)	ADMA (μM)	SDMA (μM)	L-Arginine/ ADMA
Male sham	6	117.6±16.6	0.37±0.07	0.26±0.04	328.2±39.5
Male A/I	10	101.1±14.2	0.48±0.06	0.53±0.07*	223.3±22.0*
Female sham	4	150.4±19.5	0.54±0.13	0.35±0.04	322.1±83.4
Female A/I	10	82.4±6.3*	0.46±0.08	0.41±0.05	202.1±18.2*
Kidney cortex		L-Arginine (nM/mg protein)	ADMA (nM/mg protein)	SDMA (nM/mg protein)	L-Arginine/ ADMA
Male sham	5	3.67±0.20	0.09±0.02	0.05±0.00	44.1±7.05
Male A/I	5	3.61±0.34	0.13±0.01	0.07±0.03	29.9±4.79*
Female sham	5	3.90±0.26	0.17±0.02$^{\#}$	0.06±0.01	22.9±1.63$^{\#}$
Female A/I	5	5.14±0.15*$^{\#}$	0.27±0.02*$^{\#}$	0.07±0.00	19.0±0.76*

*$p<0.05$ vs. sham, $^{\#}p<0.05$ vs. respective male.

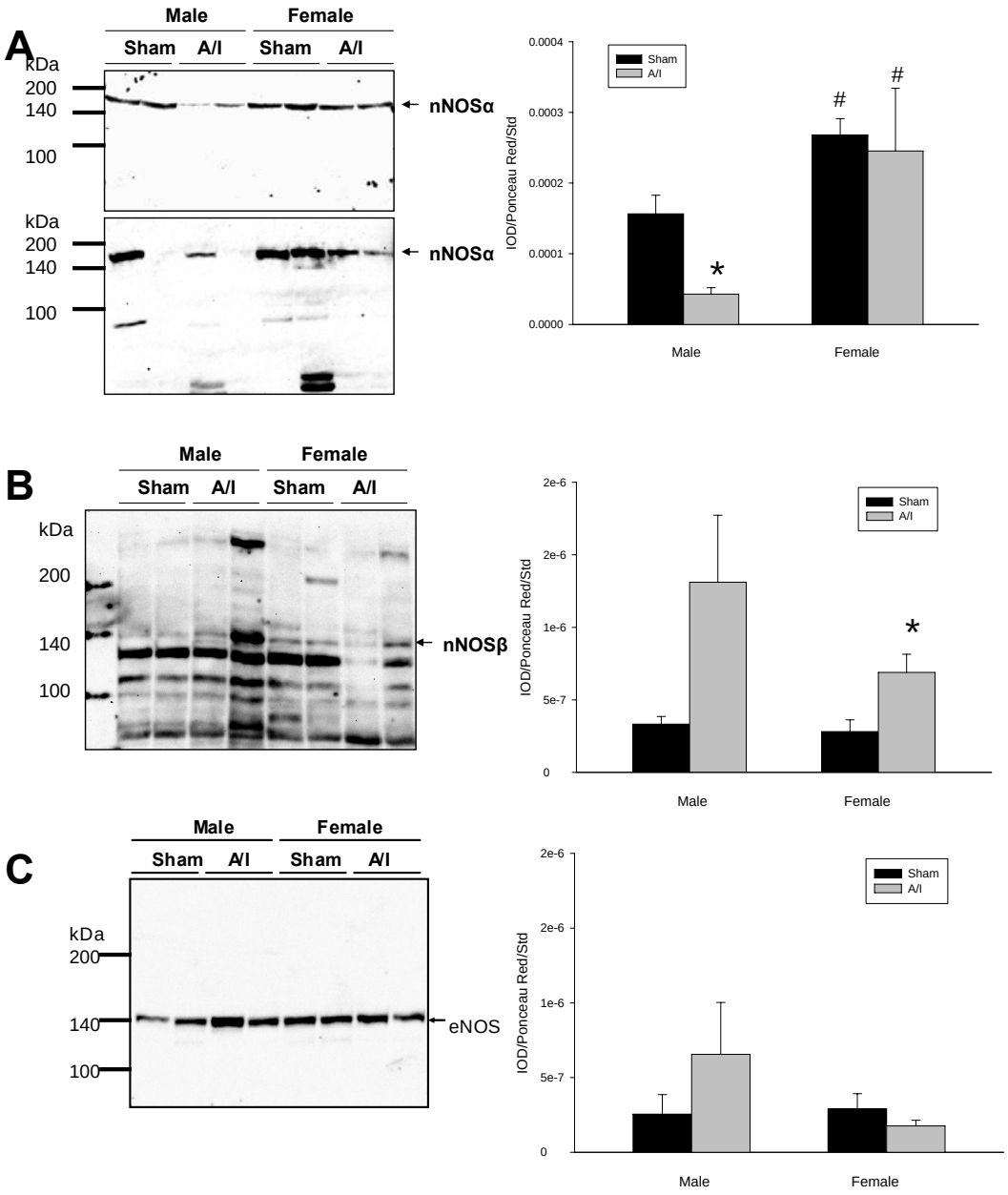

Figure 7-1. NOS isoforms expression in renal cortex. A) Relative abundance of renal cortex neuronal nitric oxide synthase α (nNOSα) by an N-terminal anti-nNOS Antibody (Kim Lau). Representative whole membranes show the nNOSα (~160 kDa) band by 2 different N-terminal nNOS antibodies: Kim Lau antibody (upper panel) vs. SC nNOS antibody (lower panel). B) Relative abundance of renal cortex neuronal nitric oxide synthaseβ (nNOSβ). C) endothelial nitric oxide synthase (eNOS). Representative membranes show nNOSβ (~140 kDa) and eNOS bands (~150 kDa). *p<0.05 vs. sham; #p<0.05 vs. respective male.

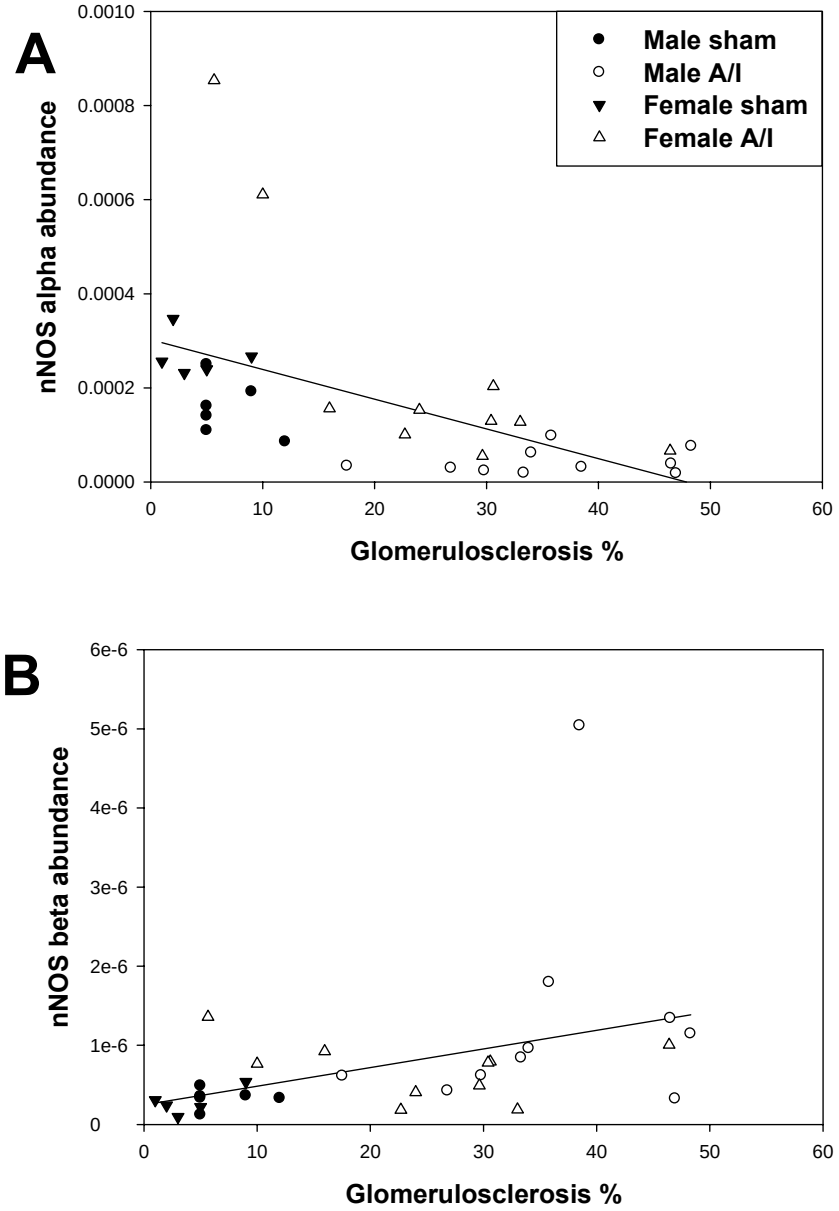

Figure 7-2. Correlation between glomerular damage and nNOS isoform abundance. A) Relative abundance of cortical neuronal nitric oxide synthaseα (nNOSα; r= -0.554, p=0.001). B) nNOSβ (r= 0.408, p<0.05).

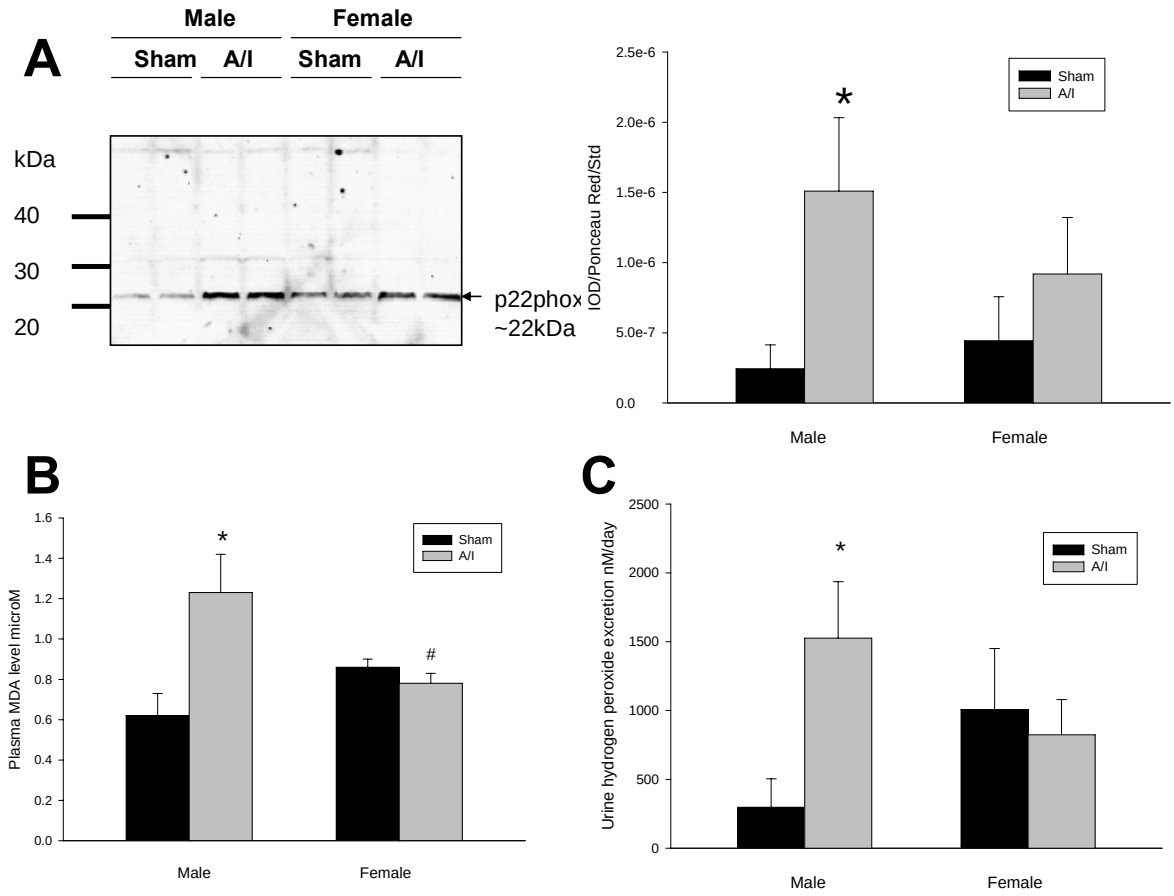

Figure 7-3. Biomarkers of oxidative stress in sham and A/I rats at 7 wk after surgery. A) Relative abundance of renal cortical $p22^{phox}$.Representative western blot shows $p22^{phox}$ bands (~22 kDa). B) Plasma MDA levels (a marker of lipid peroxydation). C) Urine hydrogen peroxide levels. *$p<0.05$ vs. sham; #$p<0.05$ vs. respective male.

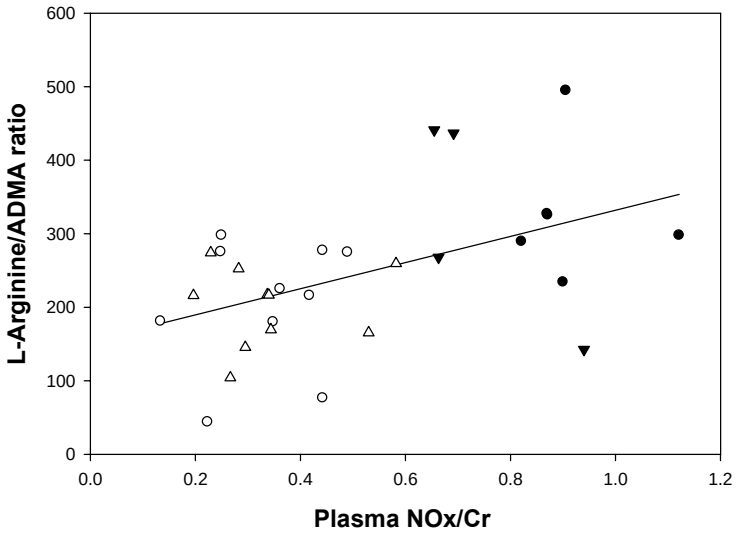

Figure 7-4. Correlation between L-arginine to ADMA ratio and plasma NOx levels (r= 0.574, p=0.001).

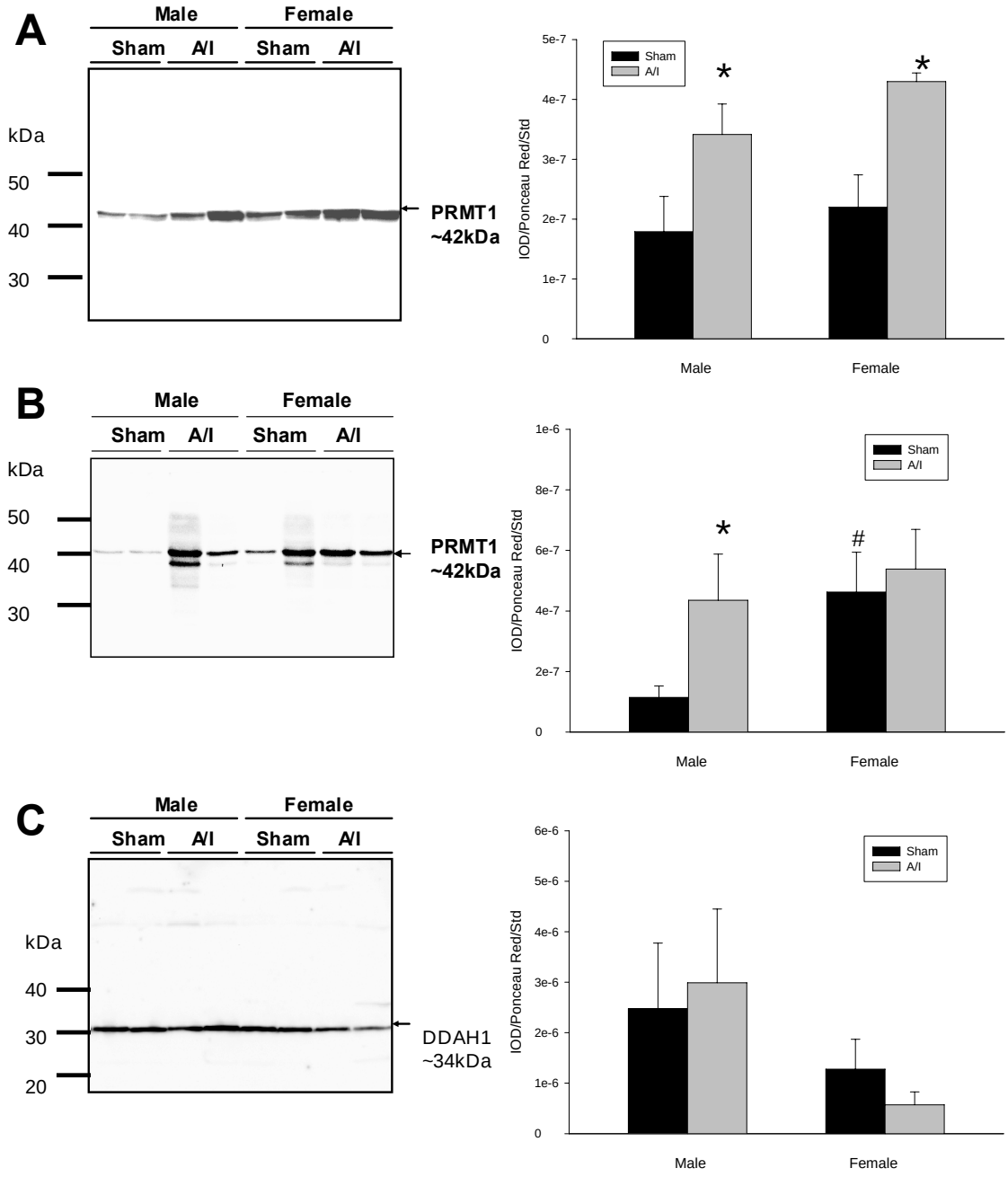

Figure 7-5. ADMA-related enzyme abundance in sham and A/I rats at 7 wk after surgery. A) Relative abundance of PRMT1 in renal cortex. B) PRMT1 in the liver. C) DDAH1 in renal cortex. D) DDAH2 in renal cortex. Representative western blots of whole membranes show PRMT1 (~42 kDa), DDAH1 (~34 kDa), and DDAH2 bands (~30 kDa). *$p<0.05$ vs. sham; #$p<0.05$ vs. respective male.

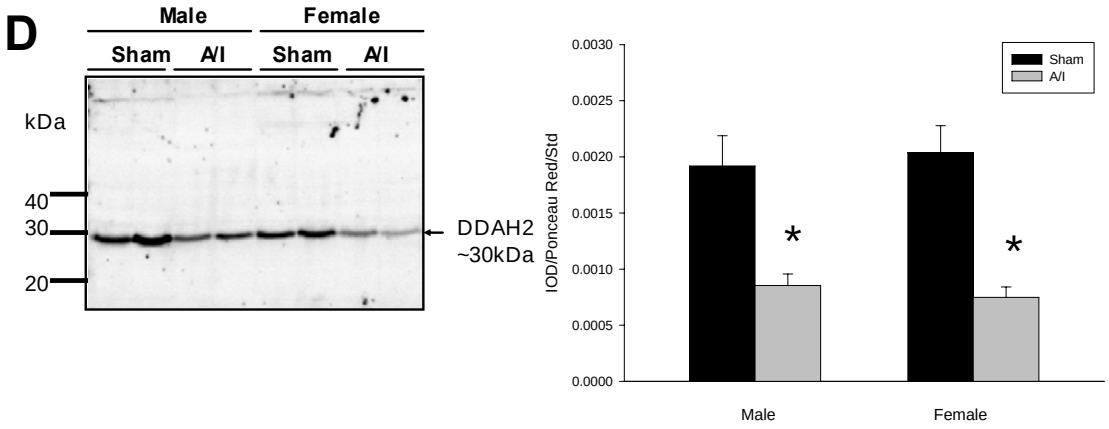

Figure 7-5. Continued

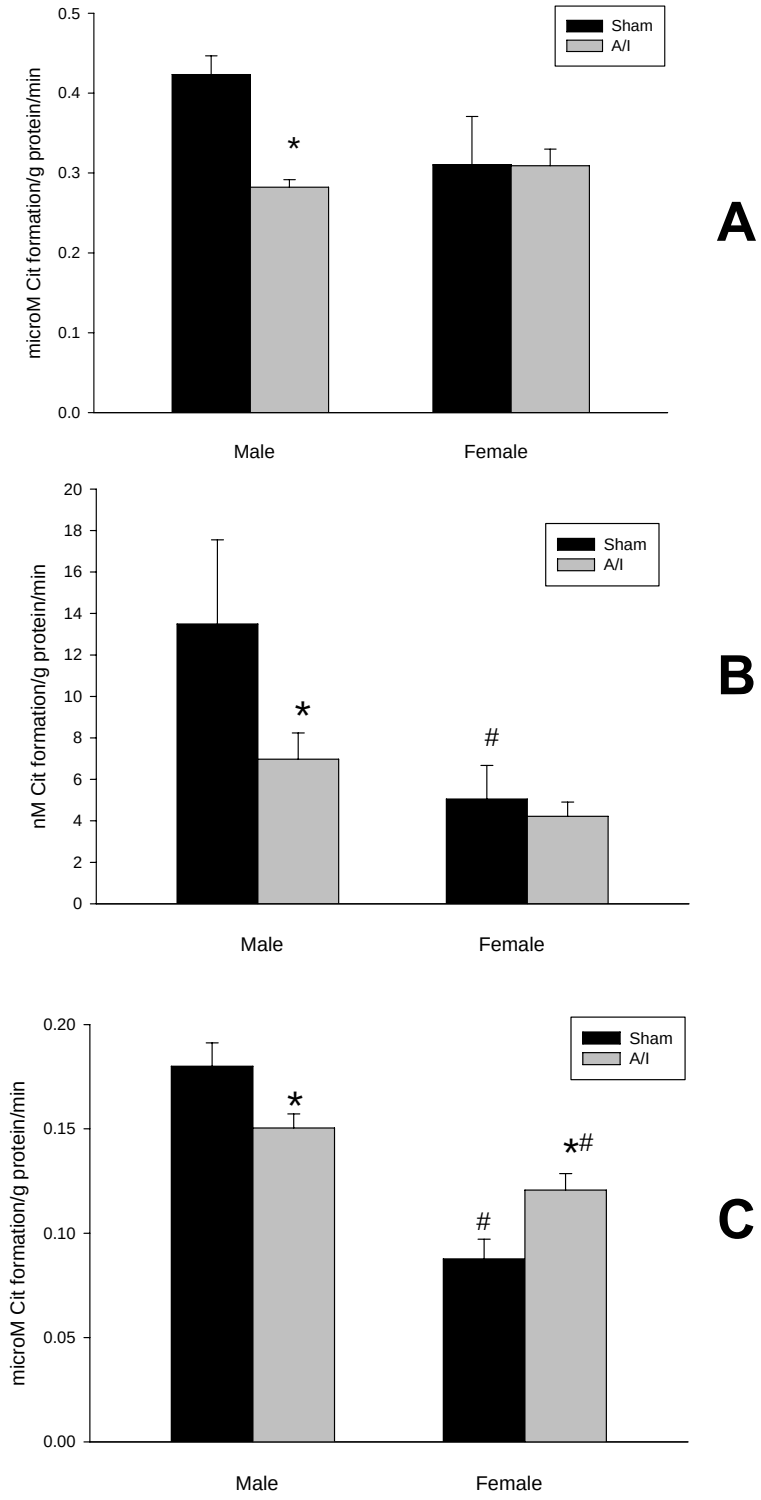

Figure 7-6. In vitro DDAH activity at 7 wk after surgery. A) In kidney cortex. B) In RBC. C) In liver. *p<0.05 vs. sham. #p<0.05 vs. respective male.

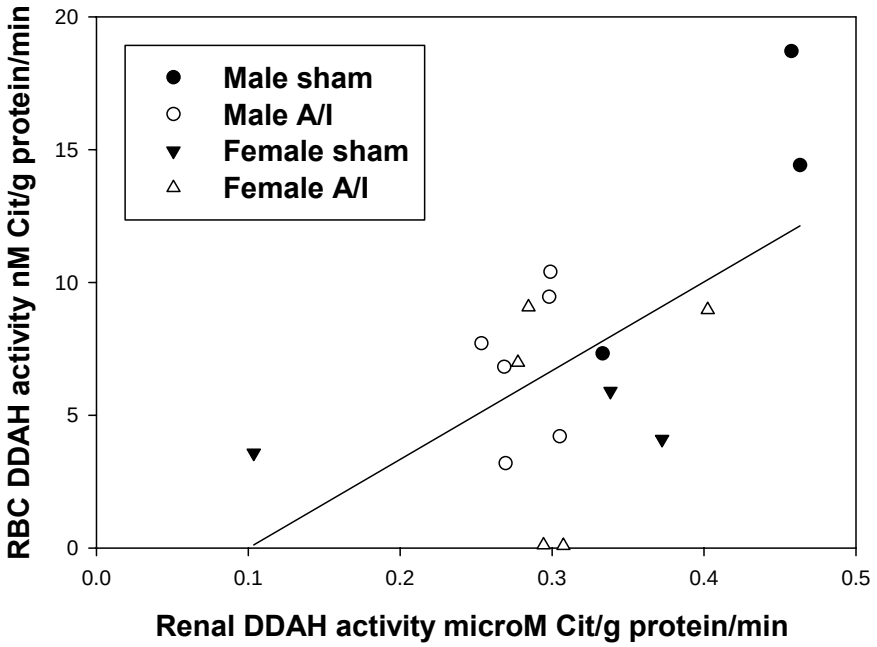

Figure 7-7. Correlation between renal DDAH activity and RBC DDAH activity ($r= 0.587$, $p<0.05$).

CHAPTER 8
CONCLUSION AND IMPLICATIONS

In this dissertation I describe five different but complementary sets of experiments intended to advance our understanding of renal NO deficiency in CKD. We have investigated the renal NOS proteins, renal and systemic oxidative stress and the renal and systemic control of ADMA.

Renal Neuronal Nitric Oxide Synthase-α and -β Isoforms Expression in Chronic Kidney Disease

In previous studies from our laboratory we have reported that in different rat CKD models, there is a fall in abundance of the renal cortical nNOSα expression that correlates with the severity of the injury. Our major findings include: (1) nNOSα expression decreases in severe CKD (e.g., 5/6 A/I, chronic GN and PAN models) (38, 130, 153); (2) Strain differences exist in nNOSα expression with rats resistant to progression of CKD (e.g., WF) showing maintained nNOSα compared to the CKD-vulnerable SD rats. This was seen in the 5/6 A/I, chronic PAN and DOCA/NaCl CKD models (38, 39, 41); and (3) Sex differences occur in the aging SD rats that correlate with susceptibility to CKD. The aged female shows maintained renal nNOSα and little age-dependent injury whereas the male shows early and progressive falls in nNOSα as CKD develops (40).

In my dissertation work I have demonstrated that (4) there exists of two isoforms of nNOS (splice variants) in the normal rat kidney; (5) while nNOSα decreases profoundly, nNOSβ expression increases in a RAPA Tx model. This increase in nNOSβ appears to be a compensatory response that helps to preserve kidney function; (6) in both 5/6 NX and A/I models where nNOSα falls, nNOSβ abundance increases in parallel with increasing glomerular damage. In these situations where the injury is more severe it seems that the increased nNOSβ

has been inadequate to prevent progression of the injury; and (7) the female rats show less structural damage, smaller falls in nNOSα and increases in nNOSβ than males with 5/6 A/I.

As shown in Figure 8-1, we compare four CKD models in this dissertation. There are two Tx-induced mild CKD models, ISO I/R and ALLO RAPA models which show slow progression of injury; the other two severe CKD models are 5/6 NX and A/I models and here the rate of progression was much faster. As shown in Table 8-1, nNOSα abundance is maintained in the ISO Tx I/R model, which displays better renal outcome compared to other CKD models. In the RAPA Tx model (another mild CKD model) there was a surprising absence of nNOSα yet a relatively good outcome. There was a significant upregulation of nNOSβ which could be viewed as compensatory, to maintain ~60% of renal function and relative preservation of structure. However, in severe progressive CKD, functional deterioration and structural damage still developed despite the upregulation of nNOSβ (e.g., 5/6 NX and A/I model) and in these models there was still significant residual nNOSα. In addition, nNOSβ abundance positively correlates to the increase of glomerular damage in 5/6 A/I model. While maintained renal cortical nNOSα is clearly critical to prevent CKD progression, the increased nNOSβ may not be adequate to prevent injury in severe progressive CKD, and could even be viewed as potentially harmful, given the positive correlation with the structural damage.

Exactly how nNOSβ influences renal function /structure is unknown. Its location is considered to be purely cytosolic (no PDZ domain) and might have similar or even higher NOS activity (no PIN binding site) vs. nNOSα in vivo (36). One hypothesis is that when nNOSα-derived NO decreases, nNOSβ expression increases and can potentially replace decreased NO production to maintain function and prevent CKD progression. However, different N-terminal truncated nNOS proteins (e.g., nNOSβ) have been shown to heterodimerize with nNOSα and

decrease NOS activity (158). Thus, an alternate possibility is that the increased nNOSβ heterodimerizes with residual nNOSα and further decreases nNOSα-derived NO production. Perhaps the positive actions of nNOSβ can only be expressed when all the nNOSa is gone, exactly as occurred in the RAPA Tx model (chapter 4). The relationship between nNOSα and –β is likely to be complex since although nNOSβ is entirely cytosolic, the "in vitro" soluble NOS activity is decreased in various severe CKD models (10, 36-41, 130, 153), showing that increased nNOSβ does not increase total nNOS activity in this setting. This could explain why increased nNOSβ in 5/6 NX and male A/I rats was not beneficial in preventing CKD progression.

Although some stimuli have been reported to up- or downregulate nNOS mRNA expression in several rat tissues (75, 156), the regulation of the nNOSβ transcript is unknown. Our data shows that renal cortical nNOSβ is upregulated in different CKD models, although the precise signal(s) remain unknown. Also, the localization of nNOSβ in kidney cortex is unknown. Bachmann et al. (9) used both N- and C-terminal anti-nNOS antibodies to recognize the same structure by immunohistochemistry and concluded that the nNOS variant of the MD is nNOSα. However, this finding does not exclude the possibility that both are present and/or that nNOSβ may exist in MD in response to renal injury. It is known that low levels of nNOS are expressed in proximal tubules, cortical collecting ducts, and perivascular nerves in kidney cortex (8) although the specific isoform is unknown. Whether the increased nNOSβ expression in different CKD models is located in MD or other segments of nephron is also unknown. Since the C-terminal Ab detects all alternatively spliced forms of nNOS, we are unable to use it to detect the localization of nNOSβ by immunohistochemistry. Although Langnaese et al. (79) developed a "specific" nNOSβ Ab to detect nNOSβ in nNOSβ overexpressing cells, their data suggests that

this Ab may cross react with other nNOS isoforms. Therefore, the location of the renal nNOS isoforms deserves further evaluation.

There have been a number of studies in the nNOSα-knockout (KO) mice (deleted exon 2) (104). However, expression of alternatively spliced variants are still detected in these mice with residual nNOS activity. Mice with complete ablation of nNOS (deleted exon 6) are viable although infertile (49) and little is known about renal control in nNOS exon 6 KO mice. Although in this dissertation we focus on nNOS expression in the kidney cortex, further study is needed to elucidate its pathophysiological role in the kidney medulla in renal disease. Future challenges to understand their relative function includes the comparison between nNOSα and full nNOS KO mice, the generation of inducible nephron site-specific knockout models, and gene silencing models targeting specific nNOS isoform to assess the physiological roles of different nNOS isoforms.

Oxidative Stress in Chronic Kidney Disease

Oxidative stress is present in CKD patients and in experimental CKD models (53, 123, 147). Superoxide (O_2^-) and hydrogen peroxide (H_2O_2) are important ROS, both of which can be made by many oxidative enzymes. On the other hand, many antioxidant enzymes counteract ROS to maintain redox balance. The complexity of the interplay between the pro-oxidants and antioxidant systems and their impact on systemic vs. renal oxidative stress makes the interpretation of in vivo studies very complicated.

Two major sources of vascular ROS are cytochrome P450 and NADPH oxidase (47). In the kidney cortex, there is a wide distribution of various NADPH oxidase complexes, thus serving as the predominant source of O_2^- generation (44). A previous study reported that renal NADPH oxidase expression increased in 5/6 NX rats (151) and our data confirms this since we observed that renal cortical NADPH oxidase-dependent O_2^- production increased in 5/6 NX rats

(133). We investigated several markers of oxidative stress in the A/I model and found that the O_2^- generating system is upregulated in male A/I rats represented by increased renal cortical $p22^{phox}$ abundance, urinary H_2O_2, and plasma MDA levels. These data suggest that NADPH oxidase may be the major source of ROS in the kidney.

Oxidative Stress and Neuronal Nitric Oxide Synthase

Our data suggests that oxidative stress is associated with loss of renal nNOSα and subsequent development of injury. We showed that 5/6 NX rats develop increased NADPH-dependent O_2^- production and decreased nNOSα expression in the kidney cortex (chapter 6). In the presence of the antioxidant vitamin E, both development of injury and loss of nNOSa are attenuated. In the 5/6 A/I model sex difference study, renal cortical nNOSα abundance was decreased in males, together with evidence of increased systemic and renal oxidative stress. In contrast, female A/I rats tended to maintain nNOSα abundance and without evidence of increased oxidative stress.

Little is known about whether oxidative stress can regulate nNOS expression in the kidney. Angiotesin II infusion decreases nNOSα but increases NADPH oxidase expression, while angiotensinogen and angiotensin 1 receptor knockout mice display increased nNOSα expression (139). These findings suggest angiotensin II may induce NADPH oxidase to downregulate nNOSα expression. It is supported by our finding in the 5/6 NX model that oxidative stress may downregulate nNOSα expression in the kidney.

Asymmetric Dimethylarginine in Chronic Kidney Disease

Elevated ADMA level has been reported in various men with ESRD and CKD, CKD models and is a risk factor for many cardiovascular disorders (146). Free plasma and tissue ADMA levels are controlled by protein turnover rate and two counterbalancing pathways, type I PRMT and DDAH. (146). Both methylation and breakdown of protein are highly regulated

processes (105, 137), however, their regulation of the formation of ADMA is not well characterized. On the other hand, ADMA is metabolized by DDAH and the kidney plays a major role for breakdown of excess ADMA (137, 146). In CKD, defective renal clearance of ADMA may cause its accumulation in the blood and/or in tissue.

We found that plasma ADMA levels are increased in 5/6 NX model (133). Our data suggest that the accumulation of ADMA is due to increased ADMA production (secondary to increased PRMT1 abundance) and decreased ADMA degradation (secondary to decreased renal DDAH activity). Matsuguma and colleagues have reported increased renal PRMT1 gene expression although they also reported decreased DDAH1 and 2 protein expression in 5/6 NX rats (90). This was contrast to our finding that DDAH1 and 2 protein abundance was unaltered in 5/6 NX rats; however, we found decreased renal DDAH activity.

Nevertheless, when we used the 5/6 A/I model there was no increase in plasma ADMA level in either sex, which was unexpected since we used the same strain of rat and since the 5/6 A/I model produces more severe injury that the 5/6 NX. The renal PRMT1 increased similarly, renal DDAH1 abundance was unchanged and DDAH2 fell similarly in both sexes with A/I. However, while there was no change in renal ADMA levels in males with A/I an increase was seen in females. In female A/I rats, an increased renal L-arginine levels also occurred which should reduce the impact of the increased renal ADMA. Interestingly, the renal L-arginine/ADMA ratios were reduced similarly after A/I in both sexes although the precise mechanism of the reduction differed.

This sex difference study has highlighted the complexity of the regulation of plasma and tissue ADMA levels since neither renal PRMT nor DDAH expression/activity can predict plasma or kidney ADMA levels in shams or 5/6 A/I. Furthermore, plasma ADMA levels do not always

predict local ADMA levels because there is likely to be interorgan regulation to control its homeostasis, i.e., ADMA formed in the heart might end up in the liver or kidney for breakdown. Also, local formation will vary and the increased renal PRMT1 might mean that net renal ADMA generation is increased in CKD. Of note, patients with normal plasma ADMA level may actually already be at risk since ADMA may accumulate in other organs (e.g., endothelium), consequently impairing their function (e.g., endothelial dysfunction). Therefore, plasma ADMA levels may not accurately reflect ADMA-associated cardiovascular risk. Other markers are needed to predict tissue ADMA levels seem important for future development of specific ADMA-lowering agents.

Another unexpected finding was that renal ADMA levels were not invariably correlated to renal DDAH activity. This again reinforces the complexity of ADMA regulation with different tissues contributing to synthesis and breakdown. However, decreased tissue DDAH activity is associated with poor renal outcome in male A/I rats, suggesting DDAH activity may be a marker in predicting outcome. We were able to detect DDAH activity in rat RBC and found that it correlates with renal DDAH activity. This may provide a useful tool as a surrogate measure of renal DDAH activity in patients with CKD and clinical studies are planned to address this.

The distinct tissue distribution of the two DDAH isoforms suggests that there may be an isoform-specific regulation of ADMA concentration and NO production (142). Wang et al. (154) recently reported that blood ADMA level was regulated by DDAH1, which was mainly expressed in kidney cortex and liver, whereas vascular NO production was primarily regulated by DDAH2, which was expressed in blood vessels. However, this is inconsistent with previous studies showing that loss of DDAH1 activity causes accumulation of ADMA as well as reduction in NO (83) and decreased DDAH2 expression in vessels was associated with elevated plasma

ADMA levels in 5/6 NX rats (136). This seems an oversimplification because both ADMA and NO are highly regulated by complicated processes, as supported by our findings. In summary, 1). We found renal cortical DDAH1 expression was unchanged in 5/6 NX and A/I models regardless to the plasma ADMA levels; 2). Plasma ADMA level cannot be predicted by individual organ PRMT1 expression, DDAH1/2 expression, and DDAH activity; 3). Renal DDAH2 expression was unaltered in 5/6 NX rats but decreased in 5/6 A/I rats; however, they all displayed decreased NO production; 4). NO production was correlated to L-aginine/ADMA ratio but not to the individual L-arginine or ADMA levels. These data points out the complexity of regulation on ADMA and NO production and indicate the need for further studies deserve to study the specific functions of DDAH isoforms. We have constructed lentiviral vectors carrying human DDAH1 or DDAH2 cDNA and we are currently studying their renoprotective effects in a chronic PAN CKD model. Hopefully, this study will give insight into the specific functions of two DDAH isoforms.

Oxidative Stress and Asymmetric Dimethylarginine

Although the link between oxidative stress and ADMA in cardiovascular disease has been reviewed (128), their relationship in renal disease is unclear. Oxidative stress is considered to increase the activity of PRMT and decrease the expression/activity of DDAH, which leads to the increase in ADMA concentrations (128). Interestingly, we found increased ADMA production (secondary to increased PRMT1 abundance) and decreased ADMA degradation (secondary to decreased DDAH activity) in 5/6 NX rats, which was associated with increased renal NADPH oxidase-dependent O_2^- production. According to the current literature, it is well established that the presence of a reactive cysteine residue in the active site of DDAH1/2 makes their activity susceptible to inhibition by S-nitrosylation as well as oxidation by ROS (72, 82, 128). In our studies, we also reported that renal DDAH activity was inhibited by either O_2^- or NO donor *in vitro* (132). However, in the 5/6 NX study, vitamin E reduced NADPH oxidase-dependent O_2^-

production, protected the kidney structure, preserved nNOSα but had no impact on the elevated plasma ADMA levels in 5/6 NX rats (133). In addition, there was no reversal of the decreased DDAH activity in the kidney. This data was unexpected since Wilcox et al. (44) suggests that NADPH oxidase is the primary renal oxidase and yet normalization with vitamin E did not reduce ADMA or restore renal DDAH activity. This could mean that O_2^- from other oxidative enzymes or other sources of ROS becomes important in generation of ROS in CKD. Alternatively it could mean that PRMT1 expression/DDAH activity is not invariably regulated by increased ROS.

Our subsequent studies in the 5/6 A/I model support this possibility since the O_2^- generating system is upregulated in male A/I rats (increased renal cortical $p22^{phox}$ abundance, urinary H_2O_2, and plasma MDA levels), tissue DDAH activity (in kidney, liver, and RBC) fell but there was no increase in either plasma or renal ADMA levels. In contrast, the female A/I rats displayed increased renal ADMA levels with no evidence of increased ROS and similar absolute DDAH activity in tissues. Whether oxidative stress can induce the accumulation of ADMA in the kidney via regulation of PRMT/DDAH needs further evaluation, as does the impact of different types of oxidative stress on the system.

Target on Nitric Oxide Pathway to Prevent Chronic Kidney Disease Progression and Cardiovascular Complications

At present, treatment aiming to retard CKD progression is limited to aggressive blood pressure control and blockade of renin-angiotensin system, with few therapies targeting the NO pathway. Because many common mechanisms of CKD progression share NO deficiency which is causally involved in both CKD progression and endothelial dysfunction, preservation of NO bioavailability becomes a therapeutic target in CKD patients. The administration of L-arginine was the most common treatment targeted to improve the NO pathway in both CKD and CVD.

Although L-arginine had a beneficial effect in experimental CKD animals (70), the data from human trials are still inconclusive (10, 15, 31).

We demonstrated that NO production is decreased in CKD and this is likely due to decreased renal nNOS abundance, increased oxidative stress, and accumulation of ADMA. Instead of L-arginine supplementation, the data presented above allows us to prevent NO deficiency in CKD patients with therapeutic approaches to (1) improve decreased renal cortical nNOSα abundance, (2) effectively suppress oxidative stress by targeting appropriate source of ROS, and (3) correct elevated ADMA levels (Figure 8-2).

Neuronal Nitric Oxide Synthase Gene Therapy

The cortical nNOSα is of critical importance in the pathogenesis of CKD progression as we demonstrated that its expression correlate to renal outcome in every CKD model studies. Although targeting nNOS with gene transfer have been used to modulate cardiac function (96), portal hypertension (163), and erectile dysfunction (88), kidney transfection is difficult due to its functional heterogeneity (141). Furthermore, since cortical nNOSα is uniquely located in MD, overexpressing nNOSα in the kidney cortex is difficult since MD-specific promoter is unavailable. Gene therapy to preserve renal nNOS is still at an early stage of development. However, nNOS in MD could be enhanced by salt restriction, diuretics, ACE inhibitors, and $NaHCO_3$ (139). Whether above interventions can preserve nNOS/NO in CKD patients deserves further evaluation.

Next, nNOS can also produce O_2^- instead of NO in the presence of deficiency of L-arginine or cofactor BH_4. Without correction of increased oxidative stress and ADMA, nNOS gene therapy could serve more harm that good, due to nNOS uncoupling. Therefore, in addition to preserving renal cortical nNOS abundance, relieving the inhibition on nNOS by manipulating oxidative stress and ADMA are essential.

Prevention of Chronic Kidney Disease Progression by Antioxidants

Traditionally, the treatment of oxidative stress is with the administration of antioxidants. We found a lack of renoprotection using short-term combined antioxidants in I/R injury although vitamin E prevents CKD progression in 5/6 NX rats. We also found female A/I rats displayed renal failure without induction of oxidative stress. As pointed out by Vaziri (148), it is clear that identification of the source of ROS and control of ROS production is a better strategy than non-selective use of antioxidants to treat different kinds of CKD. As ideal antioxidants for clinical use have not yet been discovered, a mechanism-based approach is required to gain understanding of the relative importance of the different contributors to oxidative stress in CKD. This may then lead to use of specific antioxidants to prevent the progression of CKD with different insults.

Prevention of Chronic Kidney Disease Progression by Lowering Asymmetric Dimethylarginine

Although ACE inhibitors, ARBs, hypoglycemic agents, and hormone replacement therapy (HRT) have been shown to reduce ADMA levels, specific ADMA-lowering therapy is not yet available (86). Treatment aimed at reducing oxidative stress was unable to lower plasma ADMA levels (129). Given the facts that accumulation of ADMA is associated with increased PRMT expression and decreased DDAH expression/activity, lowering ADMA levels could be approached by PRMT inhibitors or DDAH agonists. Several PRMT isoforms have been identified, each of which has its own distinct function in regulation of cellular physiology. Selective PRMT inhibitors are unavailable and anyway their inhibition may cause unwanted side effects (77). On the other hand, DDAH is emerging as a prime target for therapeutic interventions to lower ADMA. Although promising insights come from the DDAH-transgenic mice (52), selective DDAH agonist and DDAH gene therapy still awaits confirmation. Preliminary animal work showed DDAH1 gene therapy can prevent the progression in a 5/6 NX

rat model (91). A site-specific and sustained expression DDAH gene therapy for CKD patients requires further development.

Multifaceted Therapeutic Approaches in Preventing Chronic Kidney Disease Progression

As our understanding of the mechanisms of CKD continues to expand, additional targets for intervention will be identified, and it is likely that a multifaceted therapeutic approach will be required to slow the CKD progression and reduce CV complications. Chronic L-arginine therapy alone has no impact on progression of patients with mild CKD (31), indicating that the preservation of NO bioavailability may need multifaceted therapeutic approaches. Of course, such approaches as gene therapy (e.g., nNOS or DDAH), specific antioxidants, and specific ADMA-lowering agents may become viable options for CKD patients marked by NO deficiency.

Table 8-1. The nNOSα and –β isoform expression in different chronic kidney disease models

Model	Rat strain	Sex	Follow-up	%CCr	% GS	nNOSα	nNOSβ	OS	ADMA
I/R ISO	F344	M	22wk	~60%	25%	↔	ND	↑	ND
RAPA ALLO	F344 → Lewis	M	22wk	~70%	30%	↓	↑	ND	ND
5/6 NX	SD	M	15wk	~20%	40%	↓	↑	↑	↑
5/6 NX +Vit E	SD	M	15wk	~20%	25%	↔	↑	↔	↑
A/I	SD	M	7wk	~10%	40%	↓	↑	↑	↔
A/I	SD	F	7wk	~30%	30%	↔	↑	↔	↔

OS=Oxidative stress; ↑= increase; ↓=decrease; ↔=no change; ND= not detected.

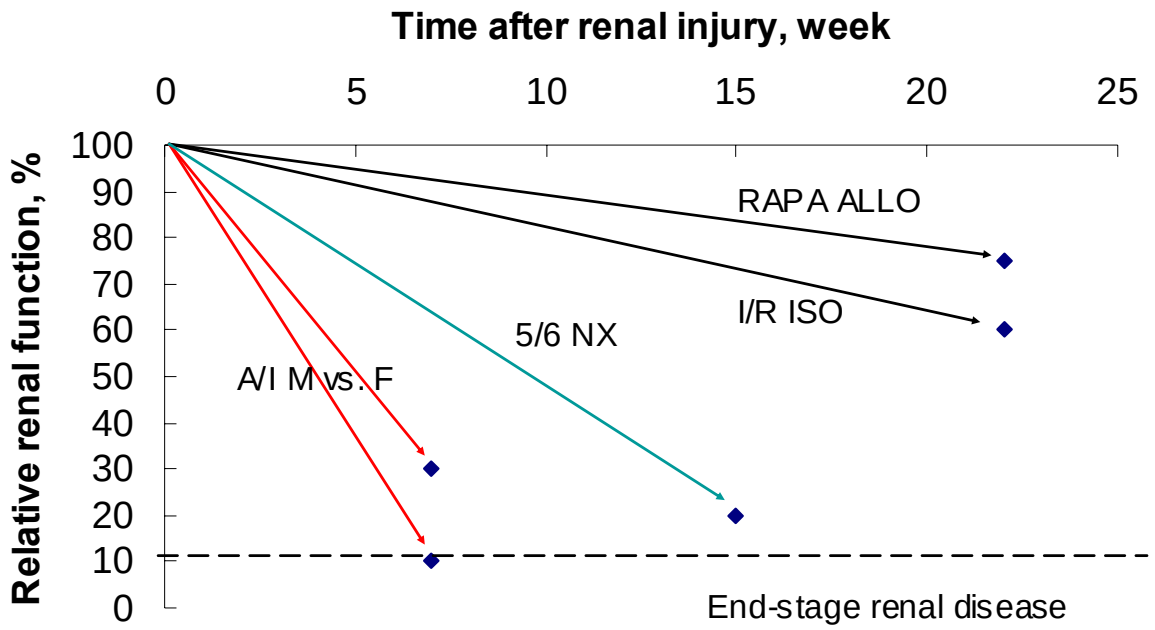

Figure 8-1. Various progression rates to end-stage renal disease in different chronic kidney disease (CKD) models. The steeper the slope, the more rapid the rate of progression and the more severe the injury.

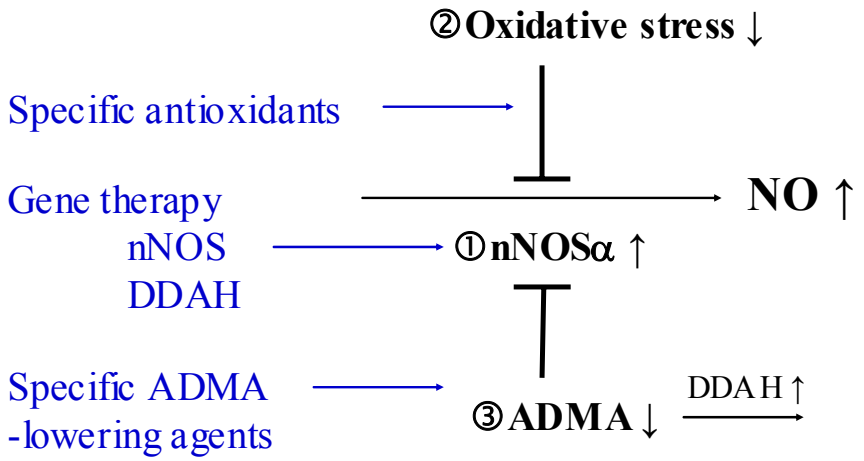

Figure 8-2. Target nitric oxide (NO) pathways in preventing chronic kidney disease (CKD) progression and cardiovascular complications. NO bioavailability can be preserved by (1) Increased renal cortical neuronal nitric oxide synthase (nNOS) abundance, (2) Decreased oxidative stress, and (3) Decreased asymmetric dimethylarginine (ADMA) by activation of dimethylarginine dimethylaminohydrolase (DDAH).

LIST OF REFERENCES

1. **Achan V, Tran CT, Arrigoni F, Whitley GS, Leiper JM and Vallance P.** all-trans-Retinoic acid increases nitric oxide synthesis by endothelial cells: a role for the induction of dimethylarginine dimethylaminohydrolase. *Circ Res* 90: 764-769, 2002.

2. **Albrecht EW, van Goor H, Smit-van Oosten A and Stegeman CA.** Long-term dietary L-arginine supplementation attenuates proteinuria and focal glomerulosclerosis in experimental chronic renal transplant failure. *Nitric Oxide* 8: 53-58, 2003.

3. **Alderton WK, Cooper CE and Knowles RG.** Nitric oxide synthases: structure, function and inhibition. *Biochem J* 357: 593-615, 2001.

4. **Arthur JM, Thongboonkerd V, Scherzer JA, Cai J, Pierce WM and Klein JB.** Differential expression of proteins in renal cortex and medulla: a proteomic approach. *Kidney Int* 62: 1314-1321, 2002.

5. **Attia DM, Verhagen AM, Stroes ES, van Faassen EE, Grone HJ, De Kimpe SJ, Koomans HA, Braam B and Joles JA.** Vitamin E alleviates renal injury, but not hypertension, during chronic nitric oxide synthase inhibition in rats. *J Am Soc Nephrol* 12: 2585-2593, 2001.

6. **Azuma H, Nadeau K, Takada M, Mackenzie HS and Tilney NL.** Cellular and molecular predictors of chronic renal dysfunction after initial ischemia/reperfusion injury of a single kidney. *Transplantation* 64: 190-197, 1997.

7. **Azzi A, Ricciarelli R and Zingg JM.** Non-antioxidant molecular functions of alpha-tocopherol (vitamin E). *FEBS Lett* 519: 8-10, 2002.

8. **Bachmann S, Bosse HM and Mundel P.** Topography of nitric oxide synthesis by localizing constitutive NO synthases in mammalian kidney. *Am J Physiol* 268: F885-98, 1995.

9. **Bachmann S and Theilig F.** Juxtaglomerular apparatus, nitric oxide, and macula densa signaling. *Adv Nephrol Necker Hosp* 30: 95-107, 2000.

10. **Baylis C.** Arginine, arginine analogs and nitric oxide production in chronic kidney disease. *Nat Clin Pract Nephrol* 2: 209-220, 2006.

11. **Baylis C.** Changes in renal hemodynamics and structure in the aging kidney; sexual dimorphism and the nitric oxide system. *Exp Gerontol* 40: 271-278, 2005.

12. **Bedford MT and Richard S.** Arginine methylation an emerging regulator of protein function. *Mol Cell* 18: 263-272, 2005.

13. **Billecke SS, Kitzmiller LA, Northrup JJ, Whitesall SE, Kimoto M, Hinz AV and D'Alecy LG.** Contribution of whole blood to the control of plasma asymmetrical dimethylarginine. *Am J Physiol Heart Circ Physiol* 291: H1788-96, 2006.

14. **Bode-Boger SM, Scalera F, Kielstein JT, Martens-Lobenhoffer J, Breithardt G, Fobker M and Reinecke H.** Symmetrical dimethylarginine: a new combined parameter for renal function and extent of coronary artery disease. *J Am Soc Nephrol* 17: 1128-1134, 2006.

15. **Boger RH.** The pharmacodynamics of L-arginine. *J Nutr* 137: 1650S-1655S, 2007.

16. **Boger RH, Schwedhelm E, Maas R, Quispe-Bravo S and Skamira C.** ADMA and oxidative stress may relate to the progression of renal disease: rationale and design of the VIVALDI study. *Vasc Med* 10 Suppl 1: S97-102, 2005.

17. **Boissel JP, Schwarz PM and Forstermann U.** Neuronal-type NO synthase: transcript diversity and expressional regulation. *Nitric Oxide* 2: 337-349, 1998.

18. **Brandes RP and Mugge A.** Gender differences in the generation of superoxide anions in the rat aorta. *Life Sci* 60: 391-396, 1997.

19. **Braunlich H, Marx F, Fleck C and Stein G.** Kidney function in rats after 5/6 nephrectomy (5/6 NX); effort of treatment with vitamin E. *Exp Toxicol Pathol* 49: 135-139, 1997.

20. **Brenman JE, Chao DS, Gee SH, McGee AW, Craven SE, Santillano DR, Wu Z, Huang F, Xia H, Peters MF, Froehner SC and Bredt DS.** Interaction of nitric oxide synthase with the postsynaptic density protein PSD-95 and alpha1-syntrophin mediated by PDZ domains. *Cell* 84: 757-767, 1996.

21. **Brenner BM.** Remission of renal disease: recounting the challenge, acquiring the goal. *J Clin Invest* 110: 1753-1758, 2002.

22. **Brigelius-Flohe R, Kelly FJ, Salonen JT, Neuzil J, Zingg JM and Azzi A.** The European perspective on vitamin E: current knowledge and future research. *Am J Clin Nutr* 76: 703-716, 2002.

23. **Cardounel AJ, Xia Y and Zweier JL.** Endogenous methylarginines modulate superoxide as well as nitric oxide generation from neuronal nitric-oxide synthase: differences in the effects of monomethyl- and dimethylarginines in the presence and absence of tetrahydrobiopterin. *J Biol Chem* 280: 7540-7549, 2005.

24. **Chander V and Chopra K.** Renal protective effect of molsidomine and L-arginine in ischemia-reperfusion induced injury in rats. *J Surg Res* 128: 132-139, 2005.

25. **Chatterjee PK, Cuzzocrea S, Brown PA, Zacharowski K, Stewart KN, Mota-Filipe H and Thiemermann C.** Tempol, a membrane-permeable radical scavenger, reduces oxidant stress-mediated renal dysfunction and injury in the rat. *Kidney Int* 58: 658-673, 2000.

26. **Chen Y, Li Y, Zhang P, Traverse JH, Hou M, Xu X, Kimoto M and Bache RJ.** Dimethylarginine dimethylaminohydrolase and endothelial dysfunction in failing hearts. *Am J Physiol Heart Circ Physiol* 289: H2212-9, 2005.

27. **Cooke JP.** Does ADMA cause endothelial dysfunction? *Arterioscler Thromb Vasc Biol* 20: 2032-2037, 2000.

28. **Curis E, Nicolis I, Moinard C, Osowska S, Zerrouk N, Benazeth S and Cynober L.** Almost all about citrulline in mammals. *Amino Acids* 29: 177-205, 2005.

29. **Cuzzocrea S, Riley DP, Caputi AP and Salvemini D.** Antioxidant therapy: a new pharmacological approach in shock, inflammation, and ischemia/reperfusion injury. *Pharmacol Rev* 53: 135-159, 2001.

30. **Dayoub H, Achan V, Adimoolam S, Jacobi J, Stuehlinger MC, Wang BY, Tsao PS, Kimoto M, Vallance P, Patterson AJ and Cooke JP.** Dimethylarginine dimethylaminohydrolase regulates nitric oxide synthesis: genetic and physiological evidence. *Circulation* 108: 3042-3047, 2003.

31. **De Nicola L, Bellizzi V, Minutolo R, Andreucci M, Capuano A, Garibotto G, Corso G, Andreucci VE and Cianciaruso B.** Randomized, double-blind, placebo-controlled study of arginine supplementation in chronic renal failure. *Kidney Int* 56: 674-684, 1999.

32. **DiJoseph JF, Fluhler E, Armstrong J, Sharr M and Sehgal SN.** Therapeutic blood levels of sirolimus (rapamycin) in the allografted rat. *Transplantation* 62: 1109-1112, 1996.

33. **Dikalov SI, Dikalova AE and Mason RP.** Noninvasive diagnostic tool for inflammation-induced oxidative stress using electron spin resonance spectroscopy and an extracellular cyclic hydroxylamine. *Arch Biochem Biophys* 402: 218-226, 2002.

34. **El Nahas M.** The global challenge of chronic kidney disease. *Kidney Int* 68: 2918-2929, 2005.

35. **Eliasson MJ, Blackshaw S, Schell MJ and Snyder SH.** Neuronal nitric oxide synthase alternatively spliced forms: prominent functional localizations in the brain. *Proc Natl Acad Sci U S A* 94: 3396-3401, 1997.

36. **Erdely A, Freshour G and Baylis C.** Resistance to renal damage by chronic nitric oxide synthase inhibition in the Wistar-Furth rat. *Am J Physiol Regul Integr Comp Physiol* 290: R66-72, 2006.

37. **Erdely A, Freshour G, Maddox DA, Olson JL, Samsell L and Baylis C.** Renal disease in rats with type 2 diabetes is associated with decreased renal nitric oxide production. *Diabetologia* 47: 1672-1676, 2004.

38. **Erdely A, Freshour G, Smith C, Engels K, Olson JL and Baylis C.** Protection against puromycin aminonucleoside-induced chronic renal disease in the Wistar-Furth rat. *Am J Physiol Renal Physiol* 287: F81-9, 2004.

39. **Erdely A, Freshour G, Tain YL, Engels K and Baylis C.** DOCA/NaCl-induced chronic kidney disease: a comparison of renal nitric oxide production in resistant and susceptible rat strains. *Am J Physiol Renal Physiol* 292: F192-6, 2007.

40. **Erdely A, Greenfeld Z, Wagner L and Baylis C.** Sexual dimorphism in the aging kidney: Effects on injury and nitric oxide system. *Kidney Int* 63: 1021-1026, 2003.

41. **Erdely A, Wagner L, Muller V, Szabo A and Baylis C.** Protection of wistar furth rats from chronic renal disease is associated with maintained renal nitric oxide synthase. *J Am Soc Nephrol* 14: 2526-2533, 2003.

42. **Fortepiani LA and Reckelhoff JF.** Role of oxidative stress in the sex differences in blood pressure in spontaneously hypertensive rats. *J Hypertens* 23: 801-805, 2005.

43. **Frein D, Schildknecht S, Bachschmid M and Ullrich V.** Redox regulation: a new challenge for pharmacology. *Biochem Pharmacol* 70: 811-823, 2005.

44. **Gill PS and Wilcox CS.** NADPH oxidases in the kidney. *Antioxid Redox Signal* 8: 1597-1607, 2006.

45. **Gordon CA and Himmelfarb J.** Antioxidant therapy in uremia: evidence-based medicine? *Semin Dial* 17: 327-332, 2004.

46. **Gornall AG and Hunter A.** A colorimetric method for the determination of citrulline. *Biochem J* 35: 650-658, 1941.

47. **Griendling KK and FitzGerald GA.** Oxidative stress and cardiovascular injury: Part I: basic mechanisms and in vivo monitoring of ROS. *Circulation* 108: 1912-1916, 2003.

48. **Griffin KA, Picken MM and Bidani AK.** Blood pressure lability and glomerulosclerosis after normotensive 5/6 renal mass reduction in the rat. *Kidney Int* 65: 209-218, 2004.

49. **Gyurko R, Leupen S and Huang PL.** Deletion of exon 6 of the neuronal nitric oxide synthase gene in mice results in hypogonadism and infertility. *Endocrinology* 143: 2767-2774, 2002.

50. **Hahn S, Krieg RJ,Jr, Hisano S, Chan W, Kuemmerle NB, Saborio P and Chan JC.** Vitamin E suppresses oxidative stress and glomerulosclerosis in rat remnant kidney. *Pediatr Nephrol* 13: 195-198, 1999.

51. **Hanna IR, Hilenski LL, Dikalova A, Taniyama Y, Dikalov S, Lyle A, Quinn MT, Lassegue B and Griendling KK.** Functional association of nox1 with p22phox in vascular smooth muscle cells. *Free Radic Biol Med* 37: 1542-1549, 2004.

52. **Hasegawa K, Wakino S, Tatematsu S, Yoshioka K, Homma K, Sugano N, Kimoto M, Hayashi K and Itoh H.** Role of asymmetric dimethylarginine in vascular injury in transgenic mice overexpressing dimethylarginie dimethylaminohydrolase 2. *Circ Res* 101: e2-10, 2007.

53. **Himmelfarb J, Stenvinkel P, Ikizler TA and Hakim RM.** The elephant in uremia: oxidant stress as a unifying concept of cardiovascular disease in uremia. *Kidney Int* 62: 1524-1538, 2002.

54. **Holden DP, Cartwright JE, Nussey SS and Whitley GS.** Estrogen stimulates dimethylarginine dimethylaminohydrolase activity and the metabolism of asymmetric dimethylarginine. *Circulation* 108: 1575-1580, 2003.

55. **Hu T, Chouinard M, Cox AL, Sipes P, Marcelo M, Ficorilli J, Li S, Gao H, Ryan TP, Michael MD and Michael LF.** Farnesoid X receptor agonist reduces serum asymmetric dimethylarginine levels through hepatic dimethylarginine dimethylaminohydrolase-1 gene regulation. *J Biol Chem* 281: 39831-39838, 2006.

56. **Huang H, He Z, Roberts LJ,2nd and Salahudeen AK.** Deferoxamine reduces cold-ischemic renal injury in a syngeneic kidney transplant model. *Am J Transplant* 3: 1531-1537, 2003.

57. **Huang PL, Dawson TM, Bredt DS, Snyder SH and Fishman MC.** Targeted disruption of the neuronal nitric oxide synthase gene. *Cell* 75: 1273-1286, 1993.

58. **Huber A, Saur D, Kurjak M, Schusdziarra V and Allescher HD.** Characterization and splice variants of neuronal nitric oxide synthase in rat small intestine. *Am J Physiol* 275: G1146-56, 1998.

59. **Hurt KJ, Sezen SF, Champion HC, Crone JK, Palese MA, Huang PL, Sawa A, Luo X, Musicki B, Snyder SH and Burnett AL.** Alternatively spliced neuronal nitric oxide synthase mediates penile erection. *Proc Natl Acad Sci U S A* 103: 3440-3443, 2006.

60. **Ibrahim HN and Hostetter TH.** The renin-aldosterone axis in two models of reduced renal mass in the rat. *J Am Soc Nephrol* 9: 72-76, 1998.

61. **Ito A, Tsao PS, Adimoolam S, Kimoto M, Ogawa T and Cooke JP.** Novel mechanism for endothelial dysfunction: dysregulation of dimethylarginine dimethylaminohydrolase. *Circulation* 99: 3092-3095, 1999.

62. **Jacobi J, Sydow K, von Degenfeld G, Zhang Y, Dayoub H, Wang B, Patterson AJ, Kimoto M, Blau HM and Cooke JP.** Overexpression of dimethylarginine dimethylaminohydrolase reduces tissue asymmetric dimethylarginine levels and enhances angiogenesis. *Circulation* 111: 1431-1438, 2005.

63. **Jaffrey SR and Snyder SH.** PIN: an associated protein inhibitor of neuronal nitric oxide synthase. *Science* 274: 774-777, 1996.

64. **Ji H, Zheng W, Menini S, Pesce C, Kim J, Wu X, Mulroney SE and Sandberg K.** Female protection in progressive renal disease is associated with estradiol attenuation of superoxide production. *Gend Med* 4: 56-71, 2007.

65. **Joles JA, Vos IH, Grone HJ and Rabelink TJ.** Inducible nitric oxide synthase in renal transplantation. *Kidney Int* 61: 872-875, 2002.

66. **Kang ES, Cates TB, Harper DN, Chiang TM, Myers LK, Acchiardo SR and Kimoto M.** An enzyme hydrolyzing methylated inhibitors of nitric oxide synthase is present in circulating human red blood cells. *Free Radic Res* 35: 693-707, 2001.

67. **Kim J, Kil IS, Seok YM, Yang ES, Kim DK, Lim DG, Park JW, Bonventre JV and Park KM.** Orchiectomy attenuates post-ischemic oxidative stress and ischemia/reperfusion injury in mice. A role for manganese superoxide dismutase. *J Biol Chem* 281: 20349-20356, 2006.

68. **Kimoto M, Miyatake S, Sasagawa T, Yamashita H, Okita M, Oka T, Ogawa T and Tsuji H.** Purification, cDNA cloning and expression of human NG,NG-dimethylarginine dimethylaminohydrolase. *Eur J Biochem* 258: 863-868, 1998.

69. **Kir HM, Dillioglugil MO, Tugay M, Eraldemir C and Ozdogan HK.** Effects of vitamins E, A and D on MDA, GSH, NO levels and SOD activities in 5/6 nephrectomized rats. *Am J Nephrol* 25: 441-446, 2005.

70. **Klahr S and Morrissey J.** L-arginine as a therapeutic tool in kidney disease. *Semin Nephrol* 24: 389-394, 2004.

71. **Knipp M.** How to control NO production in cells: N(omega),N(omega)-dimethyl-L-arginine dimethylaminohydrolase as a novel drug target. *Chembiochem* 7: 879-889, 2006.

72. **Knipp M, Braun O, Gehrig PM, Sack R and Vasak M.** Zn(II)-free dimethylargininase-1 (DDAH-1) is inhibited upon specific Cys-S-nitrosylation. *J Biol Chem* 278: 3410-3416, 2003.

73. **Knipp M and Vasak M.** A colorimetric 96-well microtiter plate assay for the determination of enzymatically formed citrulline. *Anal Biochem* 286: 257-264, 2000.

74. **Kone BC.** Nitric oxide synthesis in the kidney: isoforms, biosynthesis, and functions in health. *Semin Nephrol* 24: 299-315, 2004.

75. **Kone BC.** Localization and regulation of nitric oxide synthase isoforms in the kidney. *Semin Nephrol* 19: 230-241, 1999.

76. **Kouwenhoven EA, de Bruin RW, Heemann U, Marquet RL and IJzermans JN.** Does cold ischemia induce chronic kidney transplant dysfunction? *Transplant Proc* 31: 988-989, 1999.

77. **Krause CD, Yang ZH, Kim YS, Lee JH, Cook JR and Pestka S.** Protein arginine methyltransferases: evolution and assessment of their pharmacological and therapeutic potential. *Pharmacol Ther* 113: 50-87, 2007.

78. **Kulhanek V, Maderova V, Sindelarova K and Vojtiskova V.** Modified Determination of Ornithine-Carbamyl-Transferase Activity in Biological Material. *Clin Chim Acta* 8: 579-585, 1963.

79. **Langnaese K, Richter K, Smalla KH, Krauss M, Thomas U, Wolf G and Laube G.** Splice-isoform specific immunolocalization of neuronal nitric oxide synthase in mouse and rat

brain reveals that the PDZ-complex-building nNOSalpha beta-finger is largely exposed to antibodies. *Dev Neurobiol* 67: 422-437, 2007.

80. **Lau KS, Grange RW, Isotani E, Sarelius IH, Kamm KE, Huang PL and Stull JT.** nNOS and eNOS modulate cGMP formation and vascular response in contracting fast-twitch skeletal muscle. *Physiol Genomics* 2: 21-27, 2000.

81. **Lee MA, Cai L, Hubner N, Lee YA and Lindpaintner K.** Tissue- and development-specific expression of multiple alternatively spliced transcripts of rat neuronal nitric oxide synthase. *J Clin Invest* 100: 1507-1512, 1997.

82. **Leiper J, Murray-Rust J, McDonald N and Vallance P.** S-nitrosylation of dimethylarginine dimethylaminohydrolase regulates enzyme activity: further interactions between nitric oxide synthase and dimethylarginine dimethylaminohydrolase. *Proc Natl Acad Sci U S A* 99: 13527-13532, 2002.

83. **Leiper J, Nandi M, Torondel B, Murray-Rust J, Malaki M, O'Hara B, Rossiter S, Anthony S, Madhani M, Selwood D, Smith C, Wojciak-Stothard B, Rudiger A, Stidwill R, McDonald NQ and Vallance P.** Disruption of methylarginine metabolism impairs vascular homeostasis. *Nat Med* 13: 198-203, 2007.

84. **Leiper JM, Santa Maria J, Chubb A, MacAllister RJ, Charles IG, Whitley GS and Vallance P.** Identification of two human dimethylarginine dimethylaminohydrolases with distinct tissue distributions and homology with microbial arginine deiminases. *Biochem J* 343 Pt 1: 209-214, 1999.

85. **Lin Z, Crockett DK, Lim MS and Elenitoba-Johnson KS.** High-throughput analysis of protein/peptide complexes by immunoprecipitation and automated LC-MS/MS. *J Biomol Tech* 14: 149-155, 2003.

86. **Maas R.** Pharmacotherapies and their influence on asymmetric dimethylargine (ADMA). *Vasc Med* 10 Suppl 1: S49-57, 2005.

87. **MacAllister RJ, Parry H, Kimoto M, Ogawa T, Russell RJ, Hodson H, Whitley GS and Vallance P.** Regulation of nitric oxide synthesis by dimethylarginine dimethylaminohydrolase. *Br J Pharmacol* 119: 1533-1540, 1996.

88. **Magee TR, Ferrini M, Garban HJ, Vernet D, Mitani K, Rajfer J and Gonzalez-Cadavid NF.** Gene therapy of erectile dysfunction in the rat with penile neuronal nitric oxide synthase. *Biol Reprod* 67: 1033-1041, 2002.

89. **Maser RL, Vassmer D, Magenheimer BS and Calvet JP.** Oxidant stress and reduced antioxidant enzyme protection in polycystic kidney disease. *J Am Soc Nephrol* 13: 991-999, 2002.

90. **Matsuguma K, Ueda S, Yamagishi S, Matsumoto Y, Kaneyuki U, Shibata R, Fujimura T, Matsuoka H, Kimoto M, Kato S, Imaizumi T and Okuda S.** Molecular mechanism for

elevation of asymmetric dimethylarginine and its role for hypertension in chronic kidney disease. *J Am Soc Nephrol* 17: 2176-2183, 2006.

91. **Matsumoto Y, Ueda S, Yamagishi S, Matsuguma K, Shibata R, Fukami K, Matsuoka H, Imaizumi T and Okuda S.** Dimethylarginine dimethylaminohydrolase prevents progression of renal dysfunction by inhibiting loss of peritubular capillaries and tubulointerstitial fibrosis in a rat model of chronic kidney disease. *J Am Soc Nephrol* 18: 1525-1533, 2007.

92. **Meier-Kriesche HU, Schold JD and Kaplan B.** Long-term renal allograft survival: have we made significant progress or is it time to rethink our analytic and therapeutic strategies? *Am J Transplant* 4: 1289-1295, 2004.

93. **Miller AA, De Silva TM, Jackman KA and Sobey CG.** Effect of gender and sex hormones on vascular oxidative stress. *Clin Exp Pharmacol Physiol* 34: 1037-1043, 2007.

94. **Miller ER,3rd, Pastor-Barriuso R, Dalal D, Riemersma RA, Appel LJ and Guallar E.** Meta-analysis: high-dosage vitamin E supplementation may increase all-cause mortality. *Ann Intern Med* 142: 37-46, 2005.

95. **Modlinger PS, Wilcox CS and Aslam S.** Nitric oxide, oxidative stress, and progression of chronic renal failure. *Semin Nephrol* 24: 354-365, 2004.

96. **Mohan RM, Golding S, Heaton DA, Danson EJ and Paterson DJ.** Targeting neuronal nitric oxide synthase with gene transfer to modulate cardiac autonomic function. *Prog Biophys Mol Biol* 84: 321-344, 2004.

97. **Nakagawa T, Kang DH, Ohashi R, Suga S, Herrera-Acosta J, Rodriguez-Iturbe B and Johnson RJ.** Tubulointerstitial disease: role of ischemia and microvascular disease. *Curr Opin Nephrol Hypertens* 12: 233-241, 2003.

98. **Naoum JJ, Woodside KJ, Zhang S, Rychahou PG and Hunter GC.** Effects of rapamycin on the arterial inflammatory response in atherosclerotic plaques in Apo-E knockout mice. *Transplant Proc* 37: 1880-1884, 2005.

99. **Napoli KL, Wang ME, Stepkowski SM and Kahan BD.** Distribution of sirolimus in rat tissue. *Clin Biochem* 30: 135-142, 1997.

100. **Neugarten J, Ding Q, Friedman A, Lei J and Silbiger S.** Sex hormones and renal nitric oxide synthases. *J Am Soc Nephrol* 8: 1240-1246, 1997.

101. **Ninova D, Covarrubias M, Rea DJ, Park WD, Grande JP and Stegall MD.** Acute nephrotoxicity of tacrolimus and sirolimus in renal isografts: differential intragraft expression of transforming growth factor-beta1 and alpha-smooth muscle actin. *Transplantation* 78: 338-344, 2004.

102. **Oberbaumer I, Moser D and Bachmann S.** Nitric oxide synthase 1 mRNA: tissue-specific variants from rat with alternative first exons. *Biol Chem* 379: 913-919, 1998.

103. **Ogawa T, Kimoto M and Sasaoka K.** Purification and properties of a new enzyme, NG,NG-dimethylarginine dimethylaminohydrolase, from rat kidney. *J Biol Chem* 264: 10205-10209, 1989.

104. **Ortiz PA and Garvin JL.** Cardiovascular and renal control in NOS-deficient mouse models. *Am J Physiol Regul Integr Comp Physiol* 284: R628-38, 2003.

105. **Pahlich S, Zakaryan RP and Gehring H.** Protein arginine methylation: Cellular functions and methods of analysis. *Biochim Biophys Acta* 1764: 1890-1903, 2006.

106. **Pawlak K, Pawlak D and Mysliwiec M.** Cu/Zn superoxide dismutase plasma levels as a new useful clinical biomarker of oxidative stress in patients with end-stage renal disease. *Clin Biochem* 38: 700-705, 2005.

107. **Perico N, Cattaneo D, Sayegh MH and Remuzzi G.** Delayed graft function in kidney transplantation. *Lancet* 364: 1814-1827, 2004.

108. **Persson AE and Bachmann S.** Constitutive nitric oxide synthesis in the kidney--functions at the juxtaglomerular apparatus. *Acta Physiol Scand* 169: 317-324, 2000.

109. **Prescott LM and Jones ME.** Modified methods for the determination of carbamyl aspartate. *Anal Biochem* 32: 408-419, 1969.

110. **Ratner S and Petrack B.** Biosynthesis of urea. IV. Further studies on condensation in arginine synthesis from citrulline. *J Biol Chem* 200: 161-174, 1953.

111. **Reckelhoff JF, Kanji V, Racusen LC, Schmidt AM, Yan SD, Marrow J, Roberts LJ,2nd and Salahudeen AK.** Vitamin E ameliorates enhanced renal lipid peroxidation and accumulation of F2-isoprostanes in aging kidneys. *Am J Physiol* 274: R767-74, 1998.

112. **Reutzel-Selke A, Zschockelt T, Denecke C, Bachmann U, Jurisch A, Pratschke J, Schmidbauer G, Volk HD, Neuhaus P and Tullius SG.** Short-term immunosuppressive treatment of the donor ameliorates consequences of ischemia/ reperfusion injury and long-term graft function in renal allografts from older donors. *Transplantation* 75: 1786-1792, 2003.

113. **Roczniak A, Levine DZ and Burns KD.** Localization of protein inhibitor of neuronal nitric oxide synthase in rat kidney. *Am J Physiol Renal Physiol* 278: F702-7, 2000.

114. **Safirstein R, Miller P and Kahn T.** Cortical and papillary absorptive defects in gentamicin nephrotoxicity. *Kidney Int* 24: 526-533, 1983.

115. **Saran R, Novak JE, Desai A, Abdulhayoglu E, Warren JS, Bustami R, Handelman GJ, Barbato D, Weitzel W, D'Alecy LG and Rajagopalan S.** Impact of vitamin E on plasma asymmetric dimethylarginine (ADMA) in chronic kidney disease (CKD): a pilot study. *Nephrol Dial Transplant* 18: 2415-2420, 2003.

116. **Sartori-Valinotti JC, Iliescu R, Fortepiani LA, Yanes LL and Reckelhoff JF.** Sex differences in oxidative stress and the impact on blood pressure control and cardiovascular disease. *Clin Exp Pharmacol Physiol* 34: 938-945, 2007.

117. **Saur D, Paehge H, Schusdziarra V and Allescher HD.** Distinct expression of splice variants of neuronal nitric oxide synthase in the human gastrointestinal tract. *Gastroenterology* 118: 849-858, 2000.

118. **Scalera F, Kielstein JT, Martens-Lobenhoffer J, Postel SC, Tager M and Bode-Boger SM.** Erythropoietin increases asymmetric dimethylarginine in endothelial cells: role of dimethylarginine dimethylaminohydrolase. *J Am Soc Nephrol* 16: 892-898, 2005.

119. **Schiffrin EL, Lipman ML and Mann JF.** Chronic kidney disease: effects on the cardiovascular system. *Circulation* 116: 85-97, 2007.

120. **Schmidt RJ and Baylis C.** Total nitric oxide production is low in patients with chronic renal disease. *Kidney Int* 58: 1261-1266, 2000.

121. **Schramm L, La M, Heidbreder E, Hecker M, Beckman JS, Lopau K, Zimmermann J, Rendl J, Reiners C, Winderl S, Wanner C and Schmidt HH.** L-arginine deficiency and supplementation in experimental acute renal failure and in human kidney transplantation. *Kidney Int* 61: 1423-1432, 2002.

122. **Schulze F, Maas R, Freese R, Schwedhelm E, Silberhorn E and Boger RH.** Determination of a reference value for N(G), N(G)-dimethyl-L-arginine in 500 subjects. *Eur J Clin Invest* 35: 622-626, 2005.

123. **Shah SV, Baliga R, Rajapurkar M and Fonseca VA.** Oxidants in chronic kidney disease. *J Am Soc Nephrol* 18: 16-28, 2007.

124. **Stojanovic T, Grone HJ, Gieseler RK, Klanke B, Schlemminger R, Tsikas D and Grone EF.** Enhanced renal allograft rejection by inhibitors of nitric oxide synthase: a nonimmunologic influence on alloreactivity. *Lab Invest* 74: 496-512, 1996.

125. **Stuehr DJ and Marletta MA.** Mammalian nitrate biosynthesis: mouse macrophages produce nitrite and nitrate in response to Escherichia coli lipopolysaccharide. *Proc Natl Acad Sci U S A* 82: 7738-7742, 1985.

126. **Stuhlinger MC, Tsao PS, Her JH, Kimoto M, Balint RF and Cooke JP.** Homocysteine impairs the nitric oxide synthase pathway: role of asymmetric dimethylarginine. *Circulation* 104: 2569-2575, 2001.

127. **Sullivan JC, Sasser JM and Pollock JS.** Sexual dimorphism in oxidant status in spontaneously hypertensive rats. *Am J Physiol Regul Integr Comp Physiol* 292: R764-8, 2007.

128. **Sydow K and Munzel T.** ADMA and oxidative stress. *Atheroscler Suppl* 4: 41-51, 2003.

129. **Sydow K, Schwedhelm E, Arakawa N, Bode-Boger SM, Tsikas D, Hornig B, Frolich JC and Boger RH.** ADMA and oxidative stress are responsible for endothelial dysfunction in hyperhomocyst(e)inemia: effects of L-arginine and B vitamins. *Cardiovasc Res* 57: 244-252, 2003.

130. **Szabo AJ, Wagner L, Erdely A, Lau K and Baylis C.** Renal neuronal nitric oxide synthase protein expression as a marker of renal injury. *Kidney Int* 64: 1765-1771, 2003.

131. **Szentivanyi M,Jr, Zou AP, Mattson DL, Soares P, Moreno C, Roman RJ and Cowley AW,Jr.** Renal medullary nitric oxide deficit of Dahl S rats enhances hypertensive actions of angiotensin II. *Am J Physiol Regul Integr Comp Physiol* 283: R266-72, 2002.

132. **Tain YL and Baylis C.** Determination of dimethylarginine dimethylaminohydrolase activity in the kidney. *Kidney Int* 72: 886-9, 2007.

133. **Tain YL, Freshour G, Dikalova A, Griendling K and Baylis C.** Vitamin E reduces glomerulosclerosis, restores renal neuronal NOS, and suppresses oxidative stress in the 5/6 nephrectomized rat. *Am J Physiol Renal Physiol* 292: F1404-10, 2007.

134. **Tain YL, Muller V, Szabo A, Dikalova A, Griendling K and Baylis C.** Lack of long-term protective effect of antioxidant/anti-inflammatory therapy in transplant-induced ischemia/reperfusion injury. *Am J Nephrol* 26: 213-217, 2006.

135. **Tan B, Jiang DJ, Huang H, Jia SJ, Jiang JL, Hu CP and Li YJ.** Taurine protects against low-density lipoprotein-induced endothelial dysfunction by the DDAH/ADMA pathway. *Vascul Pharmacol* 46: 338-345, 2007.

136. **Tatematsu S, Wakino S, Kanda T, Homma K, Yoshioka K, Hasegawa K, Sugano N, Kimoto M, Saruta T and Hayashi K.** Role of nitric oxide-producing and -degrading pathways in coronary endothelial dysfunction in chronic kidney disease. *J Am Soc Nephrol* 18: 741-749, 2007.

137. **Teerlink T.** ADMA metabolism and clearance. *Vasc Med* 10 Suppl 1: S73-81, 2005.

138. **Tojo A, Kimoto M and Wilcox CS.** Renal expression of constitutive NOS and DDAH: separate effects of salt intake and angiotensin. *Kidney Int* 58: 2075-2083, 2000.

139. **Tojo A, Onozato ML and Fujita T.** Role of macula densa neuronal nitric oxide synthase in renal diseases. *Med Mol Morphol* 39: 2-7, 2006.

140. **Tojo A, Welch WJ, Bremer V, Kimoto M, Kimura K, Omata M, Ogawa T, Vallance P and Wilcox CS.** Colocalization of demethylating enzymes and NOS and functional effects of methylarginines in rat kidney. *Kidney Int* 52: 1593-1601, 1997.

141. **Tomasoni S and Benigni A.** Gene therapy: how to target the kidney. Promises and pitfalls. *Curr Gene Ther* 4: 115-122, 2004.

142. **Tran CT, Fox MF, Vallance P and Leiper JM.** Chromosomal localization, gene structure, and expression pattern of DDAH1: comparison with DDAH2 and implications for evolutionary origins. *Genomics* 68: 101-105, 2000.

143. **Ueda S, Kato S, Matsuoka H, Kimoto M, Okuda S, Morimatsu M and Imaizumi T.** Regulation of cytokine-induced nitric oxide synthesis by asymmetric dimethylarginine: role of dimethylarginine dimethylaminohydrolase. *Circ Res* 92: 226-233, 2003.

144. **Umemura T, Kitamura Y, Kanki K, Maruyama S, Okazaki K, Imazawa T, Nishimura T, Hasegawa R, Nishikawa A and Hirose M.** Dose-related changes of oxidative stress and cell proliferation in kidneys of male and female F344 rats exposed to potassium bromate. *Cancer Sci* 95: 393-398, 2004.

145. **Valdivielso JM, Crespo C, Alonso JR, Martinez-Salgado C, Eleno N, Arevalo M, Perez-Barriocanal F and Lopez-Novoa JM.** Renal ischemia in the rat stimulates glomerular nitric oxide synthesis. *Am J Physiol Regul Integr Comp Physiol* 280: R771-9, 2001.

146. **Vallance P and Leiper J.** Cardiovascular biology of the asymmetric dimethylarginine:dimethylarginine dimethylaminohydrolase pathway. *Arterioscler Thromb Vasc Biol* 24: 1023-1030, 2004.

147. **Vaziri ND.** Oxidative stress in uremia: nature, mechanisms, and potential consequences. *Semin Nephrol* 24: 469-473, 2004.

148. **Vaziri ND.** Roles of oxidative stress and antioxidant therapy in chronic kidney disease and hypertension. *Curr Opin Nephrol Hypertens* 13: 93-99, 2004.

149. **Vaziri ND.** Effect of chronic renal failure on nitric oxide metabolism. *Am J Kidney Dis* 38: S74-9, 2001.

150. **Vaziri ND, Dicus M, Ho ND, Boroujerdi-Rad L and Sindhu RK.** Oxidative stress and dysregulation of superoxide dismutase and NADPH oxidase in renal insufficiency. *Kidney Int* 63: 179-185, 2003.

151. **Vaziri ND, Ni Z, Oveisi F, Liang K and Pandian R.** Enhanced nitric oxide inactivation and protein nitration by reactive oxygen species in renal insufficiency. *Hypertension* 39: 135-141, 2002.

152. **Vos IH, Joles JA and Rabelink TJ.** The role of nitric oxide in renal transplantation. *Semin Nephrol* 24: 379-388, 2004.

153. **Wagner L, Riggleman A, Erdely A, Couser W and Baylis C.** Reduced nitric oxide synthase activity in rats with chronic renal disease due to glomerulonephritis. *Kidney Int* 62: 532-536, 2002.

154. **Wang D, Gill PS, Chabrashvili T, Onozato ML, Raggio J, Mendonca M, Dennehy K, Li M, Modlinger P, Leiper J, Vallance P, Adler O, Leone A, Tojo A, Welch WJ and Wilcox CS.** Isoform-specific regulation by N(G),N(G)-dimethylarginine dimethylaminohydrolase of rat

serum asymmetric dimethylarginine and vascular endothelium-derived relaxing factor/NO. *Circ Res* 101: 627-635, 2007.

155. **Wang X, Desai K, Juurlink BH, de Champlain J and Wu L.** Gender-related differences in advanced glycation endproducts, oxidative stress markers and nitric oxide synthases in rats. *Kidney Int* 69: 281-287, 2006.

156. **Wang Y, Newton DC and Marsden PA.** Neuronal NOS: gene structure, mRNA diversity, and functional relevance. *Crit Rev Neurobiol* 13: 21-43, 1999.

157. **Wasowicz W, Neve J and Peretz A.** Optimized steps in fluorometric determination of thiobarbituric acid-reactive substances in serum: importance of extraction pH and influence of sample preservation and storage. *Clin Chem* 39: 2522-2526, 1993.

158. **Watanabe Y, Nishio M, Hamaji S and Hidaka H.** Inter-isoformal regulation of nitric oxide synthase through heteromeric dimerization. *Biochim Biophys Acta* 1388: 199-208, 1998.

159. **Xiao S, Wagner L, Schmidt RJ and Baylis C.** Circulating endothelial nitric oxide synthase inhibitory factor in some patients with chronic renal disease. *Kidney Int* 59: 1466-1472, 2001.

160. **Xie J, Roddy P, Rife TK, Murad F and Young AP.** Two closely linked but separable promoters for human neuronal nitric oxide synthase gene transcription. *Proc Natl Acad Sci U S A* 92: 1242-1246, 1995.

161. **Yilmaz MI, Saglam M, Caglar K, Cakir E, Sonmez A, Ozgurtas T, Aydin A, Eyileten T, Ozcan O, Acikel C, Tasar M, Genctoy G, Erbil K, Vural A and Zoccali C.** The determinants of endothelial dysfunction in CKD: oxidative stress and asymmetric dimethylarginine. *Am J Kidney Dis* 47: 42-50, 2006.

162. **Yin QF and Xiong Y.** Pravastatin restores DDAH activity and endothelium-dependent relaxation of rat aorta after exposure to glycated protein. *J Cardiovasc Pharmacol* 45: 525-532, 2005.

163. **Yu Q, Shao R, Qian HS, George SE and Rockey DC.** Gene transfer of the neuronal NO synthase isoform to cirrhotic rat liver ameliorates portal hypertension. *J Clin Invest* 105: 741-748, 2000.

164. **Zatz R and Baylis C.** Chronic nitric oxide inhibition model six years on. *Hypertension* 32: 958-964, 1998.

BIOGRAPHICAL SKETCH

Mr. Tain was born in 1967, in Tainan, Taiwan. In June 1992, Mr. Tain graduated from China Medical College, Taiwan with an M.D. degree. He later received his residency training in pediatrics and fellow training in pediatric nephrology at Chang Gung Memorial Hospital (CGMH), Taiwan. From 1999 to 2002, Mr. Tain worked as an attending pediatrician at CGMH at Kaohsiung, Taiwan. At the same time, he started his research as a graduate student in Graduate Institute of Clinical Medicine at the Chang Gung University and attained a master's degree in biomedicine in December 2002.

To expand his academic horizons, Mr. Tain came to the U.S. with a pre-doctoral fellowship award from his hospital. He was accepted into a Ph.D. graduate program in the Department of Physiology and Pharmacology, West Virginia University, in January 2003. There he worked in the laboratory of Dr. Chris Baylis, studying the progression of renal disease. In summer 2004, he moved with Dr. Baylis to the University of Florida. There, he worked as a graduate student studying nitric oxide in chronic kidney disease. He received a Bronze Medal Finalist in Medical Guild Graduate Student Research, a Graduate Fellowship for Outstanding Research Award, and an Outstanding International Student Academic Award in 2007. Mr. Tain will attain a Ph.D. in biomedical science in December 2007, and plans to return to Taiwan to work at Chang Gung Memorial Hospital in Kaohsiung, Taiwan.